New York City's Metropolitan Dome: Past and Present CO_2 Concentration Patterns from an Urban to Rural Gradient

Diana Hsueh
M.A. Candidate
Department of Ecology Evolution and Environmental Biology (E3B)
Columbia University

Abstract

Elucidating the effects of urbanization on plant physiology and function is critically important to understand how our natural ecosystems will respond to anthropogenic change. The main focus here will be on the past 150 year record of carbon dioxide (CO_2) concentrations in 10-year segments from an urban to rural transect in the greater New York City greater area as well as contemporary daily and seasonal variations of CO_2 at a high temporal scale. Variations in daily temperature ranges (DTR) will also be considered. Both stable ($\delta^{13}C$) and radiogenic ($\Delta^{14}C$) isotopes of carbon were measured in tree cores to acquire water use efficiency data and historical CO_2 concentrations, respectively. Data from meteorological stations set up in and around New York City were utilized for the analysis of current CO_2 levels. Over the past century, the tree core data show that Central Park was approximately on average 15 ppm higher than the "clean" record of Mauna Loa and the Siple Ice Core. At a finer temporal scale, the current meteorological data show a similar overall trend, however, differences are much more variable and there are instances where urban CO_2 can be as low as rural CO_2, depending on the season and meteorological conditions of the region. Differences between an urban (Harlem) to rural (LDEO) site, for example, can vary 30.6 ppm in the winter and 13.7 in the summer, with similar seasonal trends at our other sites. The maximum average nighttime temperature difference between an urban (Harlem) and a rural (BRF) site reached 5.95 °C. These data provide a baseline of CO_2 levels in and out of New York City and a means to consider looking at the effects of CO_2 and temperature on the physiology and ecology of plants growing in this region.

1. Introduction

Urban centers around the world are growing rapidly, and in 2008, for the first time in history, 50% of the world's population lived in metropolitan areas. By 2050, this percentage is expected to reach to 70% (UN, 2008). As urbanization increases globally, it is important to investigate the effects on air quality, ecosystem function and plant physiology. Ecosystem health in and near these urban centers may provide valuable information regarding how future environmental scenarios brought about by global climate change will impact ecosystem services. Urban areas are associated with and create high amounts of particulate and gaseous pollutants (Lovett et al. 2000; Gatz, 1991). Furthermore, the soils in urban environments are more acidic and contain higher levels of heavy-metals (Pouyat et al., 2008; Pouyat et al., 1995) which are likely to hinder plant growth. However, other characteristics of an urban environment may stimulate plant growth. These includes higher night-time temperatures (urban heat-island effect) (Price, 1979), higher CO_2 concentrations (Clarke and Faoro, 1966) and higher rates of nutrient deposition (Lovett et al. 2000; Gatz, 1991).

Gregg et al. (2003) attempts to shed some light on the effects of urbanization on our ecosystems by growing Eastern cottonwood (*Populus deltoides*) in four sites in New York City, two sites in Long Island and one site in upstate New York. The authors consider variables such as soils, air temperature, CO_2 concentrations, ozone concentrations, nutrient deposition and urban air pollutants to look at the health and growth of *P. deltoides* and observe that the city plants grew better than rural plants. The authors' cite the high concentration of damaging ozone as being the main reason for the reduction in growth in rural areas. The authors also conclude that higher urban temperatures, CO_2 concentrations and nitrogen deposition could not explain the increased growth in urban sites. While *P. deltoides* is native to northeastern forests, it is not as ubiquitous as other flora. Therefore, *P. deltoides* might not be the most ideal plant to look into the effects of urbanization in the NYC area if the intent is to extrapolate to the broader landscape scale of the surrounding forests. Furthermore, the authors only measured CO_2 one meter above the ground for only 48 hours each in Central Park, NYC (400 ppm) and in a rural area (350 ppm) from August 26-28, 1996 (Gregg, 1999) and then used these levels in chamber experiments to conclude that CO_2 concentrations are not significantly affecting the growth of *P. deltoids* grown in NYC. Finally, to also state that change in daily temperatures is not a factor in plant growth may also be premature. It has been shown that higher nighttime temperature increases nighttime respiration rates in P. *deltoids* which in turn results in a decrease in leaf carbohydrate concentration and therefore increases photosynthetic capacity the next day (Turnbull et al., 2002). It is logical to expect these increased rates of photosynthesis and respiration would both increase tree growth as observed by Gregg et al. (2003).

In 2004, a project similar to the Gregg et al. (2003) study was initiated, where red oaks (*Quercus rubra*) were grown from an urban to rural gradient. Again, the main goal of this project was to understand the effects of urbanization on plant physiology and ecosystem function. *Q. rubra* is more ubiquitous in the Northeastern forests in the U.S. and is therefore more representative of how local forests might respond to urbanization. The four sites that make up the urban to rural gradient are i) Central Park (CP), ii) Lamont Doherty Earth Observatory (LDEO), iii) Black Rock Forest (BRF) and iv) Ashokan Reservoir (AR) in the Catskill Park and Forest Preserve. The latitude, longitude, and elevation of these four sites can be found in Table 1 and locations of the sites can be found on the map in Figure 1. In 2006 from September 22-24 and October 21-22, photosynthesis rates (made using an open-flow gas exchange system, Li-6400, Li-Cor, Lincoln NE) were found to be highest in CP, followed by AR and lowest at the two remaining sites (Searle et al., 2007). Furthermore, during the 2008 growing season, there was a clear increase in oak seedling growth in the city with respect to the other three more rural sites (Searle, personal communication, 2008; Figure 2); however the cause of the increased growth in the city is still unclear. It is hypothesized that the combined effect of CO_2, ozone concentrations and diurnal temperature range (DTR as in Easterling et al. 1997) explains most of the differences in photosynthesis and growth rates along the transect (Searle et al., 2007).

Ozone and DTR can have a large effect on plant growth and its viability. Plants are usually very sensitive to ozone, but the extent of damage is dependent on the concentration of ozone, particular species and variety of plant. *Populus spp.* is much more sensitive to ozone than *Q. rubra* (Yun and Laurence, 1999; Samuelson and Edwards, 1993); varying the way Northeastern forests will respond to urbanization. High concentrations of ozone might cause enzyme inactivation (e.g. Fridovich, 1986), lipid peroxidation, membrane damage and DNA ruptures (Halliwell and Gutteridge, 1985). Other biochemical carbon damage includes changes in the two main carbon exchange processes, photosynthesis and respiration. Decreases in photosynthesis differ by species (Guderian et al., 1985) and is dependant on the age of the leaf; young leaves tend to recover from O_3 damage more completely than more mature leaves (Pell and Brennan, 1973). Intriguingly, ozone can both promote and limit respiration, depending on the plant, duration and concentration of ozone exposure (Lee 1967; Barnes 1972).

DTR can have a significant effect on plant height, leaf orientation, chlorophyll content, shoot orientation, internodal length, petiole and flower stalk elongation and lateral branching (Myster and Moe, 1995). Accordingly I briefly touch upon diurnal temperature range along the urban to rural transect. In most of the sections below, however, I primarily explore CO_2 and its effects on plant function and physiology, its role in ecosystems and contemporary ways of measuring current and past CO_2 concentrations.

1.1 Influences of CO_2 Concentrations

The three main influences on ambient atmospheric CO_2 concentrations are anthropogenic influences, meteorological conditions, and the natural ecology of the region. Anthropogenic influences include fossil fuel emissions, cement emissions and land use change (e.g. wood harvest and deforestation). A combined total of 488 Petagram (Pg) C (1 PgC = 10^9 metric tons) has been emitted into our atmosphere from 1850 to 2006 (Canadell et al., 2007). Anthropogenic CO_2 emissions are a major factor (90% certainty) in global climate change (IPCC, 2007a) causing noteworthy changes such as increases in sea-level, adverse effects on ecosystem health and viability, changes in fire regimes, disease transmission and overall ecosystem health upon which we depend (IPCC, 2007b).

Much of the anthropogenically derived atmospheric CO_2 originates from urban centers (vehicles, building emissions, cement production and the generation of electricity) as well as transportation vectors from the combustion of fossil fuels. The magnitude of a CO_2 dome (i.e. the buildup of CO_2 in a particular area) can be considerable over urban areas. In London, CO_2 concentrations can reach up to 20% over ambient background conditions on weekdays (Derwent et al., 1995). Phoenix exhibits 43% greater concentrations than the surrounding rural areas on weekdays (Idso et al., 2001). At larger scales, the Eastern North America and Ohio-Maryland regions show an additional 2.7 ± 1.5 ppm and 4.3 ± 1.0 ppm of added fossil fuel CO_2 relative to the Rocky Mountain Region (Hsueh et al., 2007). In rural areas however, carbon dioxide is mainly controlled by the photosynthesis and respiration of the plants in an area. A significant amount of CO_2 can also be carried *via* wind from urban areas (e.g. Woodwell et al., 1973).

Atmospheric dynamics of the Greater New York City area also play a large role in controlling local CO_2 concentrations. This region is influenced by frontal systems and storms that travel across the North American continent. Hence, many of the weather conditions that affect New York City advance from a westerly course of direction. These weather systems also play a large role in keeping air from stagnating in this region. While there is a dominant continental weather effect, oceanic influence is not negligible. Summer winds blow onshore due to the cool water surface but lessen inland (NOAA, 2009). Due to the specific meteorological characteristics of this region, wind often keeps the air from stalling over the city and thus prevents the accumulation of CO_2.

Solar radiation also plays a large role in the microclimate (i.e. near/on tall buildings, trees and point sources such as roads) of this area for two reasons. First, energy from the sun provides a means for photosynthesis to occur, thus drawing down daytime CO_2 levels during the growing season. Second, the sun heats surfaces, which causes thermal instability and convection leading to additional turbulence which helps to create a deep mixed layer minimizing CO_2 accumulation. At night, convection due to direct solar heating is nonexistent and the air stalls over the city, allowing both anthropogenic and naturally respired CO_2 to accumulate.

1.2 Effects of Elevated CO_2 on Plants and Ecosystems

The three main mechanisms in which plants and ecosystems can respond to rising CO_2 levels are photosynthesis, transpiration and respiration. To try to explain the effects of rising CO_2 on our ecosystems, scientists have used different methods; most notably Free-Air Carbon Enrichment (FACE) experiments. FACE allows investigators to look at ecosystems in normal and fully exposed air conditions.

So what have we learned? Through these cumulative experiments enhanced CO_2 levels result in an increase in plant growth rate, photosynthesis (however acclimation, typically down-regulation, can be demonstrated after an extended period of time) and biomass accumulation (Norby et al., 2005) is commonly observed. This is thought to result from a reduction in stomatal conductance and transpiration (Drake et al., 1997), which results in an increased water use efficiency (WUE). However, different C_3 functional groups show varying responses in photosynthesis (Ainsworth and Long, 2005) and C_4 plants such as corn (*Zea mays*) have conflicting results as well (Leakey et al. 2004, Leakey et al. 2006). Furthermore, a long term indirect effect of elevated CO_2 on respiration seems to increase respiration by 10% (Wang and Curtis 2002).

On an ecosystem level, elevated CO_2 has also been shown to improve nutrient, water and light use efficiency of C_3 plants (Ainsworth and Long, 2005). It is also possible that elevated CO_2 amplifies carbon uptake in the shade, improves soils-water balance, increases the carbon:nitrogen ratio and thus reduces the nutritional content in primary producers (Drake et al., 1997) and therefore affecting higher trophic levels (e.g. Knepp et al., 2007). Furthermore, not only do plant responses themselves need to be taken into consideration, soil (decomposition rates, autotrophic and heterotrophic respiration etc…) is an integral part of the carbon balance of terrestrial ecosystems and needs to be carefully considered. A frequent response is that elevated CO_2 results in an increased respiratory flux of CO_2 from soils (Zak et al., 2000). This has large implications for the long-term storage of carbon in terrestrial biosphere. In addition, increases in CO_2 have had adverse effects on crop nutrition and plant biology which can in turn affect public health (Ziska et al., 2009). Interactions of CO_2 with other abiotic factors such as temperature, ozone and nutrients (e.g. nitrogen and phosphorus) further complicate the picture (e.g. Norby and Luo, 2004; Ainsworth and Long, 2005; Shapiro et al., 2004).

Given the increased attention of rising CO_2, climate change and efforts to elucidate the effects of increased carbon dioxide on ecosystems, basic monitoring of ambient CO_2 concentrations is needed. Historical CO_2 data from urban sites are limited, yet vital to our efforts to understand urban ecosystems and the linkages between urban and rural environments (to date, measurements have mostly been in “clean” sites, notably Mauna Loa). Here I will mainly focus on CO_2 concentrations (daily, seasonal and past variations) along an urban to rural gradient since understanding the spatial and temporal variations in atmospheric CO_2 may be particularly important in understanding the observed response of plants along the gradient. The rest of the introduction is divided into two sections: i) a background about both a stable form of carbon (^{13}C) and radioactive form (^{14}C) and its use in ecological experiments/observations and ii) a general overview of the more noteworthy *in-situ* carbon dioxide measurements, CO_2 remote sensing and modeling techniques.

1.3 Carbon Isotopes

There are three main isotopes ^{12}C, ^{13}C and radiocarbon (^{14}C). The abundance is as follows: 1**:**0.011**:**10^{-12}, where the first two are stable and the last is radioactive. The heavier isotopes diffuse more slowly; have lower enzymatic reaction rates and stronger chemical bonds. These properties can be used to explore biological and physical processes in ecology.

The abundance of a particular isotope is almost always stated in a ratio (R_{sample} or $R_{standard}$) of the heavier isotope to the lighter one (ex. $^{13}C/^{12}C$). The absolute ratio is unreasonable because of the large differences in natural concentrations between isotopes mentioned above. Therefore, we express the isotope concentration of a substance relative to an internationally recognized standard [e.g. Pee Dee Belemnite (PDB) for ^{13}C; Oxalic Acid I (OX-I) for ^{14}C]:

$$\delta = \left(\frac{R_{sample}}{R_{s\tan dard}} - 1 \right) \cdot 1000 \text{ ‰} \qquad (1)$$

(The unit denoted here is termed per mil (‰) and is defined as one part per thousand: 1/1000 or 0.1%)

However, ^{14}C is expressed as a concentration and is denoted as percent modern carbon. Modern carbon is defined at background activity in 1950 and is considered to be "present". 1950 [i.e. 0 Before Present (BP)] was chosen in honor of the first publication of radiocarbon dates in 1949 (Libby et al., 1949). $\Delta^{14}C$ measurements are corrected for any isotopic fractionation that takes place during sample preparation or in the AMS by normalizing to a standard $\delta^{13}C$ value of -25‰ (Stuiver and Polach, 1977) by the equations below:

$$\Delta^{14}C = \left[\left(\frac{0.975}{1 + \frac{\delta^{13}C_{sample}}{1000}} \right)^2 \frac{R_{sample}}{R_{s\tan dard}} - 1 \right] \times 1000 \qquad (2)$$

where $R = \frac{^{14}C}{^{12}C}$ (3)

and $\delta^{13}C_{sample} = \left[\left(\frac{\frac{^{13}C}{^{12}C}(sample)}{\frac{^{13}C}{^{12}C}(s\tan dard)} \right) - 1 \right] \times 1000$ from prepared graphite (4)

The importance of these isotopes in ecosystem ecology and how they will be used here in this project is explained below.

1.3.1 ^{13}Carbon

^{13}C is a stable isotope of carbon and currently the average atmospheric δ^{13}C is ~ -8 parts permil (‰) (Keeling and Whorf, 2002). Carbon from petroleum by-products however, is depleted of ^{13}C and has values ranging from -27‰ to -45‰. Nonetheless, using ^{13}C in plants to assess fossil fuel variations is difficult for mainly two reasons. i) δ^{13}C in CO_2 sources changes if the source of the petroleum varies over time (Pataki et al., 2003b) and ii) the initial photosynthetic reactions for C_3 [RUBISCO (ribulose 1-5, biophosphate carboxlase oxygenase)] and C_4 [phosphoenolpyruvate (PEP) carboxylase] plants discriminate differently against ^{13}C. The C_4 enzyme PEP fractionates less against ^{13}C, and thus the isotopic content of C_4 plants is less responsive to other aspects that control stomatal conductance such as temperature, humidity and light compared to C_3 plants (O'Leary, 1981; Farquhar et al., 1989). Because of these complications, depleted ^{14}C (discussed below) in fossil-fuel is a more useful tracer for tracking carbon than ^{13}C because it may show less temporal variations (Pataki et al., 2003b).

Carbon isotope discrimination can be used to link plant water use efficiency (WUE) and bulk $\delta^{13}C$ values. The important steps that fractionate against ^{13}C are diffusion (4.4‰) and carboxylation (30‰). Since leaf stomata effect the rate of diffusion, plants with lower rates of stomatal conductance, and therefore higher WUE, will tend to have less negative bulk $\delta^{13}C$ values (closer to -4.4‰) than plants with higher rates of conductance, and lower WUE (which tend towards -30‰). For C_3 plants, such as Oak (*Quercus spp.*) trees, the δ-value in leaves ranges from -25‰ to -29‰ (Lambers et al., 1998, pg. 54). Other tissues such as wood, stem and roots (e.g. non-photosynthetic tissues) are approximately 2 to 4‰ more positive in $\delta^{13}C$ (O'Leary, 1981). The range of $\delta^{13}C$ values in leaves is also influenced by differences in both the environment the plant was grown in and the particular plant species. Both the stomatal conductance and the rate of CO_2 assimilation influence the ratio (p_i/p_a) of the intercellular partial pressure (p_i) and the atmospheric partial pressure (p_a) of CO_2. The discrimination is thus defined as:

$$\delta^{13}C_{air} - \delta^{13}C_{leaf} = 4.4 + 22.6\left(\frac{p_i}{p_a}\right) \tag{5}$$

This states that a high p_i/p_a results in a greater amount of discrimination (e.g. a more negative $\delta^{13}C$ number).

Furthermore, WUE is defined by the ratio of energy captured by photosynthesis per unit of water transpired and can be defined as:

$$WUE = \frac{A}{E} = \frac{g_c \cdot (p_a - p_i)}{g_w \cdot (e_i - e_a)} = p_a \frac{\left(1 - \frac{p_i}{p_a}\right)}{1.6 \cdot \left(\frac{e_i}{e_a}\right)} \tag{6}$$

where
A = rate of CO_2 assimilation
E = leaf transpiration rate

g_c = diffusive conductance for CO_2
g_w = diffusive conductance for water vapor
e_i = water pressure in the leaf
e_a = water pressure in the atmosphere
1.6 = constant related to relative rates of diffusion for CO_2 vs. H_2O

If stomatal conductance is high, WUE is low and so therefore p_i/p_a will be high. Likewise, if stomatal conductance is low, WUE is high so therefore p_i/p_a will be low (Lambers et al., 1998, pg. 54). From these equations, a correlation between WUE and $\delta^{13}C$ can be found. Generally, plants that have high WUE have a more positive $\delta^{13}C$ signature in the biomass (Farquhar and Richards, 1984; O'Leary, 1988) thus are generally undergoing some form of water stress.

1.3.2 Radiocarbon (^{14}C)

^{14}C is the radioactive isotope form of carbon and is naturally formed in the upper atmosphere where cosmic rays bombard molecules which produce neutrons, which in turn bombard Nitrogen molecules (Lingenfelter, 1963). The neutron replaces a proton in a nitrogen atom, creating a carbon atom:

$$^{14}N + n \rightarrow {}^{14}C + {}^{1}H \quad (7)$$

The ^{14}Carbon then combines with oxygen (O_2) to form a radioactive form of carbon dioxide ($^{14}CO_2$) and assimilates into the carbon cycle. Thus, ^{14}C is found in both organic and inorganic forms and in aquatic and terrestrial ecosystems such as plants, animals, coral, as carbon dissolved in water and carbonates in caves (Broecker, 2003). Approximately 45% of ^{14}C is produced in the upper troposphere and 55% in the stratosphere (Gaggeler, 1995). ^{14}C decays with a half-life of 5,730 years, in which it turns back into ^{14}Nitrogen (Broecker, 2003).

Initial radiocarbon measurements were taken by counting (with a Geiger counter) the β-particles (electrons or positrons emitted by the radioactive nuclei) that were released during decay (Libby et al., 1949). It was only later that Muller (1977) realized that Accelerator Mass Spectrometers (AMS) could be used to count the ^{14}C particles themselves. This innovation brought about an enormous improvement over counting because now only 1 mg instead of 1 g of pure carbon is now needed (Broecker, 2003).

One of the more notable long-term set of recent ambient ^{14}C measurements has been made by Levin and Kromer (2004). A series of measurements [integrated CO_2 collected by chemical absorption in sodium hydroxide (NaOH)] were taken in Europe at these four sites: Vermunt, Austria (from 1959-1986); Schauinsland, Germany (1977-present); Heidelberg, Germany (1976-2002) and Jungfraujoch in the Swiss Alps (1986-present). Jungfraujoch is regarded as tropospheric background level and two of these sites, Vermunt and Schauinsland are considered to be representative of the $^{14}CO_2$ level of tropospheric CO_2 above Central Europe.

Prior to the 20th century, concentrations of ^{14}C were controlled partly by sunspot activity (Stuiver and Quay, 1980; 1981), the Earth's changing magnetic field (Thellier, 1977; Bonhomme and Zahringe, 1969) and ocean mixing/dynamics (Hughen, 1998; Shackleton et al., 1988; Broecker et al., 1990). The values of ^{14}C in the Common Era (C.E.) prior to the 20th century have ranged from approximately -20 to 20‰. Nuclear weapon testing throughout the 1950's and 1960's produced a massive abundance of free neutrons, causing atmospheric ^{14}C to reach levels as high as 1000‰ in the Northern Hemisphere (Figure 3). This feature is commonly known as the bomb spike. Since more of these nuclear tests occurred in the Northern Hemisphere and because of the gradual mixing of CO_2 between the hemispheres, the Southern Hemisphere ^{14}C concentration lagged behind for several years till the mid-1960's (Levin et al., 1980). Since the ban in nuclear weapons testing began on August 5, 1963, ^{14}C levels in the atmosphere have steadily declined largely due to carbon uptake by the ocean and terrestrial biosphere (Nydal and Lovseth, 1983). Over the past 50 years, differences in $^{14}CO_2$ in our atmosphere have been used to study the global carbon cycle (e.g. Broecker et al. 1980; Hesshaimer et al., 1994; Randerson et al., 2002). Today, the distribution of atmospheric ^{14}C is largely determined by fossil fuel emissions known as the Suess effect (Tans et al., 1979), air-sea gas exchange (Broecker et al., 1985), carbon cycling in terrestrial ecosystems (Trumbore, 2000), natural cosmogenic production (Lingenfelter, 1963) and re-entrainment of older stratospheric air in the troposphere (Hesshaimer and Levin, 2000).

Because of the age of fossil-fuels, they contain virtually no ^{14}C. As CO_2 from fossil fuels is emitted into the atmosphere, the ^{14}C content is depleted (Suess Effect) and plants thus record this signal in their biomass. ^{14}C is a sensitive tracer to fossil fuel emissions in the current (2008) atmosphere. The addition of 1 ppm of fossil fuel CO_2 causes a reduction of ^{14}C by approximately 2.75‰, which is near the precision of present day AMSs (Turnbull et al., 2006). By measuring the ^{14}C content in biomass, regional, continental and temporal patterns can be used to map out and record fossil fuel emissions and biosphere-atmosphere exchange (e.g. Riley et al., 2008; Hsueh et al., 2007).

Our understanding of present and past variations of ^{14}C in the atmosphere is crucial due to our use of ^{14}C as a "natural" tracer. Researchers have used atmospheric concentrations of ^{14}C to determine the lifetime of carbon in a specific pool, for example, roots (e.g. Gaudinski et al., 2001) and soils (e.g. Trumbore et al., 1996). Therefore it is important to quantify "natural" ^{14}C that are not heavily influenced by local fossil-fuel to prevent misleading measurements of carbon pool ages. [On a side note, pulse-labeling of ^{14}C have also been used to answer different ecological questions. An example can be found in Carbone et al., (2007) where the authors investigated the spatial and temporal distribution of photosynthetic products by measuring the amount of ^{14}C being respired from different environmental components in a black spruce forest. In this case, sodium bicarbonate enriched in ^{14}C was acidified with acetic acid to emit the $^{14}CO_2$ into the chambers.]

A method of looking into historical ^{14}C concentrations can be determined with tree rings (Cain, 1975; Marzaioli et al., 2005); each ring records the ^{14}C isotopic content acquired during photosynthesis at that particular time (Cherubini, 2000). One of the earliest works looking at one-year segments of tree ring data from 1948-1964 is from Willkomm and Erlenkeuser (1968). Since then, many radiocarbon measurements in tree rings have been made to explore past ^{14}C levels. Some of the more notable examples are derived from oak and pine trees dating back as far as 11,919 years (Kromer et al., 1986; Becker and Kromer, 1993; Kromer and Spurk, 1998; Friedrich et al., 1999). In 2004, a new international ratified calibration curve (called IntCal04, which replaced IntCal98) was constructed that covers 0-26 kyrs BP (the entire Holocene as well as the late Pleistocene). Tree-rings from multiple locations cover the period between 0-12.4 kyrs BP and corals and foraminifera (used site-specific marine reservoir correction to convert to the atmospheric equivalent) were used to look at ^{14}C levels from 12.4-26 kyrs BP (Reimer et al., 2004).

Cain (1975) produced the first work in comparing the ^{14}C concentrations in rural and urban trees in northeastern and northwestern United States. The author looked at the years 1900 until 1970. Here I extend radiocarbon measurements of tree rings similar to Cain's (1975) study sites, but I extend both ends of his timeline, from as early as 1851 until 2008 in 10-year increments.

1.4 Measuring Real Time CO_2 Concentrations

1.4.1 In-situ Measurements

It was the ingenious foresight of Charles D. Keeling to consistently monitor the levels of atmospheric CO_2 at a relatively uncontaminated site called Mauna Loa (Keeling et al., 1976) in which the famous Keeling curve was produced. Since then, over 100 similar stations have been set up all around the world. Some of the other more notable sites include Point Barrow, Alaska (BRW), Niwot Ridge, Colorado (NWR), American Samoa (SMO) and the South Pole (SPO).

Despite ground-level efforts, these observation sites have been relatively few compared to the land area of Earth and are unequally distributed around the world. The highest density of observation sites are in North America and Europe, leaving much of the Southern Hemisphere and urban sites (where much of the CO_2 is being emitted) understudied. There has only recently been an increase in interest in urban centers (Berry and Colls, 1990a,b; Clarke and Faoro, 1966). Since then, studies have been carried out in Phoenix, Arizona (Isdo et al., 2001) as well as looking at the effects of CO_2 on different vegetation types (turf, desert, at the center and edge of the city) (Day et al., 2002). Two suburban sites in Melbourne, Australia explored Southern Hemisphere dynamics (Coutts et al., 2007). One of the longer running studies (5 years) have investigated the CO_2

concentrations and other environmental factors in the city of Baltimore, a suburban Baltimore site and organic farm (George et al., 2007). Some studies have taken this one step further by creating a mobile laboratory [e.g. Essen, Germany (Henninger and Kuttler, 2007)], and putting in eddy covariance towers to monitor CO_2 fluxes from different urban neighborhoods (Mexico City, Mexico: Velasco et al., 2005; Basel, Switzerland: Vogt et al., 2006 and Chicago, Illinois: Grimmond et al., 2002). Isotopic measurement techniques (notably ^{13}C and ^{18}O) have also provided important distinguishing means between anthropogenic and biogenic CO_2 sources (e.g. Zondervan and Meijer, 1996, Kuc and Zimnoch, 1998; Pataki et al., 2003a). A study that integrates and verifies observed CO_2 concentrations with a multiple-box transport and mixing model is valuable in simulating CO_2 concentrations in other urban sites as well (ex. Reid and Steyn, 1997: in the suburban region of Vancouver, Canada). The authors found close agreement with the model and observed and stressed the significance of the atmospheric boundary layer structure for CO_2 concentrations in a specific region. Grimmond et al. (2002) provides a detailed summary table of studies measuring CO_2 concentrations in urban sites prior to 2002. Table 2 illustrates some examples of more recent studies that have measured CO_2 in urban areas. Despite these efforts, there are still major gaps in the data; notably areas that are difficult to reach or monitored continuously. Satellites and modeling are aimed to fill these gaps.

1.4.2 Satellite Measurements

The addition of satellites to monitor CO_2 has been an important asset in the effort in deciphering the larger CO_2 picture. The first attempt at monitoring global atmospheric CO_2 concentrations via satellite was the SCanning Imaging Absorption SpectroMeter for

Atmospheric CartograpHY (SCIAMACHY) instrument on Environmental Satellite (ENVISAT) that was launched in March of 2002 by the European Space Agency (ESA). The first three years of data were compared to Carbon Tracker (see below) and it was concluded that year-to-year changes had an accuracy of roughly 1 ppm. Certain latitude bands over the Northern Hemisphere were accurate near 2 ppm over the course of a seasonal cycle (Buchwitz et al., 2007). Earlier this year on January 23rd, 2009, Japan's Aerospace Exploration Agency (JAXA) launched Greenhouse Gases Observing Satellite (GOSAT) which will measure CO_2 and CH_4 (methane) over almost the entire planet at ground level. Although the primary objective is to monitor treaty compliance from various countries, this satellite will also aid in looking at the missing carbon sink and balancing the global carbon budget (JAXA, 2009). The latest attempt was from the National Aeronautics and Space Administration (NASA) where a launch effort was made on February 24, 2009 to put another satellite, the Orbiting Carbon Observatory (OCO) as part of the A-train of satellites, but very unfortunately crashed shortly following takeoff. This satellite was supposed to supplement the Japanese satellite and gather global measurements of atmospheric CO_2 in which its main mission was to aide in finding the missing CO_2 sink (Kintisch, 2009).

1.4.3 CO_2 Emissions and Modeling CO_2 Concentrations

Various projects around the world aim to deduce the carbon sinks and sources and thus gain a greater understanding of the world's carbon cycle. Two notable projects stand out in deducing the influences of these variables over atmospheric CO_2 concentrations in North America. They are Purdue University's Vulcan Program and NOAA's Carbon Tracker and which will be described in more detail below. Both projects contribute to the North American Carbon Program (NACP) which aims to determine and understand the sinks and sources of various carbon gases such as methane (CH_4), carbon monoxide (CO) and carbon dioxide (CO_2) in North America and bordering ocean areas. A multitude of various carbon projects can be found here: http://www.nacarbon.org/nacp/

Purdue University's "Vulcan Project", lead by Dr. Kevin Gurney, aims to quantify fossil fuel CO_2 emissions in North America at smaller temporal and spatial time scales than what has been attained before. It uses images of the Earth's surface from the satellite Landsat 5, population data from the U.S. Census Bureau and CO_2 emissions from the U.S. Environmental Protection Agency (EPA) and the U.S. Department of Energy (DOE). Currently it uses emission information from the year 2002 and is averaged per county, however the research team hopes to use more recent years soon and gather emissions data at the street level. Another goal is replicating this in other countries, starting with Mexico and Canada. More detail regarding the program, refer to this website: http://www.purdue.edu/eas/carbon/vulcan/index.php and the interactive map can be found here: http://www.purdue.edu/eas/carbon/vulcan/GEarth/index.html

A relatively new utensil aimed at understanding the global carbon cycle and to lay a foundation for managing international CO_2 policies was developed at the National Oceanic and Atmospheric Administration's (NOAA's) Earth System Research Laboratory (ESRL). Called "Carbon Tracker", this project creates model forecasts of global atmospheric CO_2. It does this with an atmospheric transport model and surface exchange model based on the mixing of the air, weather forecasts [from the European Centre for Medium-Range Weather Forecasts (ECMWF)], photosynthesis and respiration of the terrestrial ecosystem, air-sea exchange of CO_2 and the emission of CO_2 via fires and fossil fuels. These model values will be evaluated against measured surface atmospheric CO_2 concentrations and then a statistical model will “correct” the simulated CO_2 by decreasing the difference between modeled and measurements. In addition, column averages are also produced and can be compared to satellite measurements. This data can be useful in estimating the net carbon source an area is generating. For example, every week for the period from 2000-2005, an approximate net flux of CO_2 across North America was calculated. It was deduced that the North American terrestrial ecosystems is taking in approximately 0.65 PgC/yr. This lowers the 1.85 PgC/year that North America emits through fossil fuels and cement production. The majority of the offset is from the deciduous forests on the East Coast (32%) and the boreal forests (22%) (Peters et al., 2007). Presently, Carbon Tracker only deals with CO_2, but other gases ($^{13}CO_2$, $^{14}CO_2$, CH_4) and other direct measurements using other methods (eddy-flux and satellite) are already being taken under consideration to expand Carbon Tracker. For more detail regarding the program, please refer to this website: http://www.esrl.noaa.gov/gmd/ccgg/carbontracker/

1.5 Past CO_2 measurements in the New York Metropolitan Area

Given CO_2’s prominence in the increasingly environmentally aware world, it is essential that basic variations of CO_2 concentrations be deciphered in both urban and rural sites. Only two dated studies have measured CO_2 over the New York City greater area. Woodwell et al., (1973) measured CO_2 concentrations at different heights in a 125 m tower at the Brookhaven National Laboratory tower at Long Island for a period of 6 years from 1965-1971. The authors showed that Brookhaven had clear seasonal trends with the photosynthesis and respiration during the summer and winter months respectively which was thought only to be evident in more rural areas. The highest concentrations the authors observed exceeded the range of the calibration of 500 ppm and their lowest concentrations were during the day in the summer, between 290 and 300 ppm. Fluctuations of 10 ppm from minute to minute were common and during the breaking of the nocturnal inversions, changes of 50 ppm were common as well. Their winter and summer differences were approximately 19 ppm at 125 m above ground level. The heavily industrialized eastern seaboard also influences the site. This partly resulted from wind directional trends of CO_2 dependent on where air masses were coming from.

The second study is from Sethuraman et al. (1981) who measured CO_2 for three weeks in December 1979 at Tiana Beach in Long Island. However the authors aimed their investigation at CO_2 concentration gradients along coastal and oceanic areas rather than studying fossil-fuel and biosphere influences. Their mean CO_2 concentration was 352 ppm and when wind was light and a strong surface-based inversion formed at night, a gradient of 10-15 ppm was observed. The authors believe that this is due to a biological release of CO_2 and little mixing in the atmosphere.

As discussed above, ground stations around the world are sparse, most are in relatively clean areas and none that we know of on a 10 km basis. Here we aim to fill in the gaps about our urban and suburban areas at a finer temporal (seasonal and diurnal) and spatial scale than ever before in the surrounding areas of New York City, NY. In addition, by exploring past CO_2 concentrations from tree cores, we hope to establish a fuller picture of how CO_2 concentrations varied in the past and present to serve as a baseline for what concentrations the local vegetation have been exposed to and how they will respond to their increasingly changing climate. Overall, we predict that New York City will be exposed to higher levels of atmospheric CO_2 concentration than rural areas.

2. Materials and Methods

The four sites that encompass the urban to rural gradient are: 1) Central Park (CP) 2) Lamont Doherty Earth Observatory (LDEO) 3) Black Rock Forest (BRF) and 4) Ashokan Reservoir (AR). The latitude, longitude and elevation can be found in Table 1. The urban to rural gradient transect is located in the State of New York which is situated near the east coast of the North American continent (Figure 1).

2.1. $\delta^{13}C$ and Radiocarbon ($\Delta^{14}C$) Analysis

2.1.1. Pilot Study

For a pilot study, 3 rough cocklebur (*Xanthium strumarium)* leaves were collected from each of the sites in November of 2006. The samples were then ground and then sent to the W.M. Keck Carbon Cycle Accelerator Mass Spectrometer at UC Irvine for $\delta^{13}C$ and $\Delta^{14}C$ analysis.

2.1.2. Tree Cores

Encouraged by the pilot study results, tree cores were then collected to look at historical CO_2 concentrations. Four *Q. rubra* cores from each of the four sites were collected and dated. CP went back to 1891, LDEO went back to 1851, BRF went back to 1871 and AR went back to 1911. The cores were cut up into 10-year segments and prepared to convert the wood into holo-cellulose through a process called lipid extraction. This is to ensure that the wood that is being measured contains sequestered CO_2 at a particular time. The exact protocol of extraction can be found in the Appendix. The samples were then ground and sent to the W.M. Keck Carbon Cycle Accelerator Mass Spectrometer at University of California, Irvine (UCI) for $\Delta^{14}C$ analysis (Xu et al., 2007). $\delta^{13}C$ analysis were also carried out at UCI; some of the gas for this analysis were taken out of the graphitization line (the device used to convert gaseous pure CO_2 into graphite for ^{14}C analysis) and measured on the Gas Bench coupled with IRMS (Isotope Ratio Mass Spectrometry - Finnigan Delta Plus). For the ^{14}C analysis, the standards Oxalic Acid I, Oxalic Acid II, Australian National University (ANU), Coal, C5 Wood Standard, Firi J-Barley and Tiri B-Belfast pine were included to make sure that there was a reduced chance of differences in measurement due to running the samples in different sets. For $\delta\ ^{13}C$ analysis, the customary V-PDB standard was used.

2.1.3. Estimating Fossil Fuel CO_2

The CO_2 that is incorporated by Q. *rubra* (C_t, with units of ppm; “t” for tree) comprises of the background factor (C_{bg}), biosphere exchange (C_b), ocean exchange (C_o), and fossil fuel emissions (C_{ff}). Likewise, the $\Delta^{14}C$ elements are Δ_t, Δ_{bg}, $\Delta_{b,}$ Δ_o, Δ_{ff}. The mass balance equations are:

$$C_t = C_{bg} + C_b + C_o + C_{ff} \tag{8}$$

$$\Delta_t \cdot C_t \approx \Delta_{bg} \cdot C_{bg} + \Delta_b \cdot C_b + \Delta_o \cdot C_o + \Delta_{ff} \cdot C_{ff} \tag{9}$$

Background CO_2 levels (C_{bg}) were estimated using measurements from combining two separate records. The first segment of the record was from DOE’s Carbon Dioxide Information Analysis Center’s (CDIAC’s) Siple Ice Core Record that spans from 1734-1983 (Friedli et al., 1986). The second segment of the record was from CDIAC’s Mauna Loa record that spans from 1958 until the present (Keeling et al., 1976). Both records taken together were splined to fill in missing years in the Siple Ice Core. 10-year averages were then taken from the splined record and are listed in Table 3.

Background $\Delta^{14}C$ levels (Δ_{bg}) were estimated using three main records. The first segment was from Levin and Kromer (2004) and contains ^{14}C measurements averaged from three Northern European mountain sites: Vermunt, Austria (1800 m), Schauinsland, Germany (1205 m) and Jungfraujoch, Switzerland (3450 m). Records from these sites span from 1959-1983, 1977-2003 and 1986-2003 respectively. The second segment comes from a tree core collected in Washington State and provides a record spanning from 1815-1975 (Stuiver and Quay, 1981). However, from this tree core record, only the data from 1951 to 1954 was used for the reasons explained below. The third segment was from INTCAL04 which covers the time period from 26,000 years ago until 0 BP (i.e. 1950). This calibration curve uses various sources such as tree rings, corals and foraminifera (for more information, refer to http://www.radiocarbon.org/IntCal04.htm). A spline was then used to fill in the missing small gaps and the resulting values used are listed in Table 4. Since the INTCAL04 stopped at 1950 and Levin and Komer picked up at 1959, the Stuiver and Quay's tree ring record was used to fill in the crucial time in which ^{14}C suddenly rose sometime in the 1950's. A spline would not be appropriate here since it would have produced a gradual increase producing unrealistic background ^{14}C measurements. ^{14}C data from 2001-2008 could not be obtained in time therefore CO_2 in ppm is not shown during this time period (Figure 10).

The AR tree core could have been used as the ^{14}C background, however, this record only goes as far back as 1911 and there is no certainty that the area is completely free of a fossil fuel influence, especially during the latter half of the 20th century. In addition, it was rather difficult in locating a tree from this site that dated back more than 100 years. There are several reasons why this might have been the case. The Catskills has a long history of logging and farming prior to the establishment of Catskill Park and Forest Preserve that was formed in 1885. Several decades later, in 1929, farm abandonments began on a large scale with efforts for forest restoration beginning soon after (Kudish, 2000). At the AR site, there are visible stone walls still present in the forest nearby, evidence of some kind of human settlement. It could not be determined when this particular location was abandoned, but there were a large number of visibly younger trees. Of the trees that were visibly older, many had heart rot in the middle, making them impossible to core. One advantage of using the AR tree core would have been that localized biospheric and oceanic influences could be removed from equation 8 and 9 since the enrichment of the ^{14}C from these effects would already be integrated in the tree core measurements in the AR and Northeastern US region. The background ^{14}C in Table 4 does not incorporate these effects since the records are from a multitude of locations. And although localized enrichments could theoretically be modeled, no explicit atmospheric model simulations of biospheric and/or oceanic effects over the time period presented here is known. However, under present (2006) atmospheric conditions, there is less than a 1‰ biospheric/oceanic enrichment influence in the Northeastern U.S. area (Hsueh et al., 2007). Our estimates of C_{ff} are made relative to these clean air regions and both biospheric exchange ($C_{b,} \Delta_b$) and oceanic exchange ($C_{o,} \Delta_o$) are ignored (equations 8 and 9). The limitations and implications of these assumptions will be discussed more fully in the Discussion.

2.2 Meteorology Stations

The meteorology stations described in this project are part of a larger project called the Lamont Atmospheric Carbon Observation Project (LACOP) which was initiated in 2006. The latitude, longitude, elevation and physical location of these sites can be found in Table 1 and a map of the locations of these stations that indicate current conditions can be found in Figure 4 and this website: http://www.ldeo.columbia.edu/outr/LACOP/. The dates in which each site was initiated, the CO_2 instrument used and the weather indices being measured at each station can be found in Table 5. For calibrating the instruments, pure nitrogen gas was used for zeroing and a cylinder of a known CO_2 concentration was used for spanning. A schematic of a typical meteorological station can be found in Figure 5. The Harlem site will have to serve as the majority of the data from an urban site instead of CP because LACOP was already set up before collaboration with the urban to rural *Q. rubra* transect began. The protocol is as follows: A sample interval every 30 seconds, logging interval every 15 minutes and then it sends data to a website *via* a telemetry system every hour or so.

While it is wet CO_2 (pCO_2) that is measured in these Li-Cor 820's and 840's, it is the dry CO_2 (xCO_2) concentrations that are reported, using the following equation:

$$xCO_2 = \frac{pCO_2}{1 - \frac{H_2O}{1000}} \tag{10}$$

Where:
xCO_2 = dry CO_2
pCO_2 = wet CO_2 (measured)
H_2O (ppt) = water concentration in parts per thousand

Water concentration can normally be obtained on a Li-Cor 840 where water is measured, but with a Li-Cor 820, where water is not measured, water concentrations can be obtained through first getting specific humidity (q; g/kg) from these variables: Relative Humidity (RH; %), Temperature (T; °C) and Pressure (P; hPa) in the following equations. If the measurement for Pressure is missing, the standard pressure at ground level was used: 1013.25 hPa which is equivalent to 1 atmosphere (atm).

$$q = \frac{X_{H_2O} \cdot M_{H_2O}}{X_{H_2O} \cdot M_{H_20} + (1 - X_{H_2O}) \cdot M_{dry}} \cdot 1000 \tag{11}$$

Where the constants are:

M_{H2O} = molar mass of water = 18.01534 g/mol^{-1}
M_{dry} = molar mass of dry air = 28.9644 g/mol^{-1}

and

$$X_{H_20} = \frac{P_{H_2O}}{P} = \text{Volume mixing ratio} \tag{12}$$

and

$$P_{H_20} = \frac{RH}{100} \cdot e \;\; = \text{Partial pressure of water} \tag{13}$$

where

P = Pressure in hPa
RH = Relative Humidity in %
T = Temperature in °C
e = vapor pressure of water

$$e = a_1 + a_2 \cdot (T) + a_3 \cdot (T)^2 + a_4 \cdot (T)^3 + a_5 \cdot (T)^4 + a_6 \cdot (T)^5 + a_7 \cdot (T)^6 \tag{14}$$

a_1 = 6.11176750
a_2 = 0.443986062
a_3 = 0.143053301E-01
a_4 = 0.265027242E-03
a_5 = 0.302246994E-05
a_6 = 0.203886313E-07
a_7 = 0.638780966E-10 (Flatau et al., 1992; -50 to 50 °C)

Once q is calculated, water in parts per thousand can be obtained:

$$water(ppt) = q \cdot \frac{M_{dry}}{M_{H_20}} \tag{15}$$

In the case for CP, Harlem's Relative Humidity and Temperature were used because NOAA's data were only collected every hour. This is done so that a Harlem and CP comparison could be evaluated at a finer temporal scale.

2.3 Statistical Methods

A one-way ANOVA was used to test for significance between the 4 sites for the δ^{13}C and Δ^{14}C measurements in the *X. strumarium* leaves pilot study.

3. Results

3.1. Pilot Study

From the δ^{13}C of the *X. strumarium* leaves (Figure 6, Table 6; using a one-way ANOVA test), it can be concluded that none of the means are significantly different from the others (ANOVA $F_{3,8}$= 3.6245, p-value=0.0645) (although there are significant differences at the 95.0% level of confidence, so it is susceptible to different interpretations). However, a visual observation seems to suggest that both BRF and the AR site have a higher WUE (thus is going under more water-stress) since the site consistently have less negative δ^{13}C values than LDEO and CP.

The Δ^{14}C of the *X. strumarium* leaves (Figure 7, Table 6) show that relative to AR, there were an additional 3.3, 5.6 and 10.5 ppm of additional fossil fuel for BRF, LDEO and CP respectively. As hypothesized, CP was the most polluted while AR was the cleanest. From a one-way ANOVA test, I can conclude that at least one of the means is significantly different from the others (ANOVA $F_{3,8}$= 41.69, p-value<0.001). From a post hoc Tukey test, there is a significant difference between all of the pairs of sites except for the one between LDEO and BRF.

3.2 Tree Cores

The $\delta^{13}C$ results from the tree cores (Figure 8, Table 7) show a linear trend up until the 1950's and in the subsequent years, the $\delta^{13}C$ for all 4 sites declined. The average $\delta^{13}C$ for the four sites prior to 1950 is as follows: CP (n=6): -24.01; LDEO (n=10): -23.75; BRF (n=8): -23.40; AR (n=4): -22.75. Given that these samples were of wood rather than leaves, it is not unusual that the average values of all four sites fell above the expected C_3 δ range of -25‰ to -29‰.

The $\Delta^{14}C$ results from the tree cores (Figure 9, Table 8) show that the data followed the bomb spike well into the 1950's and 60's. CP, denoted in dark blue, is depleted in ^{14}C as expected. Two points for LDEO, 1961-1970 and 1971-1980, were not expected and there is no means to know if those unusual data points are accurate without getting additional repetitive measurements (which were not budgeted for and are prohibitively expensive).

Using mass balance equations described in the Methods section, the results can be converted to additional fossil-fuel in ppm in comparison to a clean site (Table 9, Figure 10). This graph shows an additional green line which represents "clean" CO_2 concentration splined from the Siple Ice Core and Mauna Loa Record (Table 3). BRF and LDEO showed a divergence at the beginning of the 20th century and overall CP had an average of approximately 15 ppm higher CO_2 concentrations than the clean record. The two LDEO points for the years 1961-1970 and 1971-1980 are the same anomalous points mentioned above. Also, after 1950, several of the data points showed a divergence from the usual trend and potential reasons for this divergence can be found in the Discussion section below.

3.3 Meteorology Stations

Due to the high volume of data produced daily, the following will only highlight important seasonal and daily trends within the LACOP data collected thus far from 2007 until July of 2009. All CO_2 measurements are subject to instrumentation calibration error of ± several ppm.

Daily averaged CO_2 for the years 2007 - 2009 (Figures 11-13) show that Harlem and CP have higher CO_2 concentrations than the other more rural sites. These differences are amplified in the winter months while CO_2 summer time concentrations in the six sites (for when data is available) are similar due to photosynthesis. The minimum and maximum of actual (not daily averages) of CO_2 concentration for all the sites (Table 10) demonstrate a daily trend which will be referred to in the Discussion.

Histograms of wind direction at Harlem (n = 32,422), CP (n = 5253), LDEO (n =24,452), Piermont (n = 31,088), BRF (n = 7,606), AR (n = 7,422) and Norwalk (n = 33,631) are shown with CO_2 concentrations superimposed onto the graphs to display the average concentrations coming from the respective direction (Figure 14-20). There is no histogram of wind direction for Southold due to a lack of data. All of the graphs represent a full year of measurements (2008) with the exception of three sites: 1) AR, where only part of summer and fall were used due to inadequate data, 2) Piermont, where the latter half of 2008 and the beginning of 2009 was used to obtain a full year and 3) CP, where only March – July 2009 CO_2 and wind direction data were used. BRF has fewer measurements because of the sampling frequency (every hour instead of every 15 minutes). Likewise, wind direction data for CP (NOAA, 2009) were only available in one hour increments with many missing data scattered throughout the year.

From the Harlem and CP graphs, winds from the Northwest dominate while LDEO show that winds are all coming equally from all directions. Piermont winds are predominately coming from northerly and southerly directions while BRF winds are typically coming from the south. In general, AR winds seem to come from northerly and easterly directions and Norwalk winds appear to mostly come from Northwestern, Northeastern and Southeastern directions.

Daily averaged day and night temperature (°C) for the years 2006 – 2009 (Figure 21-24) show a clear difference between day and night temperatures (Table 11-14). May through August was chosen to represent the growing season, where temperature has the most impact on plant physiology.

4. Discussion

4.1. $\delta^{13}C$ – Tree Cores

Two important pieces of information can be gathered from the $\delta^{13}C$ data collected from the oak tree cores. First, a fossil-fuel influence can be detected since carbon-based by-products have more negative $\delta^{13}C$ values (Figure 8); however it is unclear why the trend shows an increasing negative trend after 1950. Second, the most rural AR site has a higher WUE (thus is going under more water-stress) as observed in the less negative $\delta^{13}C$ values than the other three sites (Figure 8). All four sites show a trend towards more negative $\delta^{13}C$ values since the 1950-1960 decade, perhaps suggesting both fossil fuel influence and a 50 year trend in decreasing water use efficiency. It would be interesting to compare this trend to observed precipitation trends to assess the effect of potential changes in the regional precipitation patterns on tree growth.

4.2. $\Delta^{14}C$ – Tree Cores

These results demonstrate that while NYC shows a clear signal of additional anthropogenically derived CO_2, in general, the level is surprisingly low and unlikely to have a large influence on plant growth. Historical data from tree cores show that CP, LDEO, BRF and AR had on average an additional 15, 8, 5 and 3 ppm of fossil-fuel derived CO_2 in comparison to Mauna Loa and the Siple Ice Core. There is also an interesting divergence between LDEO and BRF in the beginning of the 20th century (Figure 10), suggesting an increasing influence of New York City's CO_2 dome. However, these results here represent $\Delta^{14}C$ values that are biased toward the day-time and growing season and furthermore influenced by variables that control rates of photosynthesis. Experience with LACOP data (see below) seem to suggest that CO_2 concentration differences between urban and rural sites will increase in the non-photosynthesizing months of the year (i.e. winter).

These relatively small increases in fossil-fuel CO_2 are not enough to fully explain the increased plant growth in the city. FACE systems have mainly explored concentration ranges from 475-600 ppm (Ainsworth and Long, 2005); mostly exceeding current CO_2 levels by over 100 ppm. As mentioned before, diurnal temperature and ozone also play a crucial role in plant development in an anthropogenically changing world. It is evident that there is a larger temperature difference between urban and rural sites during the night than during the day, suggesting this signal may have a larger effect on plant growth (Figures 21-24 and Tables 11-14; discussed below). Although ozone concentration data was not collected here, more ozone monitoring needs to be done at a smaller spatial scales than is currently available. Most of the ozone monitoring has been done by the

United States Environmental Protection Agency (U.S. EPA) on a relatively sparse network (Figure 25) making an interpretation of these data difficult.

There are several hypotheses as to why the data from 1951 until about the 1980's seem to be irregular (Figure 10). The first possibility would be sample preparation and laboratory error (associated with ^{13}C and ^{14}C analysis). However, it seems unlikely however, since all samples were treated the same and thus this type of error should lead to uniform error throughout and not specific to the time period in question.

Secondly, unfortunately the width of each ring was not measured before preparing the samples. Thus, within each 10-year period, if a particular year had more growth this would have created a measurement bias toward the year which has more biomass. The time period in question was during the bomb spike and thus ^{14}C content from year to year was highly variable. More biomass from a particular year could thus produce a pronounced bias compared to other 10-year averages. After the 1980's, ^{14}C was declining, but at a slow consistent rate that was much less variable.

Third, soil respiration has a potential to play a large part in error. The age of the carbon in the soil that is released through both autotrophic and heterotrophic respiration can be on timescales of years to decades (Trumbore et al., 1996). Due to the magnification ^{14}C difference from year to year during the bomb spike, the soil is cycling back older carbon could be either emitting carbon depleted or highly enriched in ^{14}C, dependent on which years the comparison is done on. Therefore a photosynthesizing tree in the area would absorb the local air ^{14}C signal potentially caused by soil respiration and thus create a bias measurement.

Fourth, as discussed in the Methods section above, three different "clean" records were used to construct the background ^{14}C record. Perhaps the C-14 was not equally distributed (globally, on shorter time scales) since the nuclear weapons testing occurred in specific locations and at specific times around the world and the United States (Beck and Bennettt, 2002). Thus, during the period of weapons testing, the Northern European sites that were utilized to create the clean background signal may not be similar to the Northeastern United States. A way to resolve this would be to find a clean tree core from this area, which for this project, could be the AR core. However, as discussed earlier, this record does not go back far enough in time and it still may be subject to fossil-fuel influence, tree ring year bias and soil respiration. Still if this record were to be used, the average differences between the sites would be approximately 3 ppm lower than the initial estimates given above (resulting in 12, 5 and 2 ppm increases above the ambient background at CP, LDEO and BRF respectively). These estimates are similar and consistent with the single year estimates from the *X. strumarium* leaves.

Fifth, the development of cities, road and freeways in the New York City greater area as well as upstate New York could have some influence over atmospheric ^{14}C concentration. For example, Palisades Parkway was built from 1947-1958 (www.nycroads.com, 2009). This increased ease of transportation brought more vehicles which emitted ^{14}C-free gases into the more traditionally rural atmosphere in upstate New York. Similarly, the construction of the Lamont-Doherty Earth Observatory campus of Columbia University, the location of the LDEO site, also began during this time (LDEO, 2009).

Sixth, the biosphere and oceanic influences mentioned above in the Methods section could be affecting these points; however, as discussed above, they seem to have less than a 1‰ biospheric/oceanic enrichment influence in the Northeastern U.S. area under present (2006) atmospheric conditions (Hsueh et al., 2007). A combination of these six reasons is also a possibility. More analysis is needed to elucidate which, if any of these reasons may have caused this unexpected trend in the tree core data.

To compare this study with the previous findings of Cain (1975) (Table 15) the Bear Mountain (BM) results of Cain were compared to BRF, the closest site in the current study (BRF is approximately 25 km north of BM). The CP measurements of Cain (1975) are more depleted than those reported in this study's; the maximum difference is 25.7‰ for the years 1931-1940. It is uncertain as to what is causing this discrepancy, but it is possible the dating methods by Cain or any of the reasons explained above could have caused these differences. Interestingly, for the BRF and Bear Mountain comparison, the opposite occurs. The measurements for BRF are more depleted than Bear Mountain, with the maximum difference being 61.9‰ for the years 1951-1960. Since this is during the time period of rapid and dramatic ^{14}C increase, several of the reasons stated above may be at play here. The only means of deciphering these numbers would require more replicate measurements. Despite these differences, Cain's (1975) data still show that CP has on average 15 ppm increase of fossil fuel for the year 1900 until 1970 demonstrating agreement with current findings. However, BM showed a 1 ppm decrease compared to the Mauna Loa and Siple Ice Core records, indicating that this site was very clean.

4.3. Meteorology Stations

On an annual scale, the 2007 Harlem and LDEO CO_2 concentrations are quite similar in the summer and then diverge as winter approaches in 2007; LDEO concentration remains relatively constant, while the Harlem site shows an increase in atmospheric CO_2. A similar trend seems to hold true for 2008 and 2009 with the addition of BRF and AR (2008 only) sites. Interestingly in 2008, Norwalk shows a large CO_2 increase in mid-October and this trend continues well into 2009. One potential problem is that the CO_2 measuring instrument was replaced in mid October and this suggests therefore that a calibration error may have lead to an underestimation of the ambient CO_2 concentration at this site. Similarly in 2009 the temperature measurements from the Harlem station were defective from May 16th onward. In order to calculate the dry Harlem CO_2 data, temperatures from CP was used from that time onward. These data are problematic since the CP temperature data were recorded on a different logging interval and thus required approximation. Also, sometime prior to early May (Julian Day: ~125), the sampling pump at the Harlem site became loose, potentially compromising the data quality.

Seasonal and daily CO_2 concentrations can vary considerably between the urban and rural sites (Figure 26). In the winter, the average CO_2 concentration was 432.2 and 401.6 ppm for Harlem and LDEO respectively. In the summer, the average CO_2 concentration was 399.0 and 385.3 ppm for Harlem and LDEO respectively. The effects of photosynthesis are obvious during the daylight summer months in both Harlem and LDEO, with a more pronounced effect for LDEO. The Harlem record shows an indication of the morning traffic hour signal in both seasons. Winter and summer nighttime hours seem to be quite similar at LDEO while Harlem shows an elevated CO_2 in the winter in comparison to Summer night hours. These trends suggest that without the moderating effect of photosynthesis during the growing season, human activities can dramatically increase localized urban CO_2 levels, especially in the winter.

As predicted, wind speed and solar radiation play an important role in controlling the local CO_2 concentration, and CO_2 seem to be inversely related to these meteorological indices much of the time (Figures 27 and 28). This indicates that winds and meteorological factors play a more important effect in the winter (Figure 27) while solar radiation via its effect on photosynthesis plays a more important effect in the summer (Figure 28). Rain can have a substantial effect on CO_2 as well reducing the variation in the ambient concentrations (Figure 29). For example in Harlem, during the time period of August to September of 2008, the days without rain events have CO_2 concentrations that vary between 360 – 480 ppm. However during the more intense rain storms, the range of CO_2 concentrations is confined near 380 ppm. The observations suggest that rain tends to mix the atmospheric boundary layer and prevent CO_2 from building up.

The winds coming into New York City (both Harlem and CP) carries air with a signature of CO_2 in rural areas to the north and west [Harlem NW and N = ~408 ppm vs. Harlem SE = 429 ppm (maximum CO_2 concentration)]. This aids in flushing out much of the CO_2 that accumulates from point sources in the city (Figure 14 and 15). Interestingly, CP shows a relatively uniform CO_2 concentration from all directions. Perhaps the moderating effect of the photosynthesis from the surrounding trees explains these trends. However, a full year of data will be needed to understand this particular microclimate. LDEO sees a signal of New York City (to the Southeast; as high as 404.2 ppm) as well as the surrounding smaller cities and suburban areas to the Southwest (as high as 406.1 ppm; Figure 16). The northern and some southeastern direction of the winds in Piermont bring air from relatively clean areas from the north and suburban influence from the southeast (Figure 17). BRF seem to receive an increase in CO_2 levels from the south (~400 ppm) and since the vast majority of the winds arrive from the south, this would substantially influence overall CO_2 concentrations (Figure 18). This may be the influence of traffic from route 9W which runs through a valley to the South of the monitoring station. For AR (Figure 19), it would seem that this site would receive air from the relatively clean Catskills to the north, however, northern winds are most polluted (as high as 406.9 ppm), and is possibly a CO_2 signal coming from Albany, NY, located approximately 100 km to the north-northeast. AR also seems to be receiving some polluted air from the Northeast where a sizeable city Kingston lies. It is unclear if this overall pattern would hold for the entire year since data was only collected for a portion of the summer in 2008. However if this trend holds, it would impact the interpretation and possible use of the AR tree ring record as the clean background sources as discussed above. Norwalk's directional CO_2 concentrations are more uniform (Figure 20); however, the slightly higher CO_2 concentrations come from the west and northeast. Westerly winds (containing CO_2 as high as 390.4 ppm) may be from NYC and New Jersey, while the northeastern signal (as high as 398.8 ppm) could be from New Haven and Hartford, CT, located 55 km and 115 km northeast respectively.

Temperature differences could have a prominent effect on plant physiology. As mentioned above, high nighttime temperatures have been shown to increase respiration and thus photosynthetic capacity the following day (Turnbull et al., 2002). Canopy layers, seasonality, soil water availability, leaf properties (nitrogen content, specific leaf area and sugars) and pre-existing vs. newly emerged leaves all have had different respiration responses to increases in nighttime temperature (Griffin et al., 2002; Xu and Griffin, 2006 and Ow et al., 2008). There can be considerable temperature differences between urban and rural areas and thus it is logical to expect complex physiological responses. Harlem and CP are only 4.5 km from each other, yet they have dramatically different microclimates; Harlem being surrounded by buildings while CP is mostly forested. From 2006 to 2009, the average differences between the sites during the day spanned anywhere from 0.95 to 2.37 °C while at night, the differences ranged from 1.48 to 3.19 °C (Tables 11-14). For other sites in comparison to Harlem in 2008, LDEO, BRF and AR had an average night difference of 5.21, 5.95 and 3.75 °C difference (Table 13) respectively. Although these current differences in temperature are not as large as many experimental treatments in the studies mentioned above, trends from the past few decades seem to point towards increasing differences of temperature in the future (Georgescu et al., 2009).

Overall, data from LACOP shows that the New York City CO_2 concentrations can be as low as rural areas depending on the season, time of day and weather patterns. This may be due to the unique coastal location of New York City. However for the most part, average CO_2 concentrations in the city are higher. In general, studies that have investigated urban CO_2 concentrations support our findings. Urban areas around the world show a seasonal cycle with a maximum in the winter and a daily variation of a daytime afternoon minimum during the growing season and maximum in the early morning (Table 10). And although the general pattern is present in all cities, variations in the temporal and spatial CO_2 concentrations differ slightly (see Grimmond et al., 2002 and Table 2). Each is unique to the meteorological conditions, natural ecology (e.g. photosynthetic capacity, length of growing season etc…) and local temporal and spatial anthropogenic emission patterns of the area.

Our results are in agreement with Woodwell (1973) where fluctuations in CO_2 follow a pronounced diurnal, seasonal trend and also related to wind direction as well. However, while the authors detected changes as much as 50 ppm, the urban (Harlem) site changed as much as 110.1 ppm (February 13, 2008; ~9:30 am) within the span of a logging interval (15 minutes), suggesting that variations in CO_2 can become increasingly variable as more emissions are produced. The authors' winter/summer difference in CO_2 concentrations at 125 m above ground is 19 ppm; in comparison to LACOP, both urban and rural sites show a greater difference (Figure 26). The variation can be as large as 43 ppm for urban sites and 31 ppm (during the daylight hours) for more rural sites.

Data from LACOP are purely observational and the causes of the elevated CO_2 concentrations observed can not be determined with certainty. There are many factors that influence CO_2 concentrations and it is hard to determine if one is more influential than the others. All of the factors mentioned, including solar radiation, wind speed, cloud cover, seasonal variations, and plant and anthropogenic activities are intertwined to affect the air quality. Based on the data collected, it can not be determined if a site's CO_2 concentration is due to the density of trees in an area vs. proximity to an urban/rural area. Furthermore, the origin of the increased carbon can not be determined or separated into sources, from respiring plants or fossil fuel emissions. Further studies could be conducted with stable isotope (^{13}C and ^{18}O) measurements to better constrain these potential sources of atmospheric CO_2 (e.g. Zondervan and Meijer, 1996, Kuc and Zimnoch, 1998; Pataki et al., 2003a). The precise placement of the MET station (rooftop or ground level at the same coordinates) could also possibly influence the measured CO_2 concentrations depending on the location and environmental conditions (night/day; wind and solar radiation conditions) which themselves are dynamic. Furthermore, high-winds are positively correlated with low stomatal conductance which could translate to lower rates of CO_2 assimilation and photosynthesis, further complicating the interpretation of these results (e.g. Freeman et al., 1982). Despite these limitations, our main focus here is simply quantifying the urban and rural CO_2 conditions in light of the environmental conditions affecting plant growth. Clearly the unique characteristics of the NYC location and microclimate result in relatively low CO_2 concentrations (close to ambient) and therefore are unlikely to be the cause of increased plant growth in the city (e.g. Gregg et al., 2003). In this respect, NYC may be unique as some other large urban centers such as Baltimore and Phoenix have all reported higher levels of anthropogenically derived local CO_2 enhancements (George et al., 2007; Isdo et al., 2001). It is not possible to confirm that O_3 is the only culprit in increased urban plant growth without additional data measured in smaller spatial scales. Furthermore, DTR data presented here warrants further investigation on temperature effect on urban and rural plant growth.

5. Conclusion, Future Work and Implications

From the tree core data, CP shows a clear lead in the most added fossil-fuel CO_2 site, followed by LDEO, BRF and AR. At a finer temporal scale, the overall trend remains constant, however there are instances where urban CO_2 can be as low as rural CO_2 (ex. summer at night), depending on the season and meteorological conditions of the region.

Fossil fuel emissions are expected to increase, despite any agreements that come out of Copenhagen in December 2009. Thus gradients of both ^{14}C and ambient CO_2 concentrations are projected to become amplified. However, in the next few decades, overall ^{14}C levels in the atmosphere are expected to arrive at a minimum shortly and then start to increase. Ironically, this is because of the amount of fossil fuel we emit into our atmosphere will lessen the flux of ^{14}C into the oceans allowing ^{14}C to accumulate in the atmosphere (Caldeira et al., 1998). Monitoring "natural" abundances of ^{14}C is important for ecosystem ecologists who use radiocarbon as a tracer.

Future work needs to include ^{14}C analysis from every year during the period of the bomb spike (1950-1970) to elucidate that time period and clear up any discrepancies. For LACOP, the use of stable isotopes such as ^{13}C and ^{18}O should be helpful in elucidating the source of the carbon, be it respiring plants or fossil fuel emissions. Other combustion products such as carbon monoxide (CO) and acetylene (C_2H_2) may also provide very good correlations for CO_2 (e.g. Potosnak, 1999). A system placed on the side of a building could be used to measure CO_2 concentrations at different heights to assess how CO_2 concentrations differ with altitude in the various urban and rural settings. A canopy model could be generated to look at the effects of diurnal variation of CO_2, temperature and light on photosynthesis. Measurements of other factors that are tied to air quality such as ozone and particulate pollution can be useful to compare to CO_2 concentrations.

There are several implications for monitoring past and present CO_2 concentrations, especially with LACOP. This network can be used to study the basic physics, biology and chemistry in the environment and how it relates to climate change, the urban CO_2 dome and anthropogenic influence on plant physiology. Furthermore, the continuous CO_2 concentration measurements produce a baseline before any CO_2-reducing policies are passed and thus could be used to assess the effectiveness of these policies (e.g. Mayor Bloomberg's PlaNYC initiatives such as Million-Trees and future congestion pricing proposals). Using different forecasted weather indices, modeling future CO_2 concentrations for up to 24 hour periods in advance may also be possible. These data could be compared with Carbon Tracker. LACOP also has potential in partnering with educational institutions to educate the next generation and the public about air quality, sustainability and climate change.

***

Acknowledgements

I have been indebted to many during the course of this work. I would like to especially thank my three advisors, Kevin L. Griffin, Wade R. McGillis and Matthew Palmer for advising me throughout my work.

I would like to thank those who have assisted me in some capacity during field, lab work and/or feedback on this project:
William Schuster and Matthew Munson at Black Rock Forest
Brendan Buckley, William Wright and Dan Stahle from the Tree Ring Lab at LDEO
Matthew Brown at the Central Park Conservancy
Christa Brelsford, Arturo Ilano, Maxwell Martin, Yun Zheng, Stephanie Searle, EB Tupper, Acadia Roher, Sam Thomas, Charlene Lee, Jennifer Levy, Nicholas Mirotchnick, Miriam Marlier, Mary Heskel and Natalie Boelman

And to those who assisted me with invaluable advice in regards to the radiocarbon laboratory work: Wallace S. Broecker, Susan E. Trumbore, Xiaomei Xu, John R. Southon, James T. Randerson and Diane E. Pataki.

And for site logistics:
National Oceanic and Atmospheric Administration (NOAA): National Weather Service and the Future Leaders Institute Elementary School

The radiocarbon analysis was carried out with grants from the Comer Science and Education Foundation and Lamont Climate Center

Additional financial assistance for LACOP was provided by:
HSBC in the Community (USA) Inc.
Betsy and Jesse Fink Foundation
Frank and Joanne Gumper

To my extraordinary classmates and friends who have been my constant anchor throughout my time spent at Columbia University.

Last, but definitely not least, I want to thank my family and especially my loving parents who have helped me immeasurably throughout my life to get me where I am today.

References

Ainsworth, E. A., and S. P. Long (2005), What have we learned from 15 years of free-air CO_2 enrichment (FACE)? A meta-analytic review of the responses of photosynthesis, canopy, *New Phytologist*, *165*(2), 351-371.

Barnes, R. L. (1972), Effects of chronic exposure to ozone on photosynthesis and respiration of pines, *Environ. Pollut.*, *3*, 133-138.

Beck, H. L., and B. G. Bennett (2002), Historical overview of atmospheric nuclear weapons testing and estimates of fallout in the continental United States, *Health Physics*, *82*(5), 591-608.

Becker, B., and B. Kromer (1993), The Continental Tree-Ring Record - Absolute Chronology, C-14 Calibration and Climatic-Change at 11 Ka, *Palaeogeography Palaeoclimatology Palaeoecology*, *103*(1-2), 67-71.

Berry, R. D., and J. J. Colls (1990a), Atmospheric Carbon-Dioxide and Sulfur-Dioxide on an Urban Rural Transect 1. continuous measurements at the Transect Ends, *Atmospheric Environment Part a-General Topics*, *24*(10), 2681-2688.

Berry, R. D., and J. J. Colls (1990b), Atmospheric Carbon-Dioxide and Sulfur-Dioxide on an Urban Rural Transect 2. Measurements along the Transect, *Atmospheric Environment Part a-General Topics*, *24*(10), 2689-2694.

Bonhomme, N., and J. Zahringe (1969), Paleomagnetism and Potassium Argon Age Determinations of Laschamp Geomagnetic Polarity Event, *Earth and Planetary Science Letters*, *6*(1), 43-46.

Broecker, W. S. (2003), Radiocarbon, in *Treatis on Geochemistry: Surface and Ground Water, Weathering, and Soils*, edited by J. I. Drever, et al., pp. 245-260, Elsevier Science, Amsterdam, The Netherlands.

Broecker, W. S., et al. (1980), Modeling the Carbon System, *Radiocarbon*, *22*(3), 565-598.

Broecker, W. S., et al. (1985), The Distribution of Bomb Radiocarbon in the Ocean, *Journal of Geophysical Research-Oceans*, *90*(NC4), 6953-6970.

Broecker, W. S., et al. (1990), The Distribution of Radiocarbon in the Glacial Ocean, *Global Biogeochemical Cycles*, *9*, 263-288.

Buchwitz, M., et al. (2007), First direct observation of the atmospheric CO_2 year-to-year increase from space, *Atmospheric Chemistry and Physics*, *7*(16), 4249-4256.

Cain, W. F. (1975), Carbon-14 in Tree Rings of Twentieth Century America, Ph.D. thesis, University of California, San Diego, United States -- California.

Caldeira, K., et al. (1998), Predicted net efflux of radiocarbon from the ocean and increase in atmospheric radiocarbon content, *Geophysical Research Letters*, *25*(20), 3811-3814.

Canadell, J. G., et al. (2007), Contributions to accelerating atmospheric CO_2 growth from economic activity, carbon intensity, and efficiency of natural sinks, *Proceedings of the National Academy of Sciences of the United States of America*, *104*(47), 18866-18870.

Carbone, M. S., et al. (2007), Allocation and residence time of photosynthetic products in a boreal forest using a low-level C-14 pulse-chase labeling technique, *Glob. Change Biol.*, *13*(2), 466-477.

Cherubini, P. (2000), Tree-ring research beyond the climate change: “Quo vadis?” *Dendrochronologia*, *18*, 91-93.

Clarke, J. F., and R. B. Faoro (1966), An evaluation of CO_2 measurements as an indicator of air pollution, *J. Air Pollut. Control Assessment*, *16*, 212-218.

Clarke, J. F., and R. B. Faoro (1966), An evaluation of CO_2 measurements as an indicator of air pollution, *J. Air Pollut. Control Assessment*, *16*, 212-218.

Coutts, A. M., et al. (2007), Characteristics influencing the variability of urban CO_2 fluxes in Melbourne, Australia, *Atmospheric Environment*, *41*(1), 51-62.

Day, T. A., et al. (2002), Temporal patterns in near-surface CO_2 concentrations over contrasting vegetation types in the Phoenix metropolitan area, *Agricultural and Forest Meteorology*, *110*(3), 229-245.

DEC (2009). Retrieved October, 2009, from http://www.dec.ny.gov/chemical/29992.html.

Derwent, R. G., et al. (1995), Analysis and Interpretation of Air-Quality Data from an Urban Roadside Location in Central London over the Period from July 1991 to July 1992, *Atmospheric Environment*, *29*(8), 923-946.

Drake, B. G., et al. (1997), More efficient plants: a consequence of rising atmospheric CO_2?, *Annual Review of Plant Physiology and Plant Molecular Biology*, *48*, 609-639.

Easterling, D. R., et al. (1997), Maximum and minimum temperature trends for the globe, *Science*, *277*(5324), 364-367.

Farquhar, G. D., and R. A. Richards (1984), Isotopic Composition of Plant Carbon Correlates with Water-Use Efficiency of Wheat Genotypes, *Australian Journal of Plant Physiology*, *11*(6), 539-552.

Farquhar, G. D., et al. (1989), Carbon Isotope Discrimination and Photosynthesis, *Annual Review of Plant Physiology and Plant Molecular Biology*, *40*, 503-537.

Flatau, P. J., et al. (1992), Polynomial Fits to Saturation Vapor-Pressure, *Journal of Applied Meteorology*, *31*(12), 1507-1513.

Freeman, B. M., et al. (1982), Influence of Windbreaks and Climatic Region on Diurnal Fluctuation of Leaf Water Potential, Stomatal Conductance, and Leaf Temperature of Grapevines, *American Journal of Enology and Viticulture*, *33*(4), 233-236.

Fridovich, I. (1986), Biological effects of the superoxide radical, *Archives of Biochemistry and Biophysics*, *247*(1), 1-11.

Friedli, H., et al. (1986), Ice Core Record of the C-13/C-12 Ration of Atmospheric CO_2 in the Past 2 Centuries, *Nature*, *324*(6094), 237-238.

Friedrich, M., et al. (1999), Paleo-environment and radiocarbon calibration as derived from Lateglacial/Early Holocene tree-ring chronologies, *Quaternary International*, *61*, 27-39.

Gaggeler, H. W. (1995), Radioactivity in the atmosphere, *Radiochimica Acta*, *70-1*, 345-353.

Gatz, D. F. (1991), Urban Precipitation Chemistry - A Review and Synthesis, *Atmospheric Environment Part B-Urban Atmosphere*, *25*(1), 1-15.

Gaudinski, J. B., et al. (2001), The age of fine-root carbon in three forests of the eastern United States measured by radiocarbon, *Oecologia*, *129*(3), 420-429.

George, K., et al. (2007), Elevated atmospheric CO_2 concentration and temperature across an urban-rural transect, *Atmospheric Environment*, *41*(35), 7654-7665.

Georgescu, M., et al. (2009), Climatic effects of 30 years of landscape change over the Greater Phoenix, Arizona, region: 1. Surface energy budget changes, *Journal of Geophysical Research-Atmospheres*, *114*, 17.

Gregg, J. W. (1999), The Effect of Urban Compared to Rural Environments on Plant Growth in the Vicinity of New York City: The Net Response and the Relative Importance of the Different Pollutants, Dissertation thesis, 197 pp, Cornell University, Ithaca, NY.

Gregg, J. W., et al. (2003), Urbanization effects on tree growth in the vicinity of New York City, *Nature*, *424*(6945), 183-187.

Griffin, K. L., et al. (2002), Canopy position affects the temperature response of leaf respiration in Populus deltoides, *New Phytologist*, *154*(3), 609-619.

Grimmond, C. S. B., et al. (2002), Local-scale fluxes of carbon dioxide in urban environments: methodological challenges and results from Chicago, *Environmental Pollution*, *116*, S243-S254.

Guderian, R., et al. (1985), Effects of photochemical oxidants on plants, *Air Pollution by Photochemical Oxidants*, 129-333.

Halliwell, B., and M. C. Gutteridge (1985), Free radicals in biology and medicine, *Oxford University Press, Oxford*.

Henninger, S., and W. Kuttler (2007), Methodology for mobile measurements of carbon dioxide within the urban canopy layer, *Climate Research*, *34*(2), 161-167.

Hesshaimer, V., and I. Levin (2000), Revision of the stratospheric bomb (CO_2)-C-14 inventory, *Journal of Geophysical Research-Atmospheres*, *105*(D9), 11641-11658.

Hesshaimer, V., et al. (1994), Radiocarbon Evidence for a Smaller Oceanic Carbon-Dioxide Sink than Previous Believed, *Nature*, *370*(6486), 201-203.

Hsueh, D. Y., et al. (2007), Regional patterns of radiocarbon and fossil fuel-derived CO_2 in surface air across North America, *Geophysical Research Letters*, *34*(2).

Hughen, K. A., et al. (1998), Deglacial changes in ocean circulation from an extended radiocarbon calibration, *Nature*, *391*(6662), 65-68.

Idso, C. D., et al. (2001), An intensive two-week study of an urban CO_2 dome in Phoenix, Arizona, USA, *Atmospheric Environment*, *35*(6), 995-1000.

IPCC (2007a), IPCC in Climate Change 2007: The Physical Science Basis, Cambridge, UK.

IPCC (2007b), Summary for Policymakers, 22 pp, Fourth Assessment Report of the Intergovernmental Panel on Climate Change, Cambridge, UK.

JAXA. (2009). "Greenhouse gases Observing SATellite "IBUKI"(GOSAT)." Retrieved June, 2009, from http://www.jaxa.jp/projects/sat/gosat/index_e.html.

Keeling, C. D., and T. P. Whorf (2002), Monthly Atmospheric $^{13}C/^{12}C$ Isotopic Ratios for 10 SIO Stations, edited, Carbon Dioxide Information Analysis Center (CDIAC); Oak Ridge National Laboratory, Oak Ridge, TN.

Keeling, C. D., et al. (1976), Atmospheric Carbon-Dioxide Variation at Mauna-Loa Observatory, Hawaii, *Tellus*, *28*(6), 538-551.

Kintisch, E. (2009), EARTH MONITORING Loss of Carbon Observatory Highlights Gaps in Data, *Science*, *323*(5919), 1276-1277.

Knepp, R. G., et al. (2007), Foliage of oaks grown under elevated CO_2 reduces performance of Antheraea polyphemus (Lepidoptera : Saturniidae), *Environmental Entomology*, *36*(3), 609-617.

Kromer, B., and M. Spurk (1998), Revision and tentative extension of the tree-ring based C-14 calibration, 9200-11,855 cal BP, *Radiocarbon*, *40*(3), 1117-1125.

Kromer, B., et al. (1986), Radiocarbon Calibration Data for the 6th to the 8th Millennia BC, *Radiocarbon*, *28*(2B), 954-960.

Kuc, T., and M. Zimnoch (1998), Changes of the CO_2 sources and sinks in a polluted urban area (southern Poland) over the last decade, derived from the carbon isotope composition.

Kudish, M. (2000), *The Catskill Forest: A History*, 217 pp., Purple Mountain Pr Ltd.

Lambers, H., et al. (1998), *Plant Physiological Ecology*, 540 pp., Springer-Verlag, New York, NY.

LDEO. (2009). "History of Lamont." Retrieved October, 2009, from http://www.ldeo.columbia.edu/about-ldeo/history-lamont-0.

Leakey, A. D. B., et al. (2004), Will photosynthesis of maize (Zea mays) in the US Corn Belt increase in future [CO_2] rich atmospheres? An analysis of diurnal courses of CO_2 uptake under free-air concentration enrichment (FACE), *Glob. Change Biol.*, *10*(6), 951-962.

Leakey, A. D. B., et al. (2006), Photosynthesis, productivity, and yield of maize are not affected by open-air elevation of CO_2 concentration in the absence of drought, *Plant Physiology*, *140*(2), 779-790.

Lee, T. T. (1967), Inhibition of oxidative phosphorylation and respiration by ozone in tobacco mitochondria, *Plant Physiol.*, *42*, 91-696.

Levin, I., and B. Kromer (2004), The tropospheric (CO_2)-C-14 level in mid-latitudes of the Northern Hemisphere (1959-2003), *Radiocarbon*, *46*(3), 1261-1272.

Levin, I., et al. (1980), The Effect of Anthropogenic CO_2 and C-14 sources on the Distribution of C-14 in the Atmosphere, *Radiocarbon*, *22*(2), 379-391.

Libby, W. F., et al. (1949), Age Determination by Radiocarbon Content - World-Wide Assay of Natural Radiocarbon, *Science*, *109*(2827), 227-228.

Lingenfelter, R. E. (1963), Production of Carbon-14 by Cosmic-ray Neutrons, *Reviews of Geophysics*, *1*(1), 35-55.

Lovett, G. M., et al. (2000), Atmospheric deposition to oak forests along an urban-rural gradient, *Environ. Sci. Technol.*, *34*(20), 4294-4300.

Marzaioli, F., et al. (2005), Reconstruction of past CO_2 concentration at a natural CO_2 vent site using radiocarbon dating of tree rings, *Radiocarbon*, *47*(2), 257-263.

Moriwaki, R., et al. (2006), Carbon dioxide build-up within a suburban canopy layer in winter night, *Atmospheric Environment*, *40*(8), 1394-1407.

Muller, R. A. (1977), Radioisotope Dating with a Cyclotron, *Science*, *196*(4289), 489-494.

Myster, J., and R. Moe (1995), Effect of Diurnal Temperature Alternations of Plant Morphology in some Greenhouse Crops - A Mini Review, *Scientia Horticulturae*, *62*(4), 205-215.

NOAA. (2009). "New York Cntrl Pk Twr: About this Station." Retrieved March, 2009, from http://www4.ncdc.noaa.gov/cgi-win/wwcgi.dll?wwDI~StnSrch~StnID~20019453.

Norby, R. J., and Y. Q. Luo (2004), Evaluating ecosystem responses to rising atmospheric CO_2 and global warming in a multi-factor world, *New Phytologist*, *162*(2), 281-293.

Norby, R. J., et al. (2005), Forest response to elevated CO_2 is conserved across a broad range of productivity, *Proceedings of the National Academy of Sciences of the United States of America*, *102*(50), 18052-18056.

Nydal, R., and K. Lovseth (1983), Tracing Bomb C-14 in the Atmosphere 1962-1980, *Journal of Geophysical Research-Oceans and Atmospheres*, *88*(NC6), 3621-3642.

O’Leary, M. H. (1981), Carbon Isotope Fractionation in Plants, *Phytochemistry*, *20*(4), 553-567.

O'Leary, M. H. (1988), Carbon Isotopes in Photosynthesis, *Bioscience*, *38*(5), 328-336.

Ow, L. F., et al. (2008), Thermal acclimation of leaf respiration but not photosynthesis in Populus deltoides x nigra, *New Phytologist*, *178*(1), 123-134.

Pataki, D. E., et al. (2003a), Seasonal cycle of carbon dioxide and its isotopic composition in an urban atmosphere: Anthropogenic and biogenic effects, *Journal of Geophysical Research-Atmospheres*, *108*(D23).

Pataki, D. E., et al. (2003b), Tracing changes in ecosystem function under elevated carbon dioxide conditions, *Bioscience*, *53*(9), 805-818.

Pell, E. J., and E. Brennan (1973), Changes in respiration, photosynthesis, adenosin 5'-triphosphate and total adenylate content of ozonated pinto bean foliage as they relate to synptom expression, *Plant Physiol.*, *51*, 378-381.

Peters, W., et al. (2007), An atmospheric perspective on North American carbon dioxide exchange: CarbonTracker, *Proceedings of the National Academy of Sciences of the United States of America*, *104*(48), 18925-18930.

Potosnak, M. J., et al. (1999), Influence of biotic exchange and combustion sources on atmospheric CO_2 concentrations in New England from observations at a forest flux tower, *Journal of Geophysical Research-Atmospheres*, *104*(D8), 9561-9569.

Pouyat, R. V., et al. (1995), Soil Characteristics of Oak Stands along an Urban-Rural Land-Use Gradient, *Journal of Environmental Quality*, *24*(3), 516-526.

Pouyat, R. V., et al. (2008), Response of forest soil properties to urbanization gradients in three metropolitan areas, *Landsc. Ecol.*, *23*(10), 1187-1203.

Price, J. C. (1979), Assessment of the Urban Heat Island Effect through the use of Satellite Data, *Mon. Weather Rev.*, *107*(11), 1554-1557.

Randerson, J. T., et al. (2002), Seasonal and latitudinal variability of troposphere Delta(CO_2)-C-14: Post bomb contributions from fossil fuels, oceans, the stratosphere, and the terrestrial biosphere, *Global Biogeochemical Cycles*, *16*(4).

Reid, K. H., and D. G. Steyn (1997), Diurnal variations of boundary-layer carbon dioxide in a coastal city - Observations and comparison with model results, *Atmospheric Environment*, *31*(18), 3101-3114.

Reimer, P. J., et al. (2004), IntCal04 terrestrial radiocarbon age calibration, 0-26 cal kyr BP, *Radiocarbon*, *46*(3), 1029-1058.

Rigby, M., et al. (2008), First continuous measurements of CO2 mixing ratio in central London using a compact diffusion probe, *Atmospheric Environment*, *42*(39), 8943-8953.

Riley, W. J., et al. (2008), Where do fossil fuel carbon dioxide emissions from California go? An analysis based on radiocarbon observations and an atmospheric transport model, *Journal of Geophysical Research-Biogeosciences*, *113*(G4).

Samuelson, L. J., and G. S. Edwards (1993), A Comparison of Sensitivity to Ozone in Seedlings and Trees of Quercus-Rubra L., *New Phytologist*, *125*(2), 373-379.

Searle, S. (2008), 2008 Transect Harvest Data, D. Hsueh.

Searle, S., et al. (2007), Proposed Causes and Mechanisms for Variation in Photosynthesis of Quercus rubra Along an Urban to Rural Gradient, *Columbia Undergraduate Science Journal*, *2*(1), 29-40.

Sethuraman, S. (1981), Carbon-Dioxide Fluxes over the Atlantic-Ocean Estimated from Measurements at Tiana Beach, Long Island, New York, *Bound.-Layer Meteor.*, *20*(1), 19-26.

Shackleton, N. J., et al. (1988), Radiocarbon Age of Last Glacial Pacific Deep-Water, *Nature*, *335*(6192), 708-711.

Shapiro, J. B., et al. (2004), Response of Xanthium strumarium leaf respiration in the light to elevated CO_2 concentration, nitrogen availability and temperature, *New Phytologist*, *162*(2), 377-386.

Stuiver, M., and H. A. Polach (1977), Reporting of C-14 Data - Discussion, *Radiocarbon*, *19*(3), 355-363.

Stuiver, M., and P. D. Quay (1980), Changes in Atmospheric C-14 attributed to a Variable Sun, *Science*, *207*(4426), 11-19.

Stuiver, M., and P. D. Quay (1981), Atmospheric C-14 changes resulting from Fossil-Fuel CO_2 release and Cosmic-Ray Flux Variability, *Earth and Planetary Science Letters*, *53*(3), 349-362.

Tans, P. P., et al. (1979), Natural Atmospheric C-14 Variation and the Suess Effect, *Nature*, *280*(5725), 826-827.

Thellier, E. (1977), Early Research on Intensity of Ancient Geomagnetic-Field, *Physics of the Earth and Planetary Interiors*, *13*(4), 241-244.

Trumbore, S. (2000), Age of soil organic matter and soil respiration: Radiocarbon constraints on belowground C dynamics, *Ecological Applications*, *10*(2), 399-411.

Trumbore, S. E., et al. (1996), Rapid exchange between soil carbon and atmospheric carbon dioxide driven by temperature change, *Science*, *272*(5260), 393-396.

Turnbull, J. C., et al. (2006), Comparison of (CO_2)-C-14, CO, and SF_6 as tracers for recently added fossil fuel CO_2 in the atmosphere and implications for biological CO_2 exchange, *Geophysical Research Letters*, *33*(1).

Turnbull, M. H., et al. (2002), The relative impacts of daytime and night-time warming on photosynthetic capacity in Populus deltoides, *Plant Cell Environ.*, *25*(12), 1729-1737.

UN (2008), Economic & Social Affairs: World Urbanization Prospects The 2007 Revision: Executive Summary, United Nations, New York.

Universiteit Utrecht (2009). "Radiocarbon Dating." Retrieved May, 2008, from http://www1.phys.uu.nl/ams/Radiocarbon.htm.

Velasco, E., et al. (2005), Measurements of CO_2 fluxes from the Mexico City urban landscape, *Atmospheric Environment*, *39*(38), 7433-7446.

Vogt, R., et al. (2006), Temporal dynamics of CO_2 fluxes and profiles over a central European city, *Theoretical and Applied Climatology*, *84*(1-3), 117-126.

Wang, X. Z., and P. Curtis (2002), A meta-analytical test of elevated CO_2 effects on plant respiration, *Plant Ecology*, *161*(2), 251-261.

Willkomm, H., and H. Erlenkeuser (1968), University of Kiel Radiocarbon Measurements III, *Radiocarbon*, *10*(2), 328-332.

Woodwell, G. M., et al. (1973), Atmospheric CO_2 at Brookhaven, Long Island, New York - Patterns of Variation up to 125 meters, *Journal of Geophysical Research*, *78*(6), 932-940.

www.nycroads.com. (2009). "Palisades Interstate Parkway: Historic Overview." Retrieved 2009, May, from http://www.nycroads.com/roads/palisades/.

Xu, C. Y., and K. L. Griffin (2006), Seasonal variation in the temperature response of leaf respiration in Quercus rubra: foliage respiration and leaf properties, *Funct. Ecol.*, *20*(5), 778-789.

Xu, X. M., et al. (2007), Modifying a sealed tube zinc reduction method for preparation of AMS graphite targets: Reducing background and attaining high precision, *Nuclear Instruments & Methods in Physics Research Section B-Beam Interactions with Materials and Atoms*, *259*(1), 320-329.

Yun, S. C., and J. A. Laurence (1999), The response of clones of Populus tremuloides differing in sensitivity to ozone in the field, *New Phytologist*, *141*(3), 411-421.

Zak, D. R., et al. (2000), Elevated atmospheric CO_2, fine roots and the response of soil microorganisms: a review and hypothesis, *New Phytologist*, *147*(1), 201-222.

Ziska, L. H., et al. (2009), Rising CO_2, Climate Change, and Public Health: Exploring the Links to Plant Biology, *Environmental Health Perspectives*, *117*(2), 155-158.

Zondervan, A., and H. A. J. Meijer (1996), Isotopic characterisation of CO_2 sources during regional pollution events using isotopic and radiocarbon analysis, *Tellus Ser. B-Chem. Phys. Meteorol.*, *48*(4), 601-612.

Figures

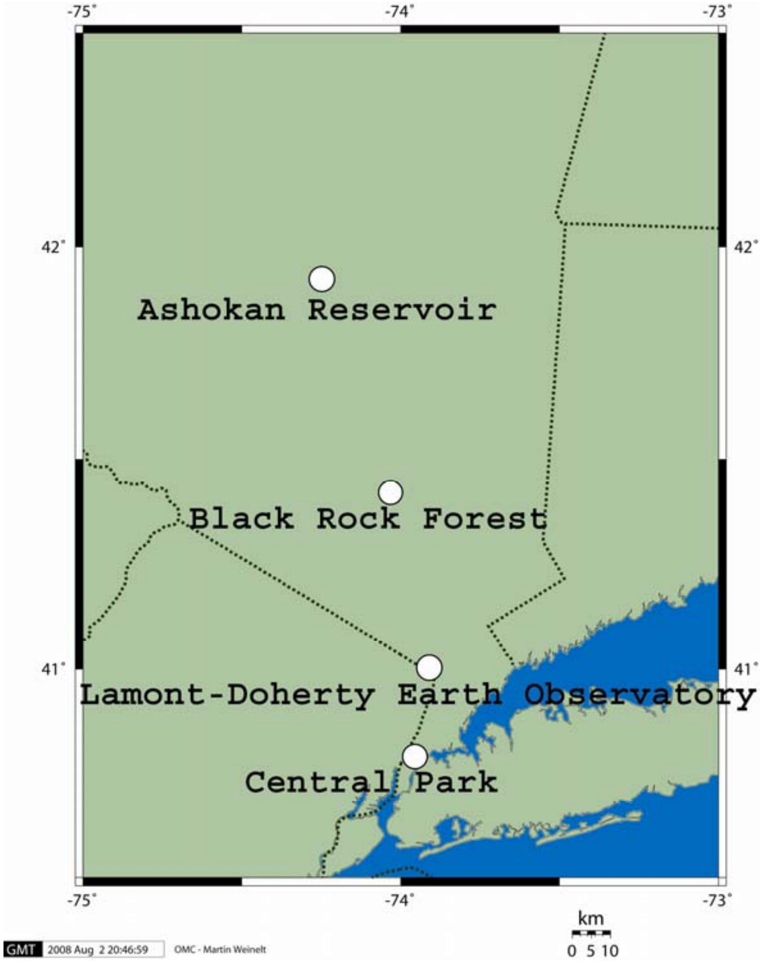

Figure 1. Locations of the sites from an urban to rural gradient extending out from New York City.

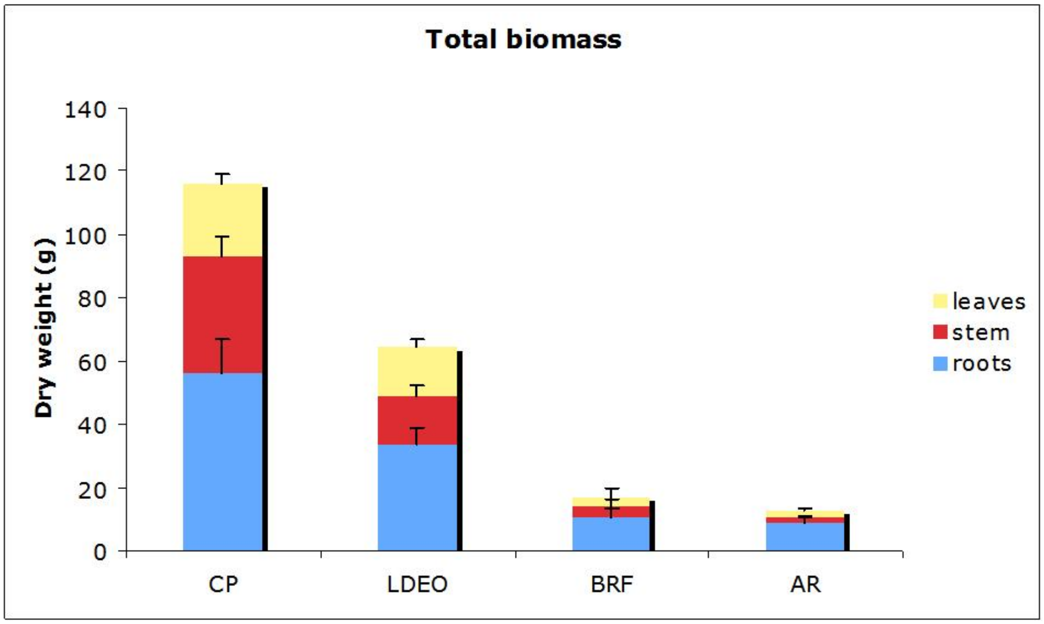

Figure 2. Total Biomass of *Quercus rubra* in the summer 2008 at sites Central Park (CP), Lamont-Doherty Earth Observatory (LDEO), Black Rock Forest (BRF) and Ashokan Reservoir (AR).

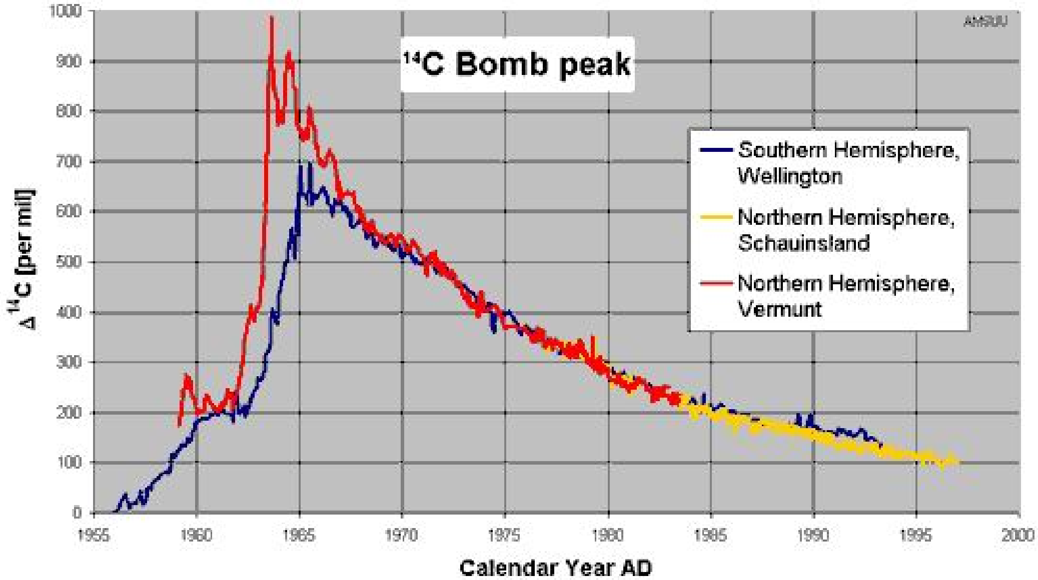

Figure 3. Radiocarbon measurements taken at three sites (Wellington, New Zealand; Schauinsland, Germany and Vermunt, Austria) that show the ^{14}C Bomb Peak in the mid-1900's. Observe the lag the Southern Hemisphere (Universiteit Utrecht, 2009)

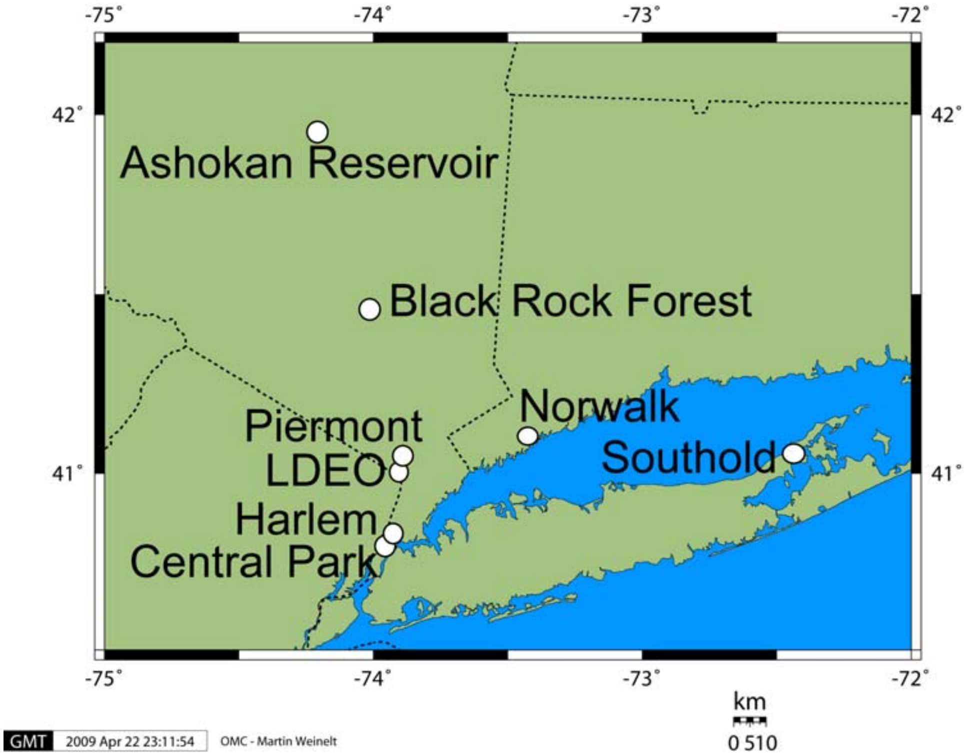

Figure 4. LACOP sites and the added Black Rock Forest (BRF) site

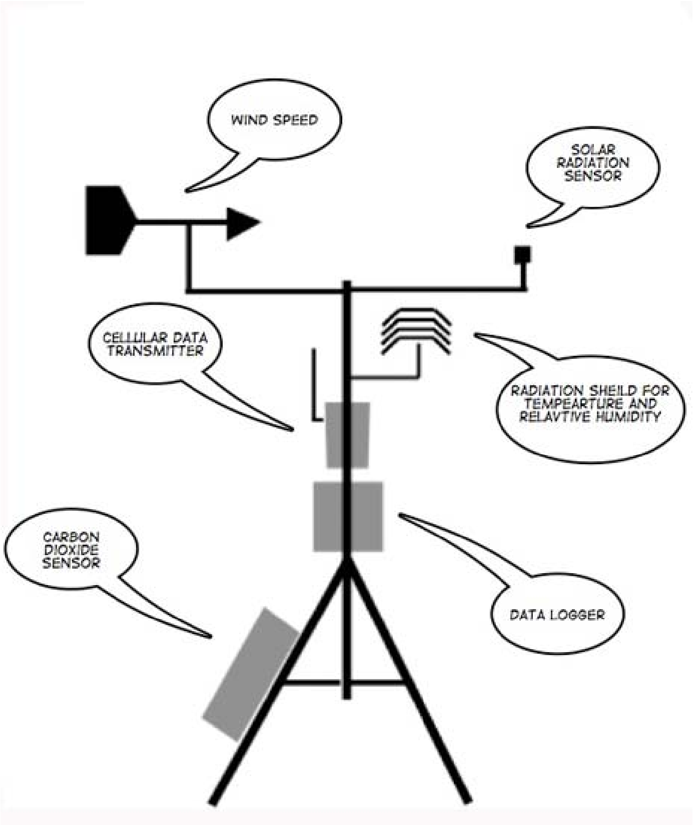

Figure 5. A graphic of a meteorological station: Taken from http://www.ldeo.columbia.edu/outr/LACOP/datacollection.html

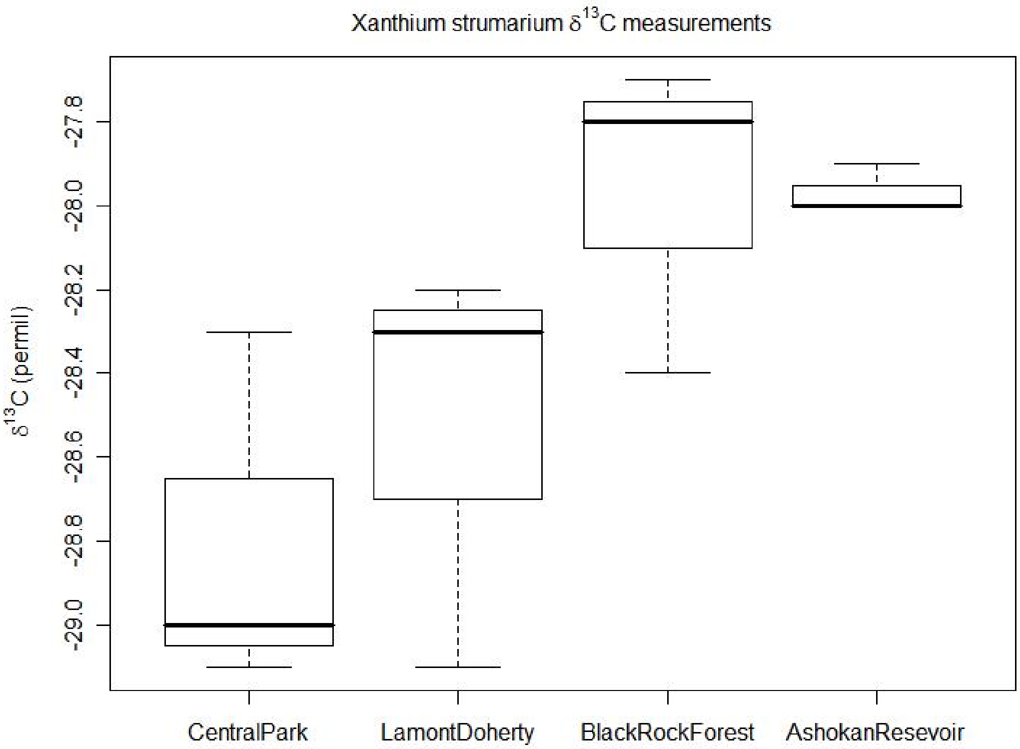

Figure 6. *Xanthium strumarium* δ^{13}C results for the sites CP, LDEO, BRF and AR

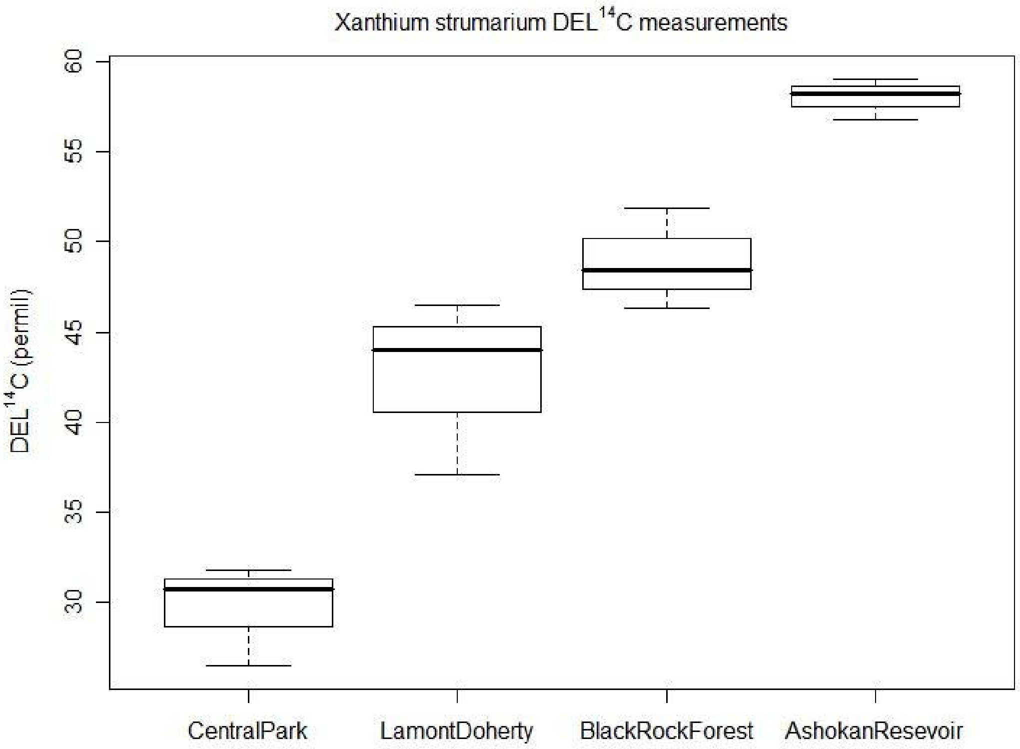

Figure 7. *Xanthium strumarium* Δ^{14}C results for the sites CP, LDEO, BRF and AR.

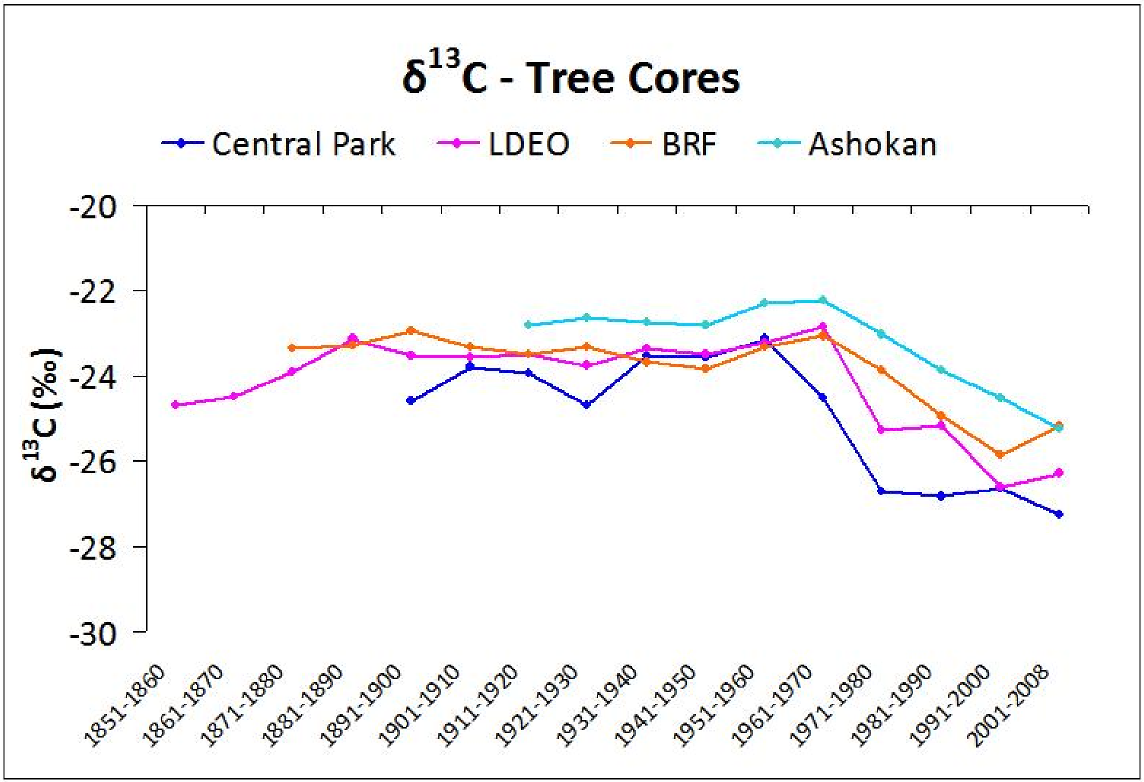

Figure 8. *Quercus rubra* δ^{13}C results for the sites CP, LDEO, BRF and AR

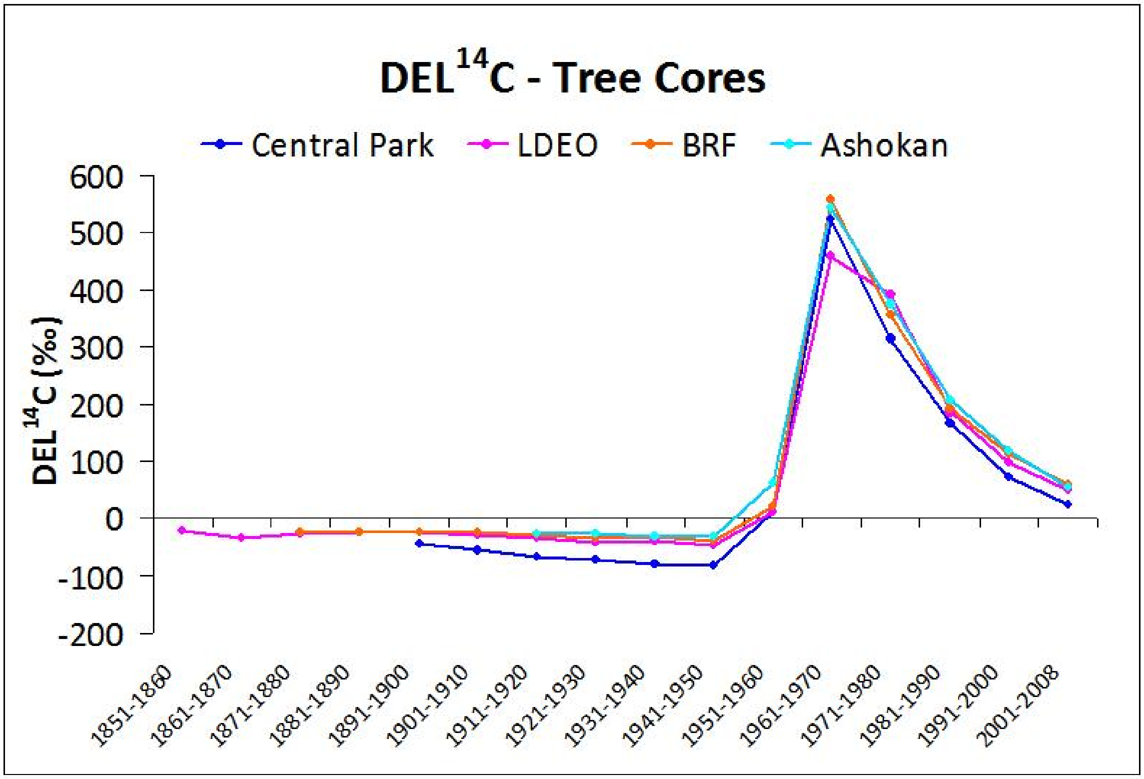

Figure 9. *Quercus rubra* Δ^{14}C results for the sites CP, LDEO, BRF and AR.

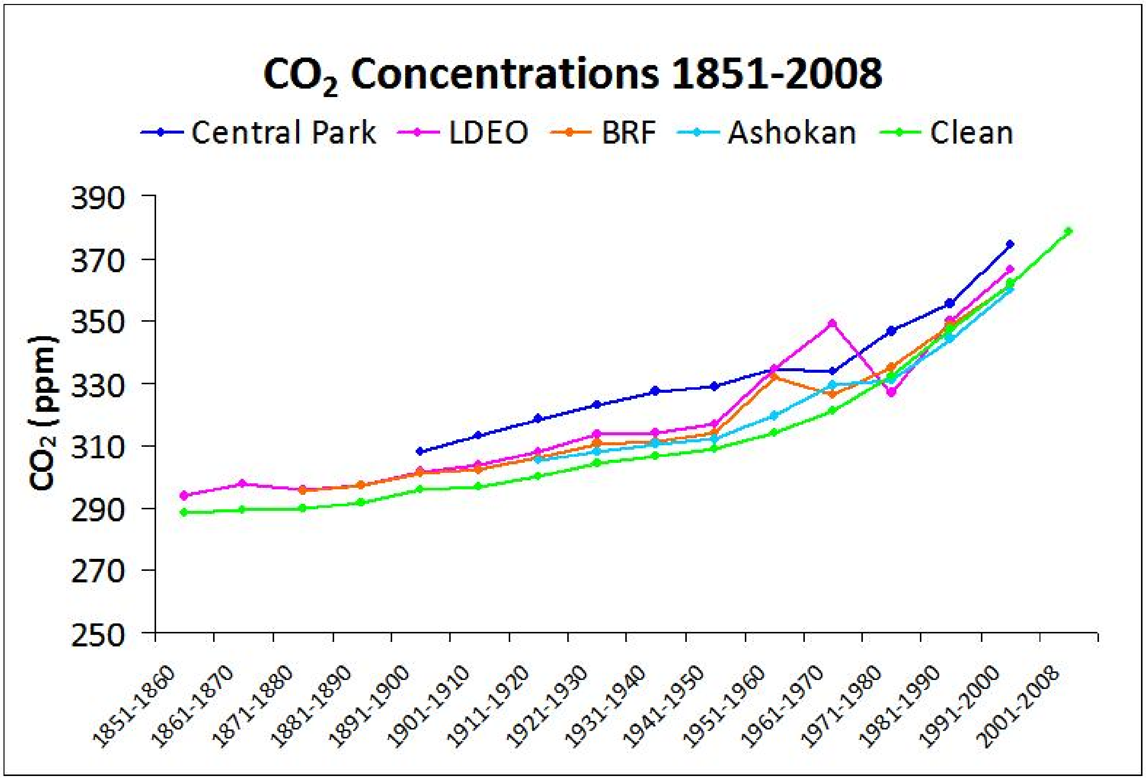

Figure 10. *Quercus rubra* $\Delta^{14}C$ results for the sites CP, LDEO, BRF and AR converted to ppm relative to the Siple Ice Core and Mauna Loa record (Table 3)

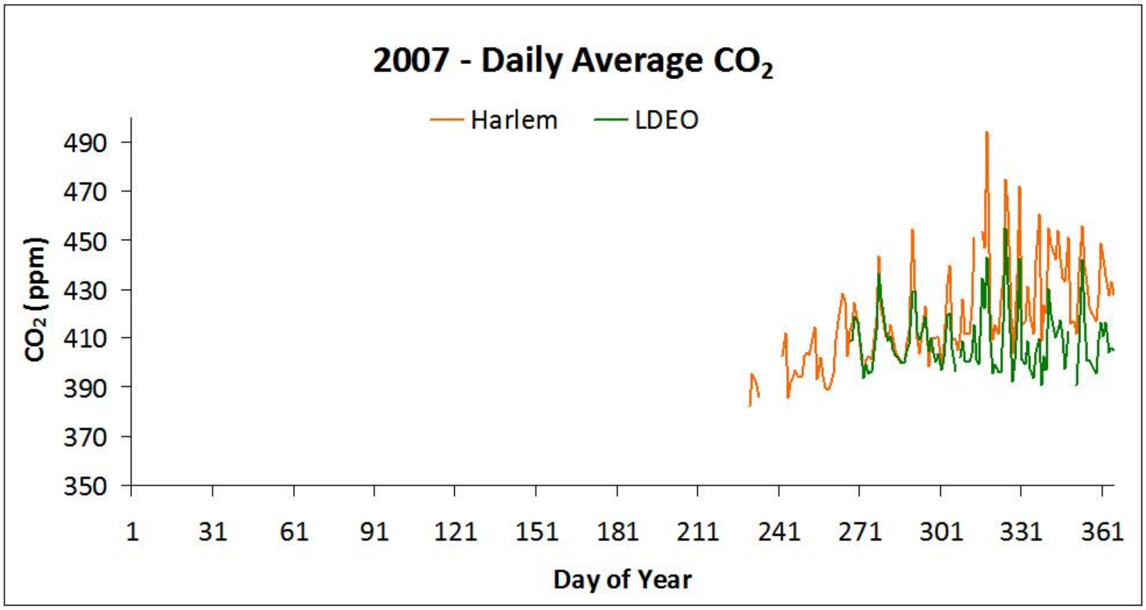

Figure 11. 2007 daily average CO_2 (ppm). Standard Deviation ranges:
Harlem: 3.2 - 71.3; LDEO: 1.3 - 39.4

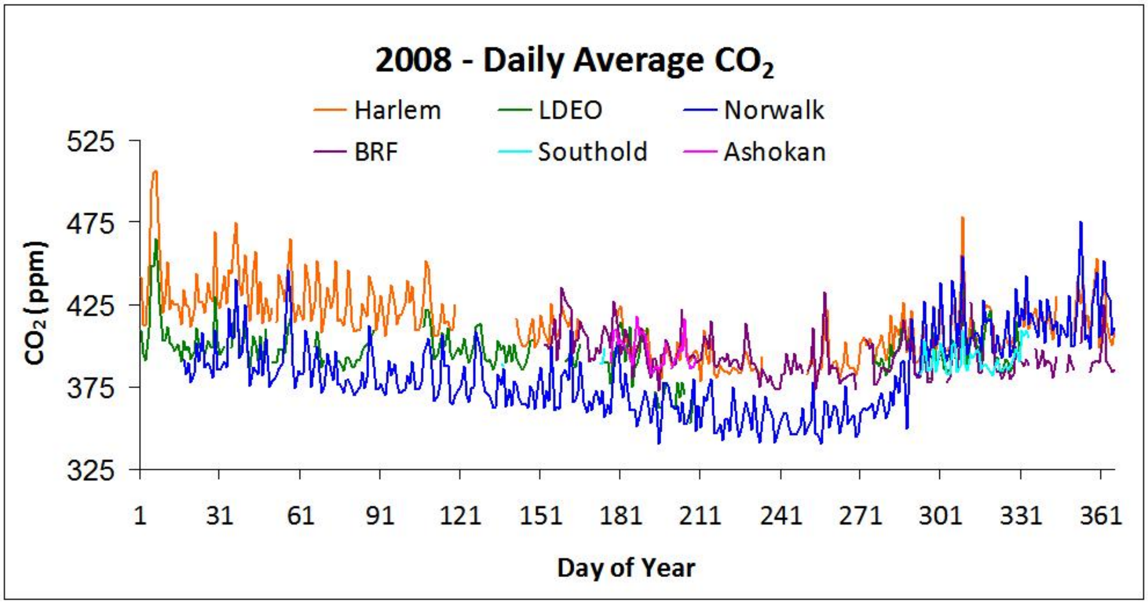

Figure 12. 2008 daily average CO_2 (ppm). Standard Deviation ranges:
Harlem: 2.7 – 50.3; LDEO: 0.9 – 34.8; Norwalk: 1.0 – 52.9; BRF: 1.6 – 39.1; Southold: 1.2 – 20.7; AR: 13.9 – 32.5

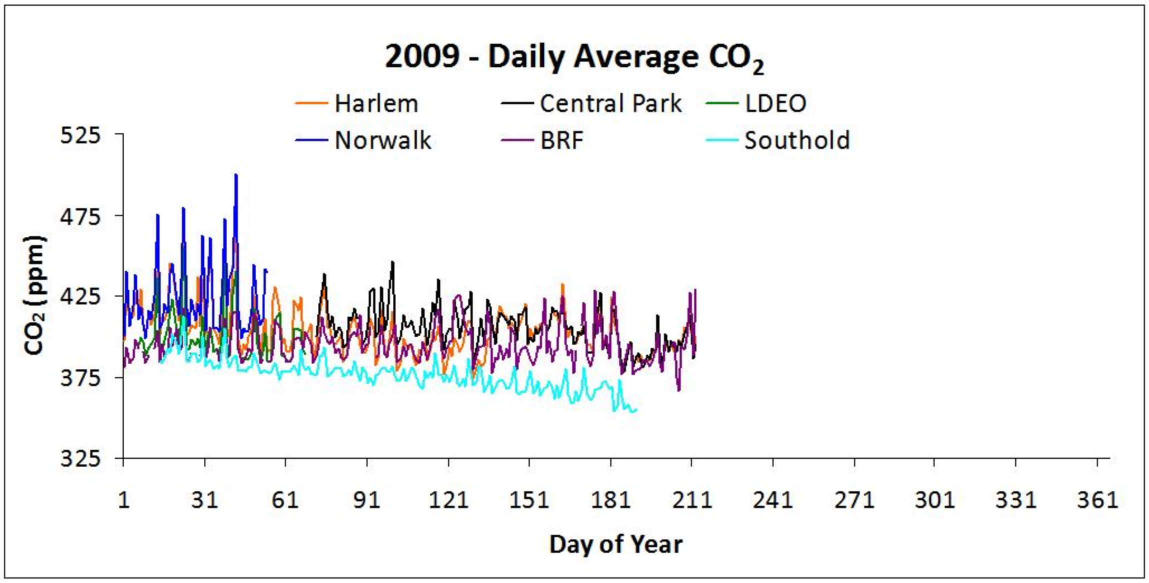

Figure 13. 2009 daily average CO_2 (ppm). Standard Deviation ranges:
Harlem: 1.8 – 54.0; Central Park: 1.7 – 41.6; LDEO: 0.7 – 40.4; Norwalk: 3.2 – 50.1; BRF: 0.8 – 46.7; Southold: 0.7 – 27.1. Caveats about Harlem data can be found in the text.

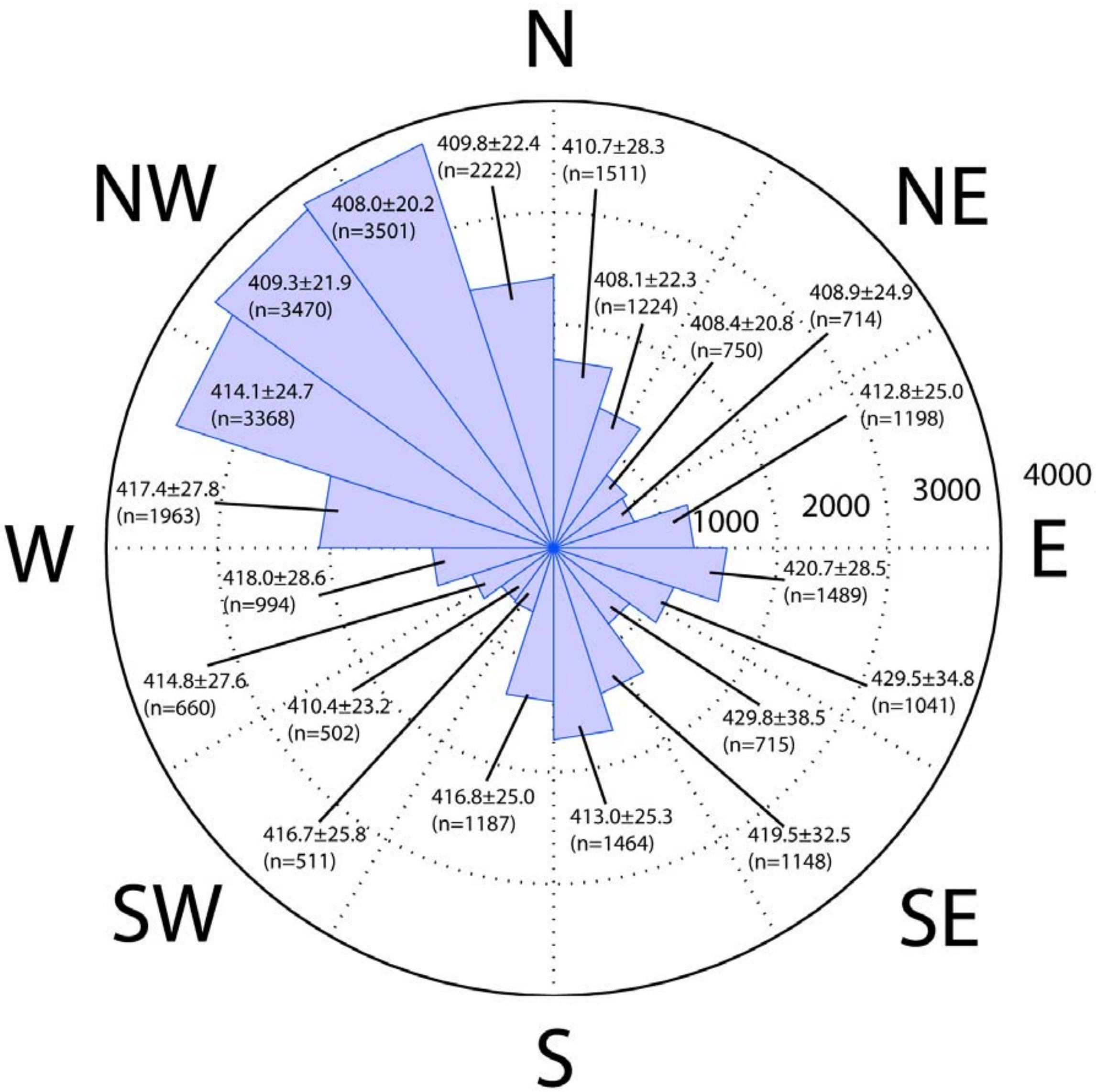

Figure 14. A histogram of wind direction and respective CO_2 concentration (ppm) ± standard deviation at Harlem in 2008. Winds from the North West bring in air with a strong signature of CO_2 in rural areas (total n = 32,422).

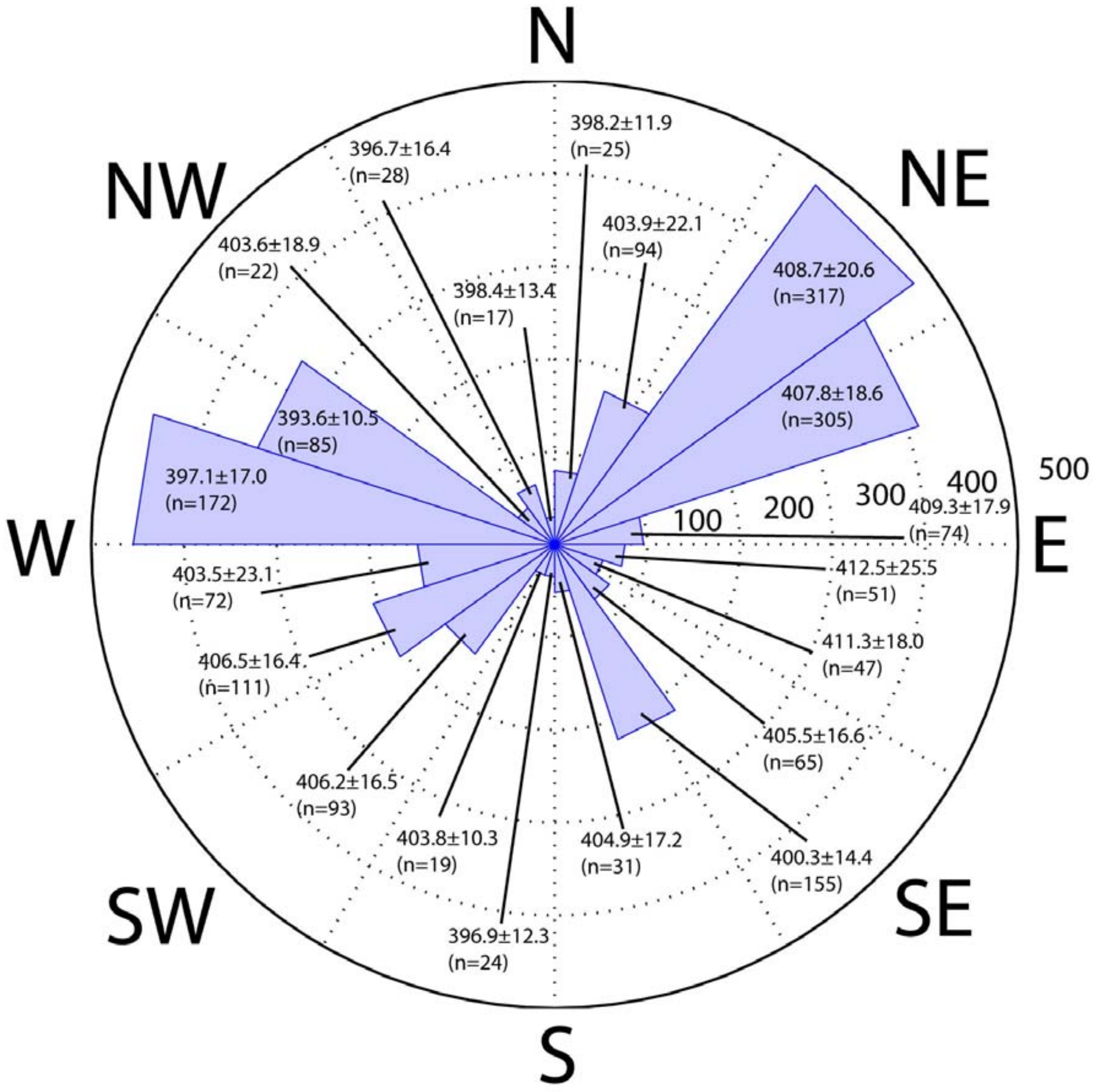

Figure 15. A histogram of wind direction at Central Park from January – July 2009. CO_2 concentrations (ppm) standard deviation is taken from March – July 2009. Due to different logging intervals, wind direction and CO_2 measurements are a few minutes off from one another. Winds from the West and North East bring in air with a strong signature of CO_2 in rural areas. (total n = 5253). The wind direction data was retrieved from the National Climatic Data Center (NCDC) (NOAA, 2009).

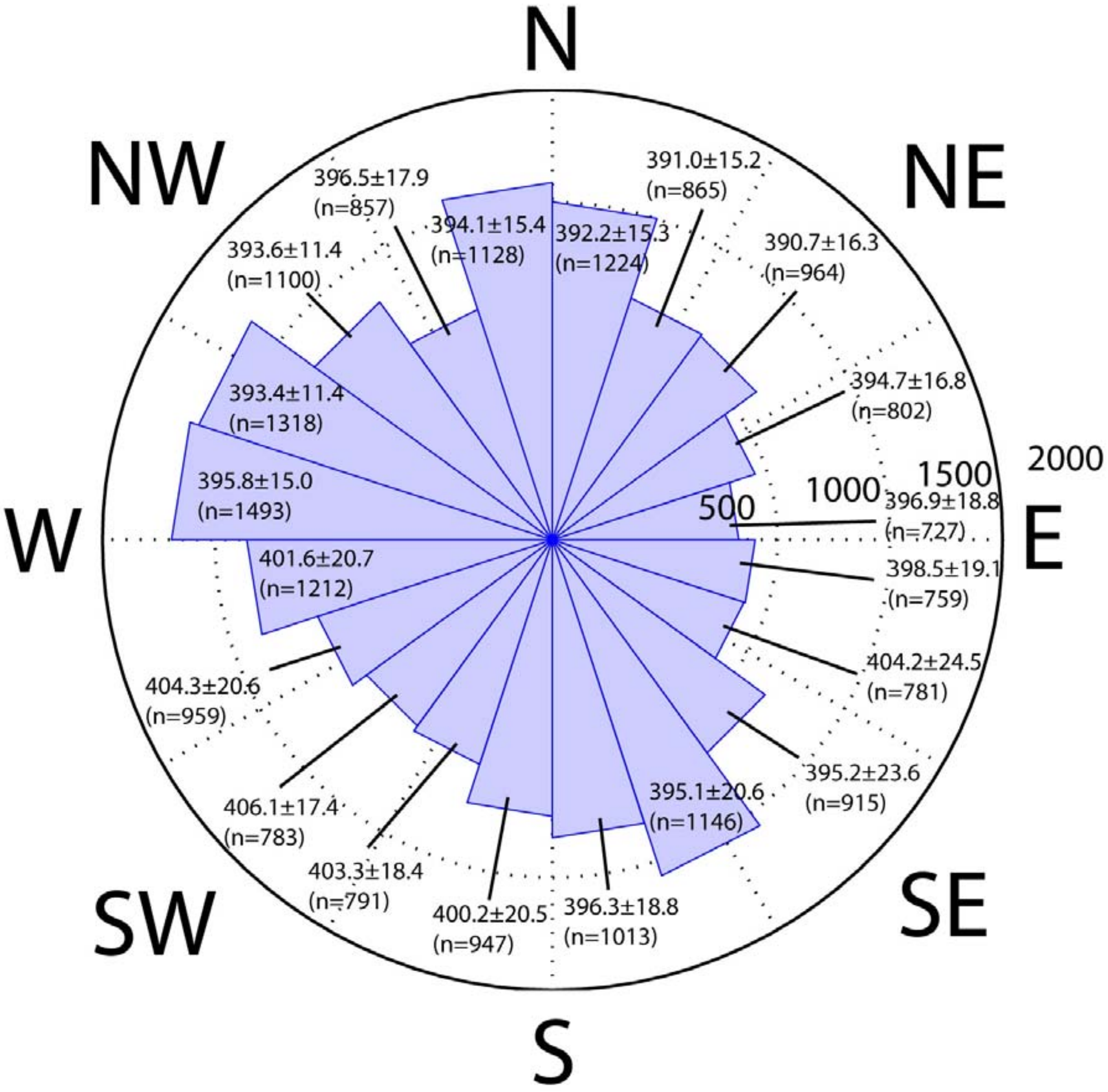

Figure 16. A histogram of wind direction at LDEO in 2008. Winds are all coming in more or less an equal direction (total n =24,452).

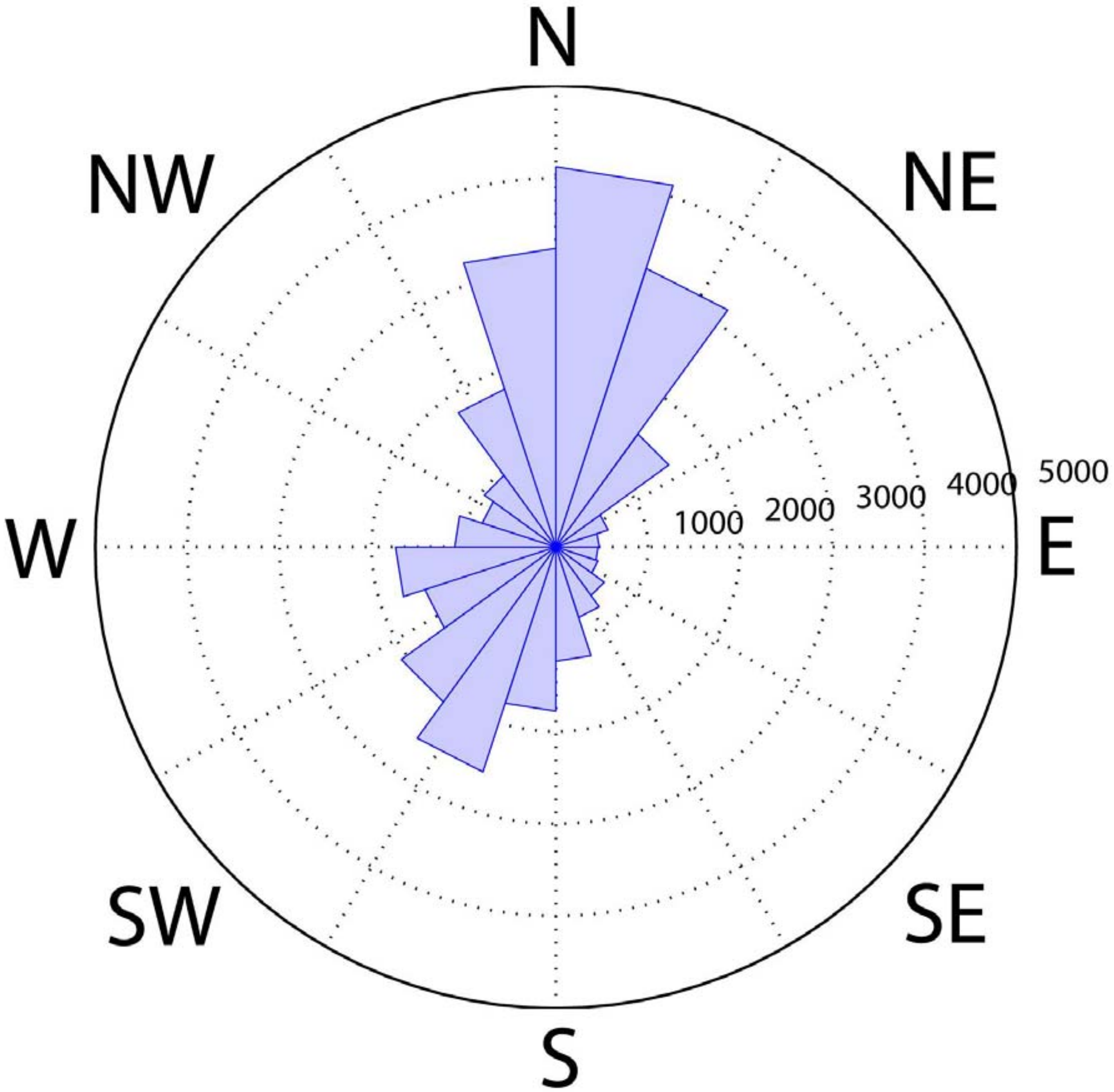

Figure 17. A histogram of wind direction at Piermont in the latter half of 2008 and beginning half of 2009. Winds are mostly coming from the North and South direction (total n = 31,088).

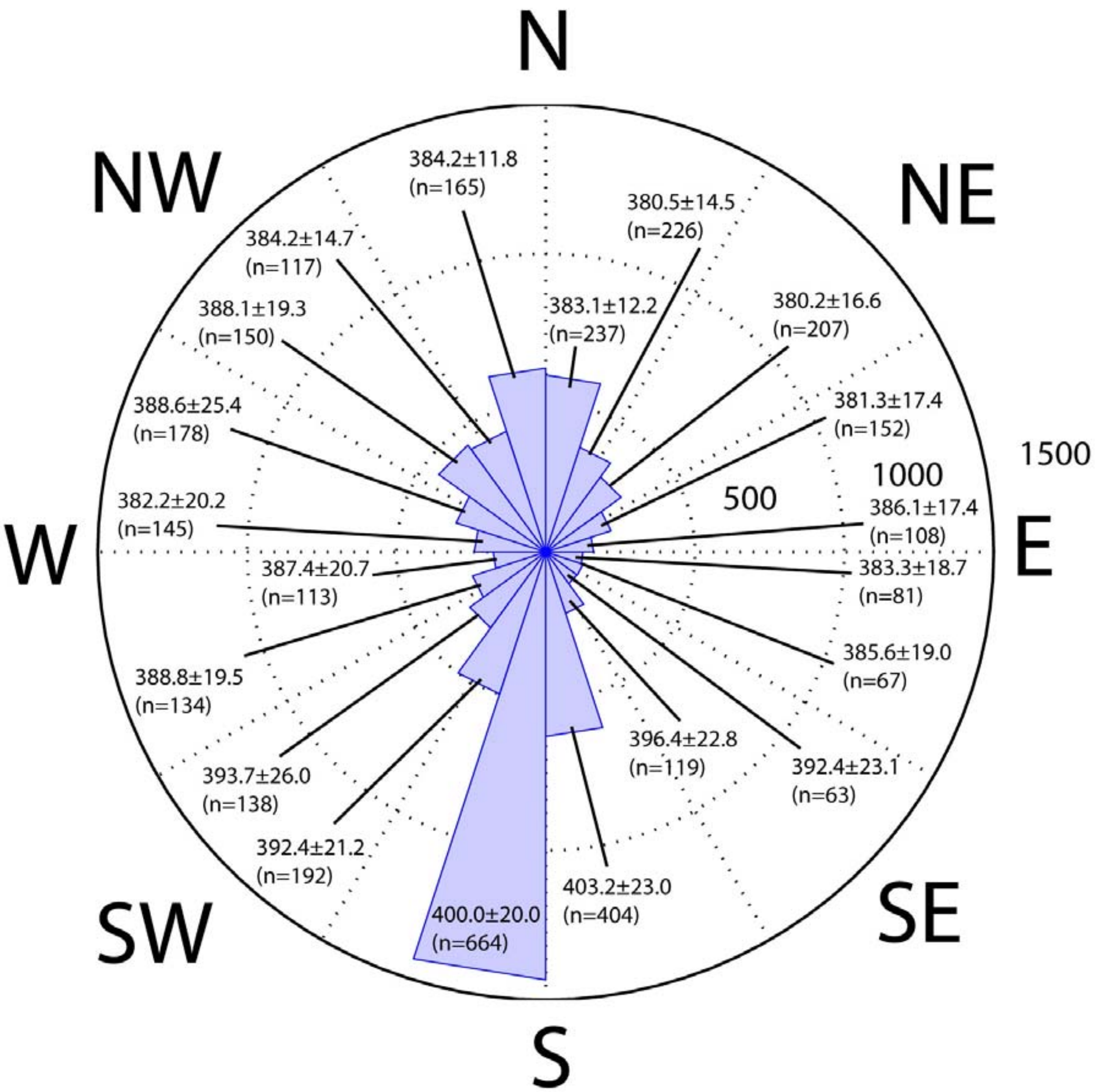

Figure 18. A histogram of wind direction at BRF in 2008. There are fewer measurements for BRF because measurements are taken every hour instead of every 15 minutes. Winds are mostly coming from a southerly direction (total n = 7,606).

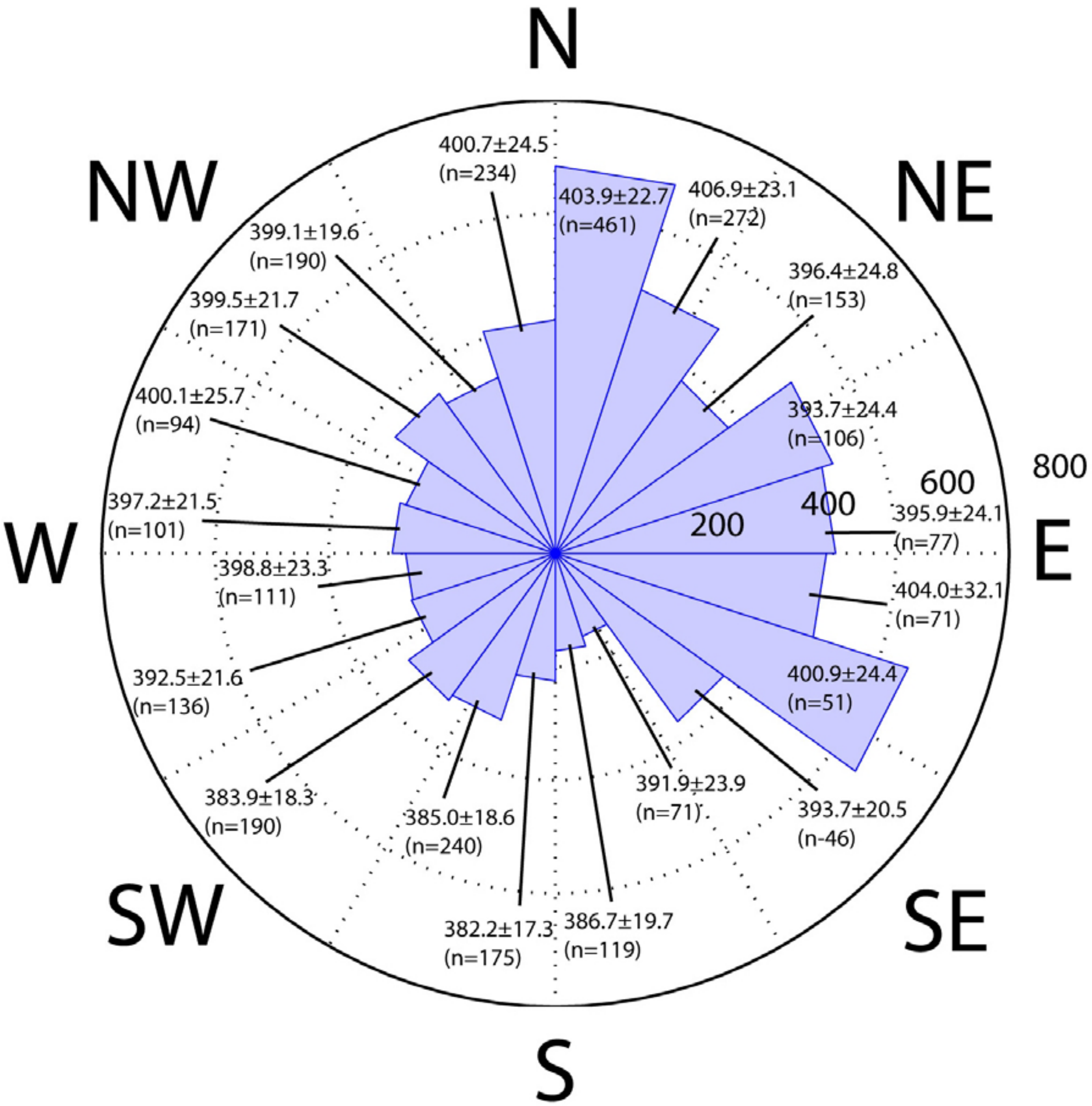

Figure 19. A histogram of wind direction at AR during the summer and part of fall in 2008. Winds are mostly coming from a northern and easterly direction (n = 7,422).

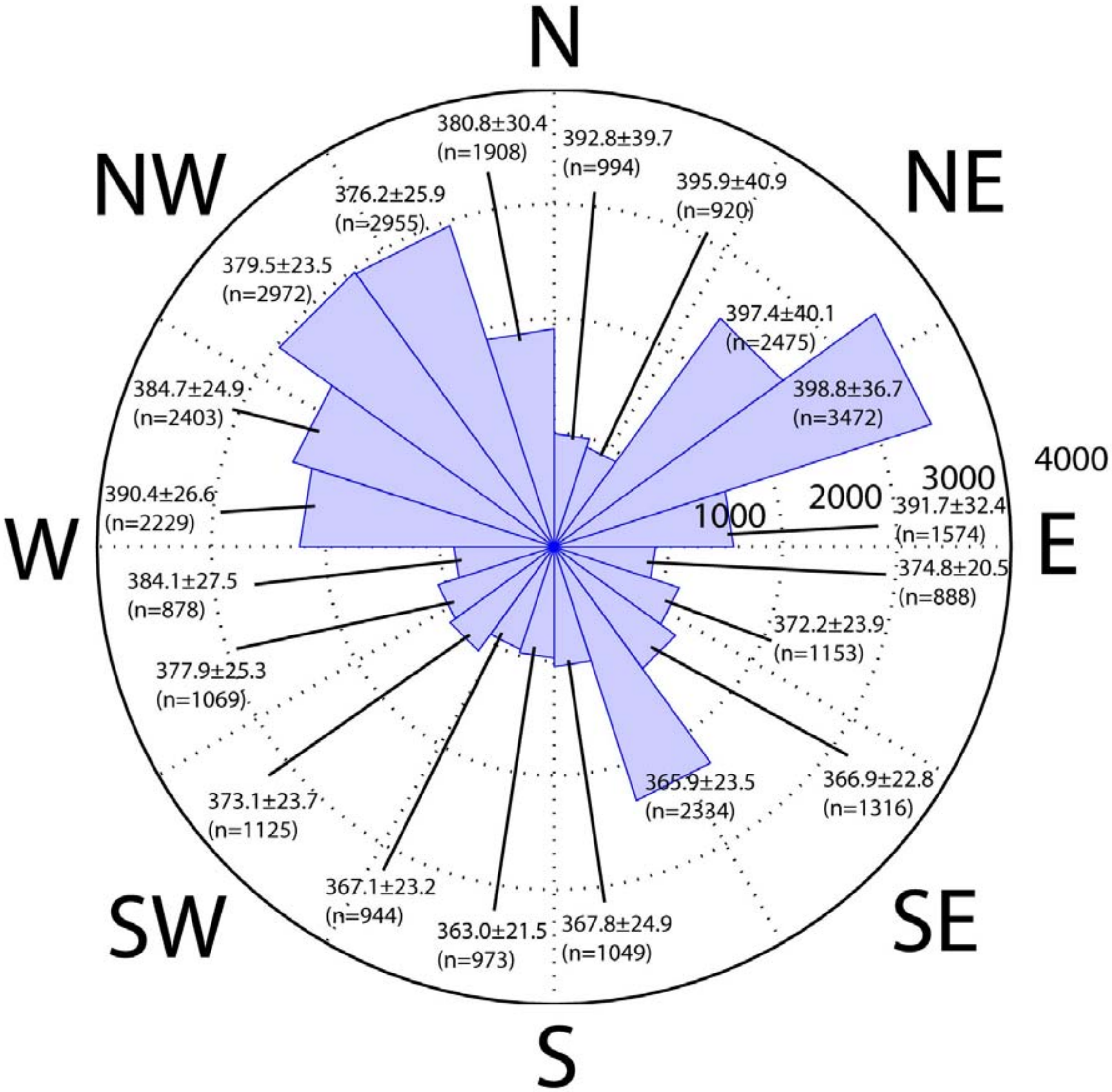

Figure 20. A histogram of wind direction at Norwalk in 2008. Winds are mostly coming from a Northwestern, Northeastern and Southeastern direction (total n = 33,631).

a)

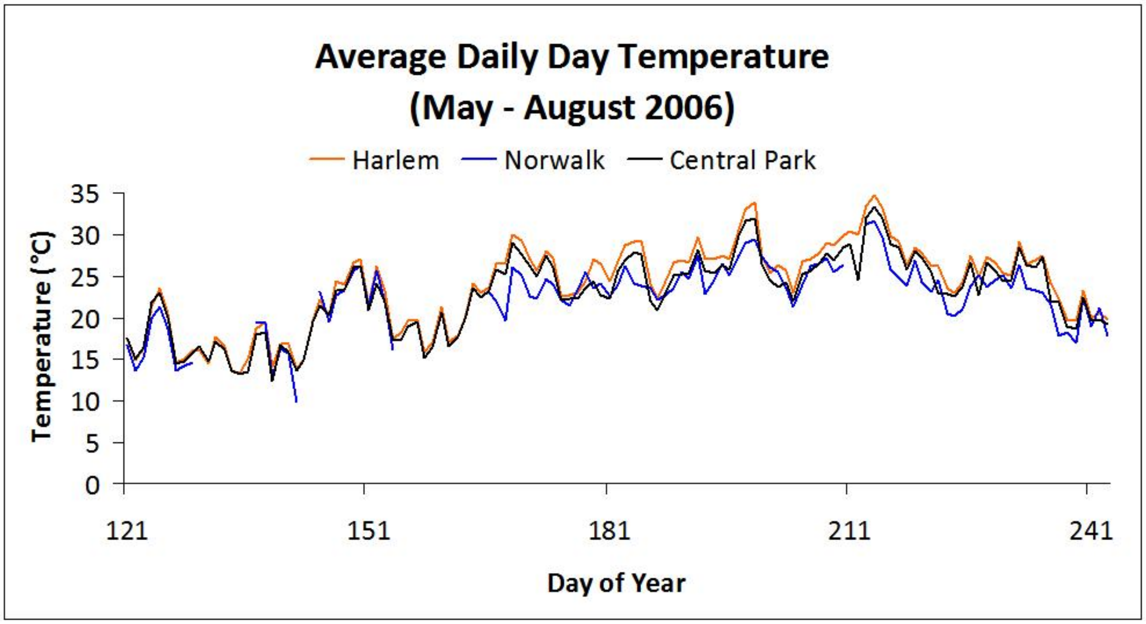

b)

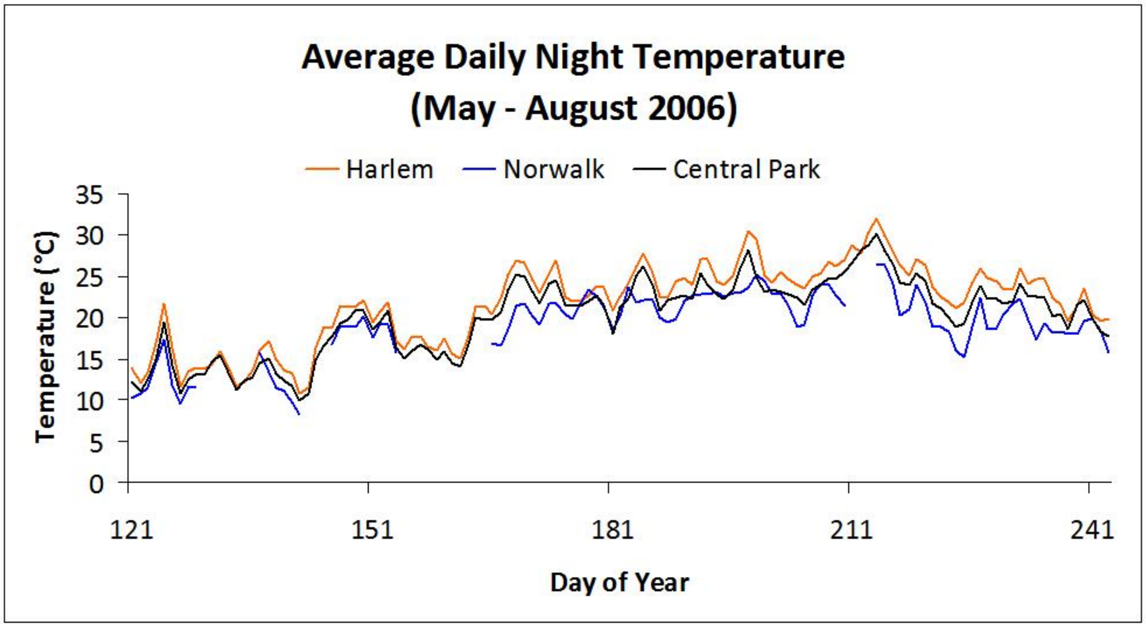

Figure 21. 2006 Day (a) and Night (b) daily averaged temperature (°C).
Standard deviation ranges during the day:
Harlem Day: 0.5 – 4.7; Central Park Day: 0.5 – 4.0; Norwalk Day: 0.5 – 5.5
Standard deviation ranges during the night:
Harlem Night: 0.4 – 3.9; Central Park Night: 0.3 – 3.9; Norwalk Night: 0.3 – 5.5

a)

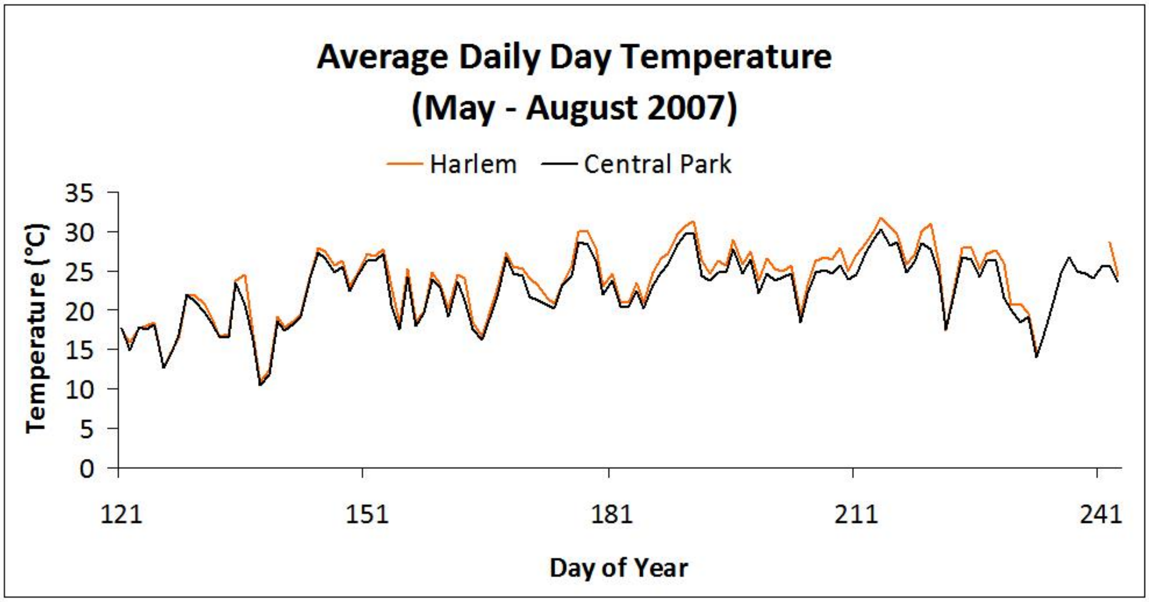

b)

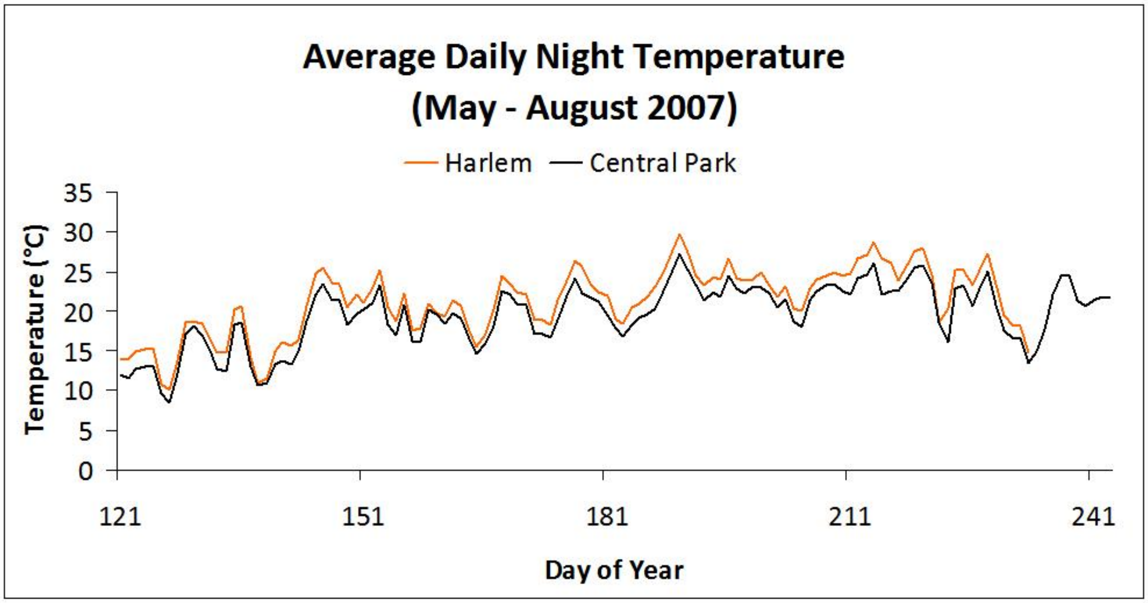

Figure 22. 2007 Day (a) and Night (b) Daily averaged temperature (°C).
Standard deviation ranges during the day:
Harlem Day: 0.4 – 5.3; Central Park Day: 0.5 – 5.0
Standard deviation ranges during the night:
Harlem Night: 0.2 – 5.4; Central Park Night: 0.2 – 5.1

a)

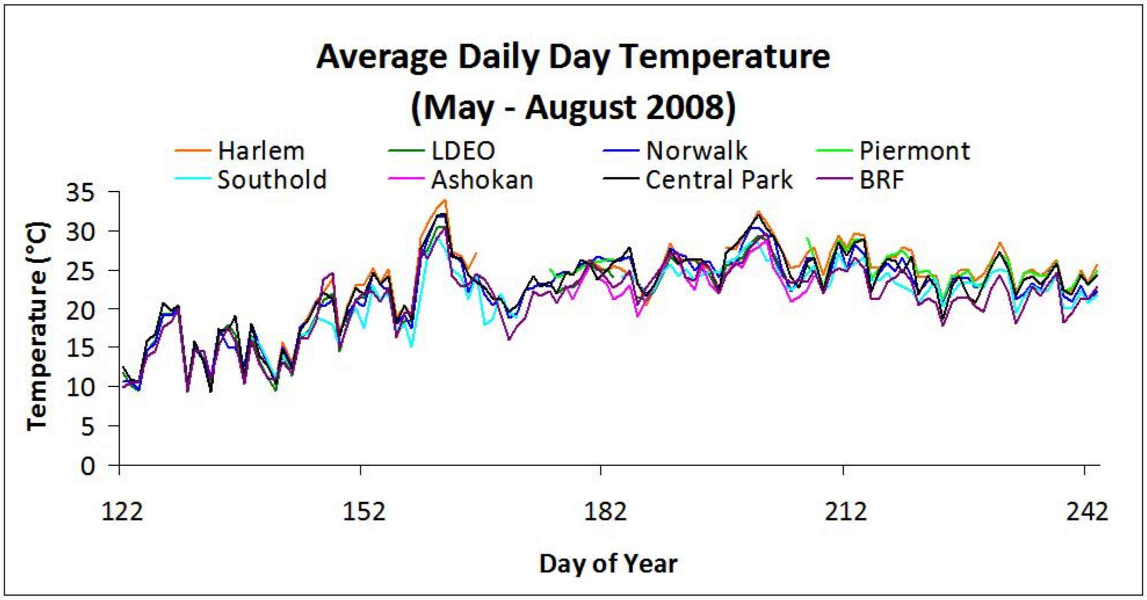

b)

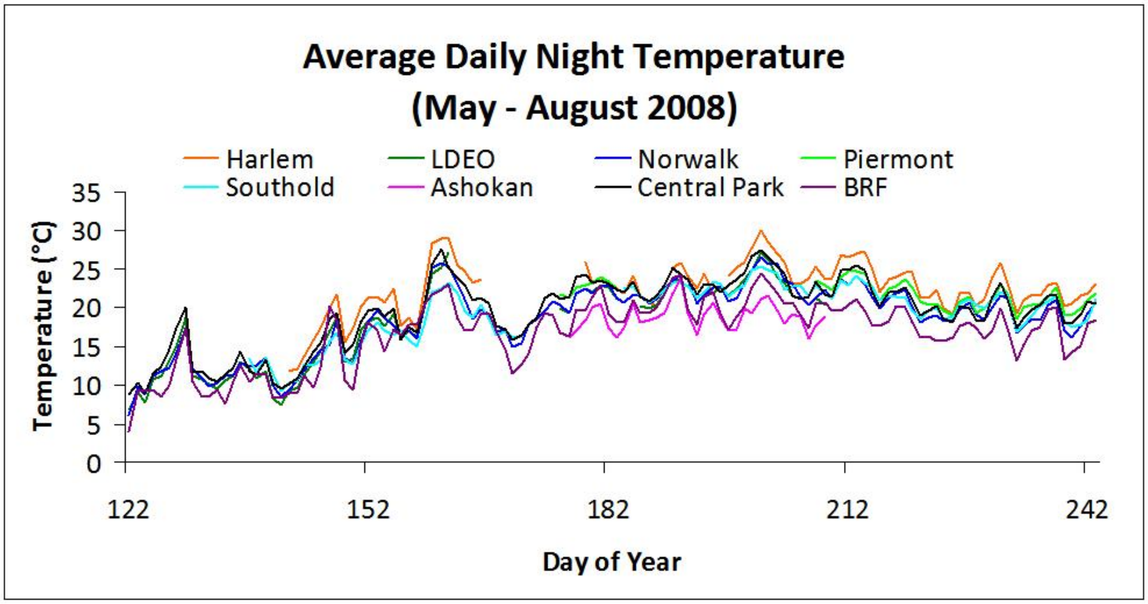

Figure 23. 2008 Day (a) and Night (b) Daily averaged temperature (°C).
Standard deviation ranges during the day:
Harlem Day: 1.0 – 6.7; Central Park Day: 0.6 – 6.0; LDEO Day: 0.4 – 6.0; BRF Day: 0.2 – 6.8; Norwalk Day: 0.4 – 6.5; Piermont Day: 0.4 – 4.5; Southold Day: 0.6 – 4.4; AR Day: 1.4 – 5.6
Standard deviation ranges during the night:
Harlem Night: 0.3 – 6.9; Central Park Night: 0.4 – 6.0; LDEO Night: 0.3 – 5.5; BRF Night: 0.4 – 5.9; Norwalk Night: 0.4 – 6.1; Piermont Night: 0.2 – 2.6; Southold Night: 0.3 – 4.2; AR Night: 0.4 – 3.6

a)

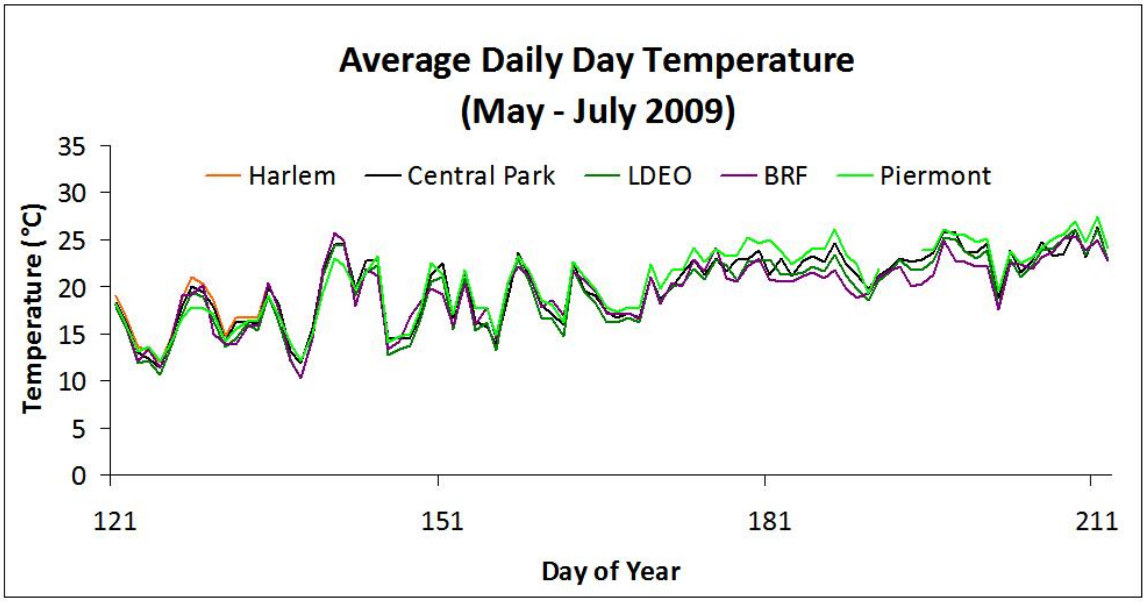

b)

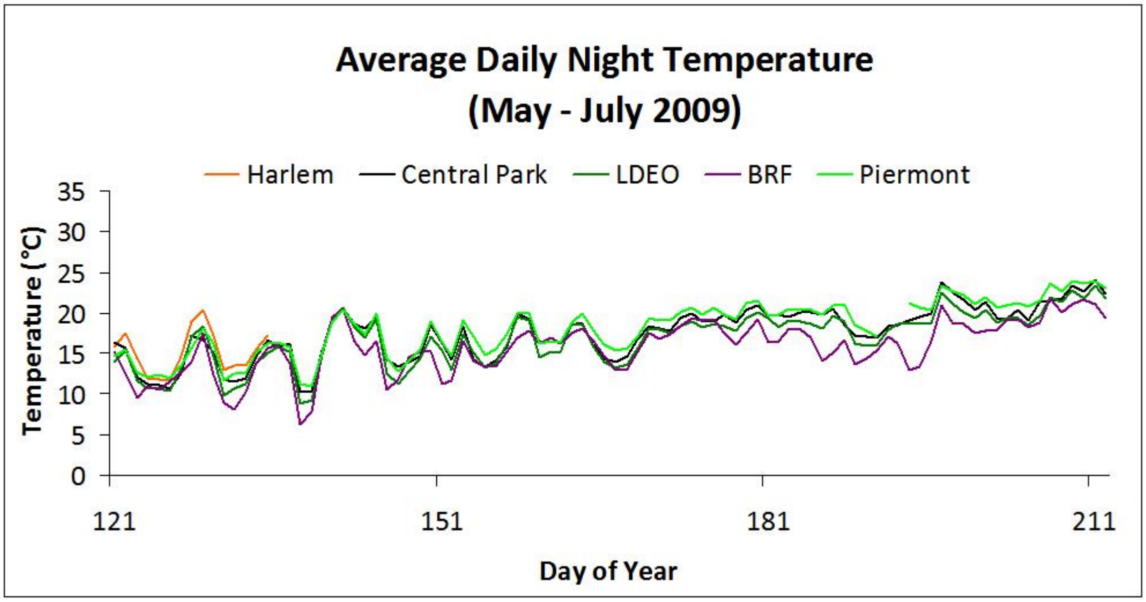

Figure 24. 2009 Day (a) and Night (b) Daily averaged temperature (°C).
Standard deviation ranges during the day:
Harlem Day: 0.7 – 3.7; Central Park Day: 0.5 – 4.5; LDEO Day: 0.3 – 5.4; BRF Day: 0.3 – 7.8; Piermont Day: 0.3 – 4.6
Standard deviation ranges during the night:
Harlem Night: 0.2 – 4.1; Central Park Night: 0.2 – 4.4; LDEO Night: 0.3 – 4.8; BRF Night: 0.2 – 6.4; Piermont Night: 0.3 – 3.9

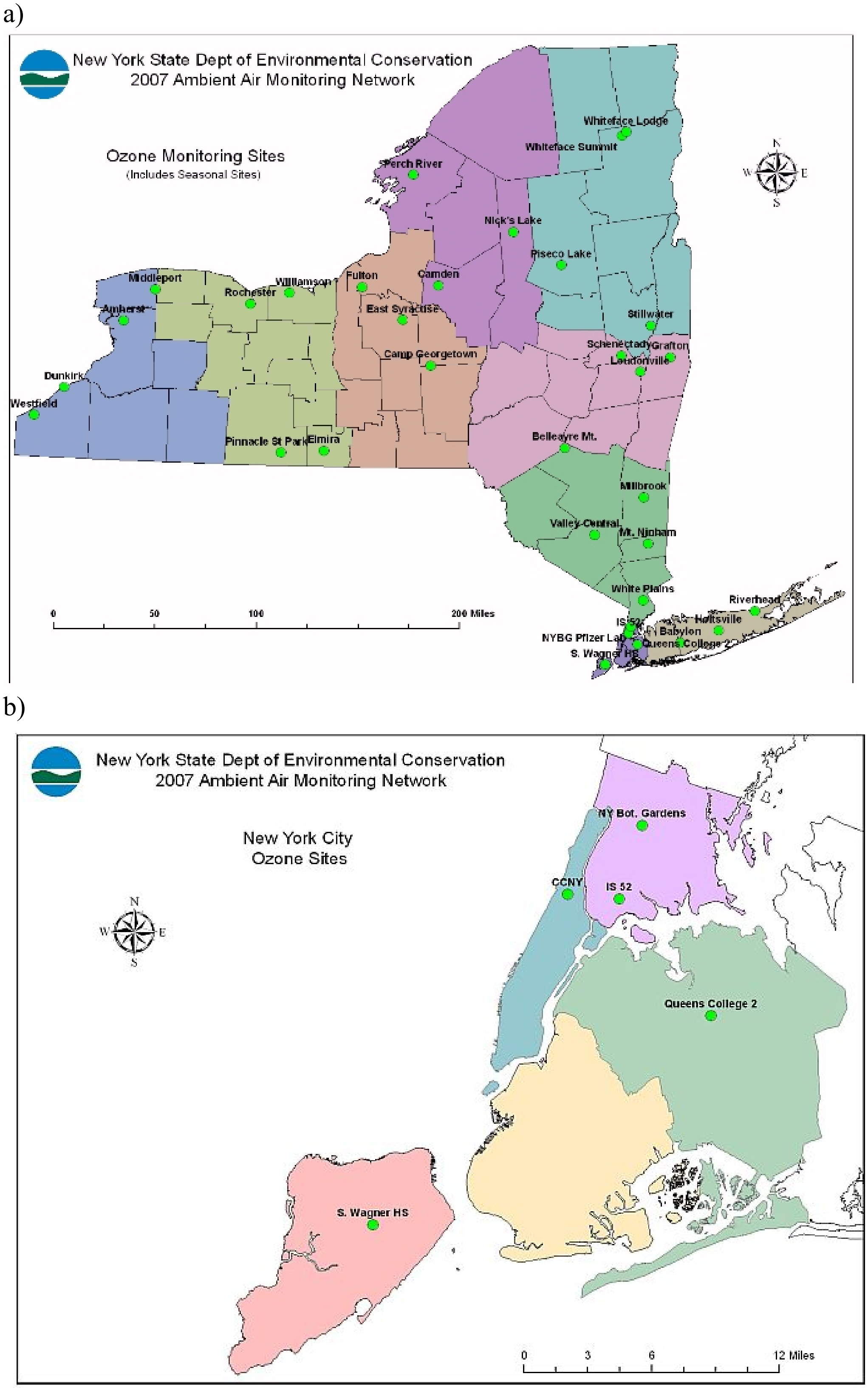

Figure 25. New York State Dept. of Environmental Conservation 2007 Ambient Air Monitoring Network in a) New York State and b) New York City (DEC, 2009).

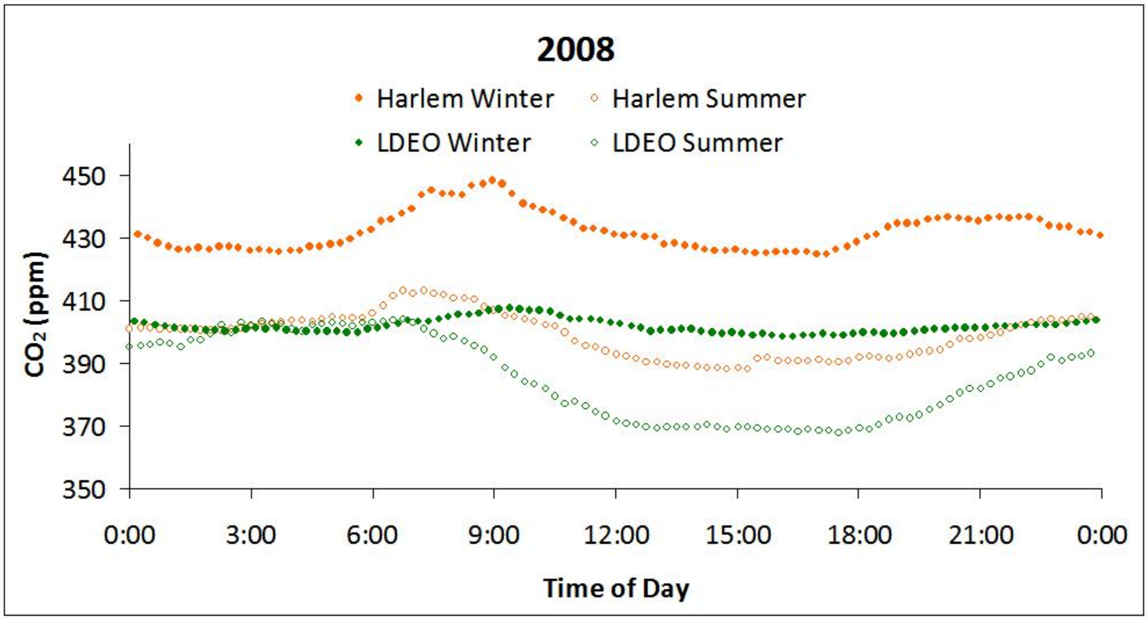

Figure 26. Seasonal and daily variation of CO_2 concentrations over the course of the day comparing an urban (Harlem) vs. rural (LDEO) site in 2008. Winter was averaged over the months January, February and March while summer was averaged over the months June, July and August. LDEO summer only consisted of the majority of June and July due to inadequate data for August.

a)

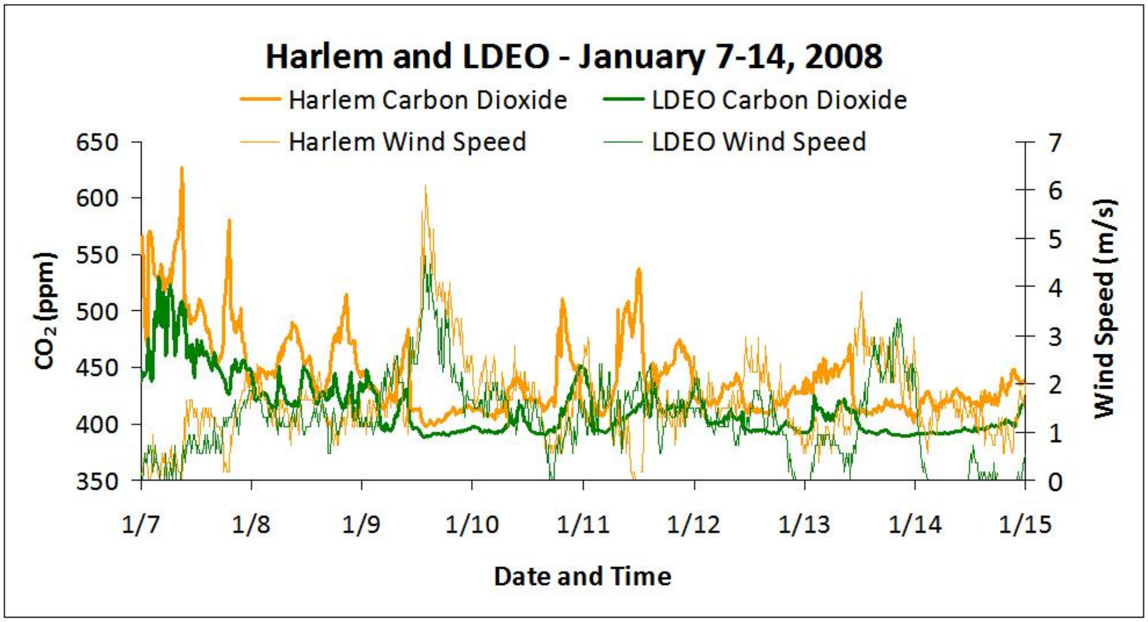

b)

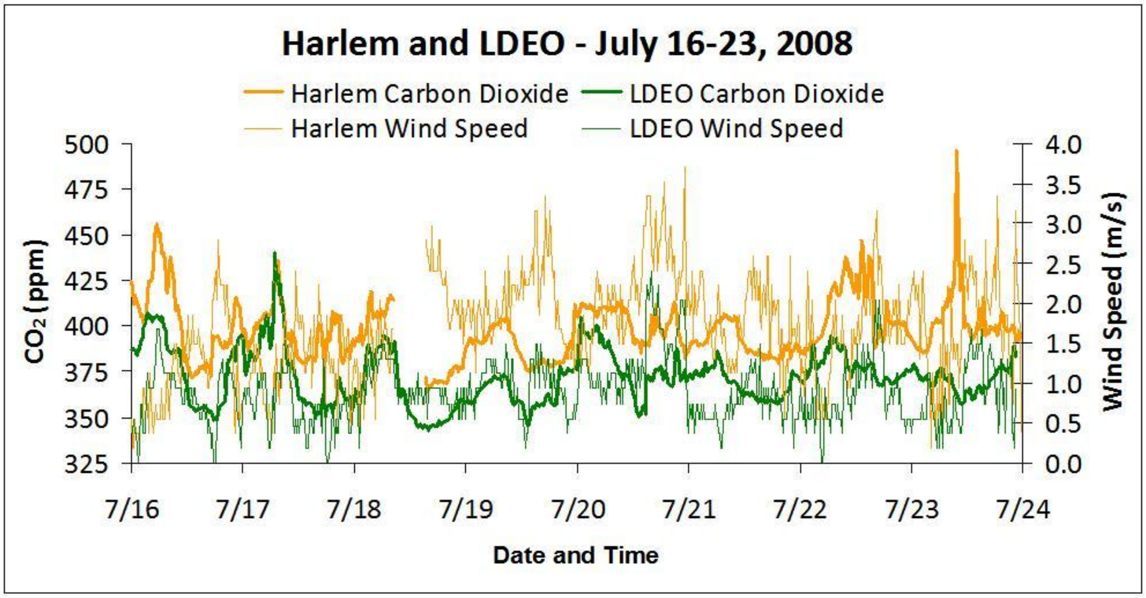

Figure 27. Effect of wind on CO_2 in Harlem and LDEO in winter (a) and summer (b). Date and Time tick marks represent midnight.

a)

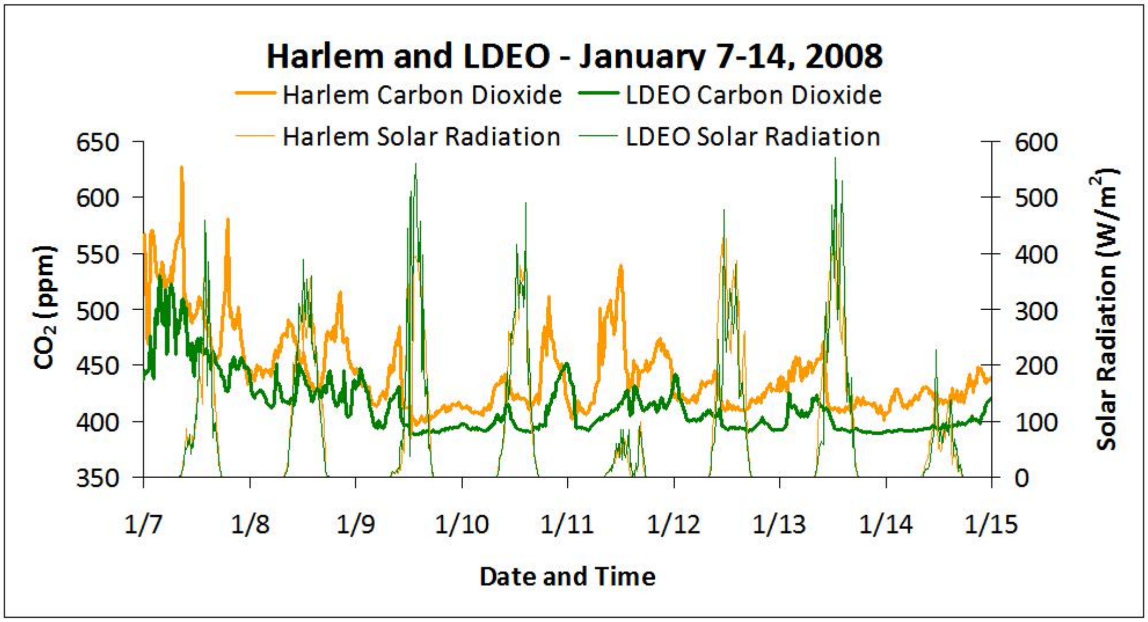

b)

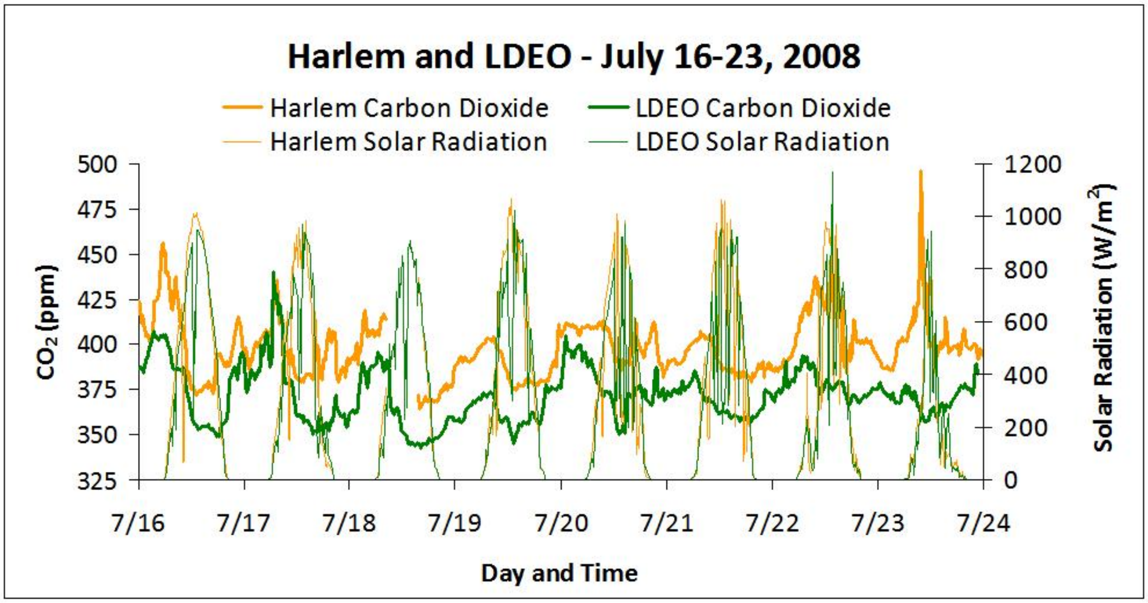

Figure 28. Effect of Solar Radiation on CO_2 in Harlem and LDEO in winter (a) and summer (b). Date and Time tick marks represent midnight

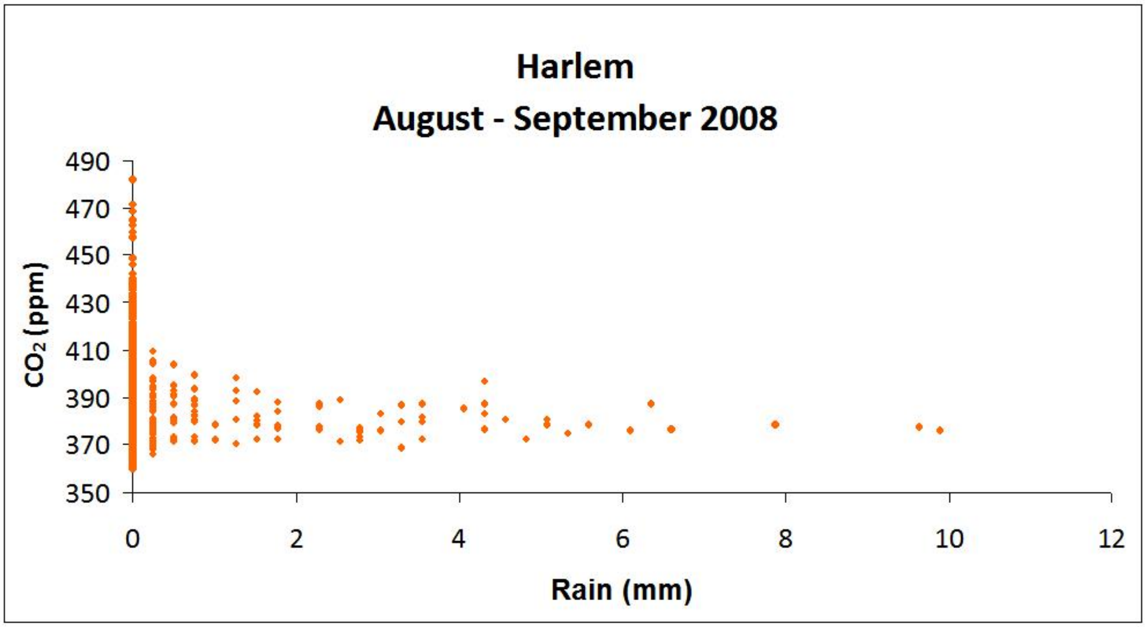

Figure 29. Effect of Rain on CO_2 in Harlem from August until September 2008.

Tables

Table 1. Latitude, Longitude, Elevation and Location of each site

Site	Latitude (°, N)	Longitude (°, W)	Elevation (m)	Location
Central Park (CP)	40.780	73.970	28	Ground Level
Harlem	40.808	73.950	8	Roof
LDEO	41.005	73.908	128	Top of Satellite Tower
Piermont	41.043	73.897	5	Roof
Black Rock Forest (BRF)	41.430	74.020	115	Ground Level
Ashokan Reservoir (AR)	41.925	74.248	233	Ground Level
Norwalk	41.101	73.418	3	Roof
Southold	41.058	72.429	10	Roof

Table 2. Recent examples of studies with continuous measurements of CO_2 concentrations in urban sites

Author / Location	Measurement method	Instrument Used	Range of CO_2 concentrations	Bkg Conc. Mauna Loa (ppm)
Grimmond et al., 2002 northwest suburb of Chicago, Illinois	June 14 - August 11, 1995 every 15 minutes	LI-COR 6262	Average: 384 ppm Night Avg: 405 ppm (max 441 ppm) Day Avg: 370 ppm (min: 338 ppm)	June 1995: 363.03 July 1995: 361.55 Aug. 1995: 358.94
Day et al., 2002 4 sites in Phoenix, Arizona 1) urban: grass turf 2) rural: grass turf 3) urban: native desert 4) rural: native desert	March 15 - April 3, 2000 every 5 minutes	LI-COR 800	Urban Center: Avg. of 396 ppm Rural Area: Avg. of 377 ppm 8 ppm difference during the day (383 vs. 375 ppm) 24 ppm difference during the night (409 vs. 385 ppm)	March 2000: 370.38 April 2000: 371.63
Pataki et al., 2003a 3.5 km east of downtown Salt Lake City	January - December 2002 every 5 minutes	LI-COR 7000	Nighttime average values: Winter: 390 - 480 ppm Spring/Summer: 375 - 400 ppm Afternoon: ± 5 ppm of bkg value: 372.2 ppm	2002: 373.17
Henninger and	50 mobile trips:	infrared	Average rural for entire period:	2002: 373.17

Kuttler, 2007 Essen, Germany	2002 - 2005 day/night/weekdays/weekends 1.5 m a.g.l.	radiation absorption	379 ± 5.04 ppm average urban for entire period: 408 ± 20.66 ppm	2003: 375.78 2004: 377.52 2005: 379.76
George et al., 2007 3 sites: 1) Baltimore city center (urban) 2) 11km west of Baltimore (suburban) 3) Buckeystown, MD (rural)	2002 - 2006 every 15 minutes	Quibit Systems: S151	Urban [CO$_2$] increased by 16% from 2002 to 2006 Avg range of [CO$_2$]: 443-459 ppm Highest [CO$_2$] in the 5 years: 488 ppm (urban site) 442 ppm (suburban site) 422 ppm (rural site)	2002: 373.17 2003: 375.78 2004: 377.52 2005: 379.76 2006: 381.85
Vogt et al. 2006 Sperrstrasse in Basel	June/July 2002 10 tower heights 10 min periods averaged to hourly values	LICOR-6262 & LICOR-7500	1.5 and 31 m: avg. diurnal range: 362 to 423 ppm Low heights (0.1 m): as high as 600 ppm	June 2002: 375.44 July 2002: 373.91
Velasco et al., 2005 Iztapalapa: southeast Mexico City	25 m tower on roof of building (total height: 37 m) April 7-29, 2003 every 30 minutes	NOAA open-path ifrared gas analyzer (IRGA)	range of 398 to 444 ppm Avg: 421 ppm lowest in afternoon: avg: 375 ppm	April 2003: 377.75
Coutts et al., 2007 near Melbourne CBD 1) suburb of Preston 2) suburb of Surrey Hills	1) Preston: Feb 2004 - June 2005 2) Surrey Hills: Feb 2004 - July 2004 every 30 minutes	LI-COR 7500	Preston: Summer avg daily range: 362-370 ppm Winter avg daily range: 370-378 ppm Surrey Hills: Summer avg daily range: 356-370 ppm Winter avg daily range: 359-370 ppm	2004: 377.52 2005: 379.76
Moriwaki et al., 2006 residential area in Kugahara, Tokyo, Japan	29 m tower 11 tower levels November to December 2004 every 4 minutes	LI-COR 7000 and LI-COR 7500	Avg. diurnal CO$_2$: 406 to 444 ppm; amplitude of the diurnal variation is 38 ppm	Nov. 2004: 276.15 Dec. 2004: 377.51

Rigby et al., 2008 London 1) Urban: Queen's Tower - on the Imperial College - campus in South Kensigton 2) Rural: Royal Holloway - University of London - in Egham, Surrey	July 2006 - June 2007 every 15 minutes	Vaisala CARBOCAP GMP343 and LI-COR 6252	seasonal amplitude: ~25 ppm Spring/Autumn: Day: Urban site - few ppm higher than rural site Nighttime: rural site significantly elevated than urban site Winter: Urban values elevated above rural max increase of 10 ppm at 9 am	2006: 381.85 2007: 383.71

Table 3. 10-year averages of splined Siple Ice Core and Mauna Loa CO_2 records

Years	**CO_2 (ppm)**
1851-1860	288.455
1861-1870	289.370
1871-1880	289.854
1881-1890	291.992
1891-1900	295.635
1901-1910	297.049
1911-1920	300.502
1921-1930	304.336
1931-1940	306.701
1941-1950	309.090
1951-1960	313.983
1961-1970	321.162
1971-1980	332.140
1981-1990	346.913
1991-2000	361.783
2001-2008	378.554

Table 4. 10-year averages of splined Northern Europe, Washington State and INTCAL04 records

Years	$\Delta^{14}CO_2$ (‰)
1851-1860	-3.518
1861-1870	-4.635
1871-1880	-5.211
1881-1890	-4.773
1891-1900	-3.254
1901-1910	-5.28
1911-1920	-9.532
1921-1930	-14.058
1931-1940	-17.85
1941-1950	-22.839
1951-1960	79.228
1961-1970	584.05
1971-1980	370.8
1981-1990	196.33
1991-2000	111.32
2001-2008	-

Table 5. CO_2 Instrument used and weather indices measured at each site.

Site	Date Initiated	CO_2 Instrument	Rain (mm)	Pressure (kPa)	Solar Radiation (W/m^2)	Wind Speed (m/s)	Gust Speed (m/s)	Wind Direction (°)	Air Temp (°C)	Relative Humidity (%)	Soil Temp (°C)
Central Park	March-09	Li-Cor 820 or 840	-	-	-	-	-	-	-	-	-
Harlem	Jan-06	Li-Cor 820 or 840	X	X	X	X	X	X	X	X	-
LDEO	Dec-07	Li-Cor 820 or 840	-	-	X	X	X	X	X	X	-
Piermont	June-08	-	X	X	X	X	X	X	X	X	-
Black Rock Forest	May-08 (CO_2)	Li-Cor 7500	X	X	X	X	-	X	X	X	-
Ashokan Reservoir	June-08	Li-Cor 820 or 840	X	-	X	X	X	X	X	X	X
Norwalk	Jan-08	Li-Cor 820 or 840	-	-	X	X	X	X	X	X	-
Southold	May-08	Li-Cor 820 or 840	-	-	X	X	X	X	X	X	-

Table 6. $\delta^{13}C$ and $\Delta^{14}C$ of three different *Xanthium strumarium* leaves per site

	Central Park	**±[b]**	**LDEO**	**±[b]**	**Black Rock Forest**	**±[b]**	**Ashokan Reservoir**	**±[b]**
$\delta^{13}C$ (‰)	-28.3	0.15	-29.1	0.15	-27.7	0.15	-27.9	0.15
	-29.0	0.15	-28.3	0.15	-28.4	0.15	-28.0	0.15
	-29.1	0.15	-28.2	0.15	-27.8	0.15	-28.0	0.15
$\Delta^{14}C$ (‰)[a]	31.8	1.7	37.1	1.9	48.4	1.8	56.8	2.1
	26.5	1.9	44.0	1.8	51.9	1.8	58.2	1.7
	30.7	1.7	46.5	2.1	46.3	1.9	59.0	2.0

[a] $\Delta^{14}C$ sample preparation backgrounds have been subtracted, based on measurements of ^{14}C-free coal

[b] Precision error of Mass Spectrometer (for $\delta^{13}C$) and Accelerator Mass Spectrometer (for $\Delta^{14}C$)

Table 7. $\delta^{13}C$ (‰) tree core *Quercus rubra* measurements from 1851-2008

Years	**Central Park**	**±**[a]	**LDEO**	**±**[a]	**Black Rock Forest**	**±**[a]	**Ashokan Reservoir**	**±**[a]
1851-1860	-	-	-24.70	0.15	-	-	-	-
1861-1870	-	-	-24.49	0.15	-	-	-	-
1871-1880	-	-	-23.91	0.15	-23.35	0.15	-	-
1881-1890	-	-	-23.16	0.15	-23.28	0.15	-	-
1891-1900	-24.58	0.15	-23.54	0.15	-22.94	0.15	-	-
1901-1910	-23.78	0.15	-23.59	0.15	-23.33	0.15	-	-
1911-1920	-23.92	0.15	-23.50	0.15	-23.52	0.15	-22.80	0.15
1921-1930	-24.68	0.15	-23.77	0.15	-23.32	0.15	-22.64	0.15
1931-1940	-23.53	0.15	-23.38	0.15	-23.67	0.15	-22.75	0.15
1941-1950	-23.57	0.15	-23.49	0.15	-23.83	0.15	-22.82	0.15
1951-1960	-23.14	0.15	-23.22	0.15	-23.32	0.15	-22.32	0.15
1961-1970	-24.53	0.15	-22.85	0.15	-23.05	0.15	-22.25	0.15
1971-1980	-26.72	0.15	-25.28	0.15	-23.88	0.15	-23.02	0.15
1981-1990	-26.83	0.15	-25.15	0.15	-24.94	0.15	-23.86	0.15
1991-2000	-26.64	0.15	-26.61	0.15	-25.85	0.15	-24.52	0.15
2001-2008	-27.24	0.15	-26.27	0.15	-25.17	0.15	-25.22	0.15

[a] Precision error of the Mass Spectrometer measurements

Table 8. $\Delta^{14}C$ (‰) tree core *Quercus rubra* measurements from 1851-2008

Years	**Central Park**	**±[a]**	**LDEO**	**±[a]**	**Black Rock Forest**	**±[a]**	**Ashokan Reservoir**	**±[a]**
1851-1860	-	-	-21.4	2.0	-	-	-	-
1861-1870	-	-	-33.2	2.0	-	-	-	-
1871-1880	-	-	-25.3	2.0	-24.4	1.4	-	-
1881-1890	-	-	-22.6	2.1	-23.1	1.2	-	-
1891-1900	-43.7	1.9	-22.7	2.2	-22.4	1.5	-	-
1901-1910	-56.8	1.9	-27.9	2.1	-23.0	1.2	-	-
1911-1920	-66.1	2.0	-34.6	2.0	-27.7	1.4	-25.2	1.3
1921-1930	-71.1	1.9	-43.2	1.9	-33.5	1.3	-27.1	1.3
1931-1940	-80.0	1.9	-40.7	1.9	-32.4	1.3	-30.7	1.3
1941-1950	-82.0	1.9	-47.0	1.9	-38.6	1.3	-32.0	1.3
1951-1960	11.6	1.3	12.7	2.0	21.4	1.4	61.3	1.4
1961-1970	523.1	3.1	458.3	3.0	557.5	2.4	543.7	2.0
1971-1980	313.5	2.6	392.6	3.0	357.8	2.2	375.8	2.2
1981-1990	167.1	2.4	185.3	2.5	190.7	2.2	206.2	1.9
1991-2000	74.2	2.2	97.3	2.3	112.5	2.2	117.2	1.9
2001-2008	25.5	2.1	48.7	2.1	60.2	2.1	53.0	1.3

[a] Precision error of the Accelerator Mass Spectrometer measurements

Table 9. Derived CO_2 concentrations (ppm) from $\Delta^{14}C$ (‰) measurements for years 1851-2008

Years	Central Park	LDEO	Black Rock Forest	Ashokan Reservoir
1851-1860	-	293.717	-	-
1861-1870	-	297.905	-	-
1871-1880	-	295.837	295.571	-
1881-1890	-	297.319	297.462	-
1891-1900	308.123	301.527	301.424	-
1901-1910	313.273	303.977	302.451	-
1911-1920	318.717	308.317	306.108	305.332
1921-1930	323.029	313.600	310.452	308.409
1931-1940	327.412	314.016	311.313	310.753
1941-1950	328.999	316.912	314.167	312.024
1951-1960	334.973	334.611	331.747	319.282
1961-1970	334.017	348.855	326.637	329.564
1971-1980	346.635	326.945	335.318	330.939
1981-1990	355.591	350.140	348.555	344.061
1991-2000	374.268	366.394	361.398	359.886
2001-2008	-	-	-	-

Table 10. Minimum and Maximum CO_2 concentrations (ppm) at each site

		from Aug. 2007		2008		up to July 2009	
Site		**Min**	**Max**	**Min**	**Max**	**Min**	**Max**
CP	Date – Time	-	-	-	-	7/30 - 4:30 pm	3/16 - 8:00 am
	CO_2 (ppm)	-	-	-	-	361.5	579.3
Harlem	Date – Time	8/18 - 5:01 pm	11/14 - 9:12 am	7/31 - 7:15 pm	2/13 - 9:12 am	7/30 - 5:45 pm	2/2 - 8:30 am
	CO_2 (ppm)	374.5	676.1	358.5	695.5	367.5	598.9
LDEO	Date – Time	12/7 - 0.37 am[a]	11/14 - 11:52 am	7/18 - 4:00 pm	1/7 - 3:37 am	2/1 - 12:26[b]	2/7 - 11:20 am
	CO_2 (ppm)	379.3	545.5	342.4	530.3	370.8	592.6
BRF	Date – Time	-	-	8/27 - 5:00 pm	9/26 - 4:00 pm	7/25 - 8:00 am	6/24 – 4:00 am
	CO_2 (ppm)	-	-	352.1	501.2	344.4	495.8
AR	Date – Time	-	-	7/19 - 12:00 pm	7/23 - 4:00 pm[c]	-	-
	CO_2 (ppm)	-	-	355.5	484.3	-	-
Norwalk	Date – Time	-	-	7/29 - 11:48 am	12/18 - 11:33 pm	1/1 - 2:33 pm[d]	2/11 - 9:33 am
	CO_2 (ppm)	-	-	323.2	582.8	392.1	655.5
Southold	Date – Time	-	-	11/21 - 4:15 pm[e]	11/28 - 2:15 pm[e]	7/7 - 3:15 pm	1/23 - 9:15 am
	CO_2 (ppm)	-	-	368.8	451.4	338.9	451.7

[a] data was only acquired from mid-Sept onward. Therefore min/max is not representative of the whole year

[b] data could not be acquired from mid-March until July. Therefore min/max is not representative of the whole year

[c] data was only acquired from mid-June until mid-July. Therefore min/max is not representative of the whole year

[d] data was only acquired until late-February. Therefore min/max is not representative of the whole year

[e] data was only acquired from mid-October until late November. Therefore min/max is not representative of the whole year

Table 11. Average temperature (°C) difference between sites from May - August 2006[a]

	Harlem		CP		Norwalk	
	Day[b]	Night[c]	Day	Night		
Harlem	-	-	-	-	-	-
CP	0.95	1.48	-	-	-	-
Norwalk	1.03	2.33	0.08	0.86	-	-

[a] differences are relative to the horizontal site heading temperature
(i.e. negative sign is when the horizontal site's temperature
is lower than that of the vertical site's temperature)

[b] Day is defined as when Solar Radiation measurements > 0.625

[c] Night is defined as when Solar Radiation measurements = or < 0.625

Table 12. Average temperature (°C) difference between sites from May - August 2007[a]

	Harlem		CP	
	Day[b]	Night[c]	Day	Night
Harlem	-	-	-	-
CP	1.00	1.70	-	-

[a] differences are relative to the horizontal site heading temperature
(i.e. negative sign is when the horizontal site's temperature
is lower than that of the vertical site's temperature)

[b] Day is defined as when Solar Radiation measurements > 0.625

[c] Night is defined as when Solar Radiation measurements = or < 0.625

Table 13. Average temperature (°C) difference between sites from May - August 2008[a]

	Harlem		CP		LDEO		BRF		AR		Piermont		Norwalk		Southold	
	Day[b]	Night[c]	Day	Night	Day	Night	Day	Night	Day	Night	Day	Night	Day	Night	Day	Night
Harlem	-	-	-	-	-	-	-	-	-	-	-	-	-	-	-	-
CP	2.37	3.19	-	-	-	-	-	-	-	-	-	-	-	-	-	-
LDEO	4.53	5.21	2.16	2.02	-	-	-	-	-	-	-	-	-	-	-	-
BRF	3.88	5.95	1.51	2.76	-0.65	0.75	-	-	-	-	-	-	-	-	-	-
AR	1.18	3.75	-1.19	0.56	-3.35	-1.45	-2.70	-2.20	-	-	-	-	-	-	-	-
Piermont	-0.18	0.91	-2.55	-2.28	-4.71	-4.30	-4.06	-5.04	-1.37	-2.84	-	-	-	-	-	-
Norwalk	2.70	4.05	0.33	0.86	-1.83	-1.16	-1.18	-1.91	1.52	0.30	2.88	3.14	-	-	-	-
Southold	2.96	3.21	0.59	0.02	-1.57	-2.00	-0.92	-2.75	1.77	-0.55	3.14	2.30	0.26	-0.84	-	-

[a] differences are relative to the horizontal site heading temperature
(i.e. negative sign is when the horizontal site's temperature
is lower than that of the vertical site's temperature)

[b] Day is defined as when Solar Radiation measurements > 0.625

[c] Night is defined as when Solar Radiation measurements = or < 0.625

Table 14. Average temperature (°C) difference between sites from May - July 2009[a]

	Harlem[b]		CP		LDEO		BRF		Piermont	
	Day[c]	Night[d]	Day	Night	Day	Night	Day	Night	Day	Night
Harlem	-	-	-	-	-	-	-	-	-	-
CP	-	-	-	-	-	-	-	-	-	-
LDEO	-	-	0.65	0.72	-	-	-	-	-	-
BRF	-	-	0.60	1.80	-0.05	1.08	-	-	-	-
Piermont	-	-	-0.38	-0.59	-0.05	-1.31	-0.98	-2.39	-	-

[a] differences are relative to the horizontal site heading temperature (i.e. negative sign is when the horizontal site's temperature is lower than that of the vertical site's temperature)

[b] Day is defined as when Solar Radiation measurements > 0.625

[c] Night is defined as when Solar Radiation measurements = or < 0.625

Table 15. Comparison of Cain (1975) with contemporary measurements

Year(s)	Central Park (Cain, 1975)[a]	±	Central Park	±	Bear Mountain[b] (Cain, 1975)[a]	±	Black Rock Forest[b]	±
1871-1880	-	-	-	-	-	-	-24.4	1.4
1881-1890	-	-	-	-	-	-	-23.1	1.2
1891-1900	-	-	-43.7	1.9	-	-	-22.4	1.5
1900	-37.0	3.9	-	-	3.8	4.0	-	-
1901-1910	-	-	-56.8	1.9	-		-23.0	1.2
1905	-	-	-		6.4	4.3	-	-
1910	-52.0	4.0			-4.3	4	-	-
1911-1920			-66.1	2.0			-27.7	1.4
1915	-67.1	4.3			-5.4	4.0	-	-
1920	-64.9	3.9			-17	4	-	-
1921-1930	-66.5	3.1 - s.e.[c]	-71.1	1.9			-33.5	1.3
1925-1930					-21.4	2.9 - s.e.	-	-
1931-1940	-54.3	3.8 - s.e	-80.0	1.9	-18.13	1.6 - s.e.	-32.4	1.3
1941-1950	-66.6	1.7 - s.e.	-82.0	1.9	-23.78	1.6 - s.e.	-38.6	1.3
1951-1960	19.3	32.1 - s.e.	11.6	1.3	83.31	36.2 - s.e.	21.4	1.4
1961-1970	510.4	56.5 - s.e.	523.1	3.1	602.81	62.0 - s.e.	557.5	2.4
1971-1980			313.5	2.6			357.8	2.2
1981-1990			167.1	2.4			190.7	2.2
1991-2000			74.2	2.2			112.5	2.2
2001-2008			25.5	2.1			60.2	2.1

[a] Cain, W. F. (1975). Carbon-14 in Tree Rings of Twentieth Century America. United States -- California, University of California, San Diego.

[b] Black Rock Forest is approximately 25 km north of Bear Mountain

[c] Standard error is denoted as "s.e.". All other error bars are due to the precision error of the Accelerator Mass Spectrometer measurements

Appendix

Modified from Susan Trumbore's Lab Extraction Method
Modified Last on 10/13/09 by Diana Hsueh
Questions? Contact Diana: hsueh.diana@gmail.com

Cellulose Lipid Extraction and Bleaching Protocol

Safety Precautions

Always wear safety glasses for eye protection and gloves to prevent contamination and chemical spill injuries. **Wearing safety glasses cannot be stressed enough.** You **never** know when a small fracture in glassware or liquid nitrogen dewers can cause it to shatter or explode unexpectedly. Always wear close toed shoes and long pants. Long sleeved shirt highly recommend.

Materials and Chemicals-- Amount for One Extraction Batch

Exacto Knife and tweezers to cut sample up
Ankom tissue digestion paper (paper located in the bottom cabinet to the left of the hood)
Heat Sealer (located in the bottom cabinet to the left of the hood)
Laboratory Scale (one that can measure in mg – or enough decimals in g so that you know mg)
Rounded-bottom hot plate (located next to the yellow flammable cabinet to the left of the hood)
Soxhlet Apparatus (see *Figure 1.*) - parts located in the bottom cabinet to the left of the hood
Vacuum Grease or Vaseline
Heavy-Duty metal clamp to restrict water flow
Plastic Tubing for water flow (one thick-walled-yellow tube; one clear tube)
Round metal clamps to secure plastic tubing to water source and soxhlet apparatus
Boiling Chips (Boileezers)
Toluene -- ~260 ml
Ethanol --- ~520 ml
DI Water
Long Tweezers
A 1000 mL beaker
A 500 mL round bottom flask
Sodium chlorite --- ~12-24 g
Glacial acetic acid --- ~ 6-12 ml
Scoopula
Heated Stir Plate
Watch Glass
Thermometer
3 pronged Clamp
Aluminum Foil
Drying Oven
Small Glass Vials
Scissors
Methanol
Kimwipes
<u>Optional:</u>
    A 5000 µl pipette
    A 5000 µl pippet tip
    6750 Freezer/Mill – Located underneath the hood
    Liquid Nitrogen

Modified from Susan Trumbore's Lab Extraction Method
Modified Last on 10/13/09 by Diana Hsueh
Questions? Contact Diana: hsueh.diana@gmail.com

Lipid Extraction

**Note: Use the pre-made sheet (below) for note-taking for your convenience:

wght of scint. vial (mg): = weight of the empty scintillation vial
wght of scint.vial+unprocessed sample (mg): = weight of scintillation vial + unprocessed sample
subtract to calculate the weight of the unprocessed sample
wght of glass vial (mg): = weight of the glass vial
wght of glass vial+processed sample (mg): = weight of the glass vial + processed sample
subtract to calculate the weight of the processed sample

1. Sample Preparation:

**Note: If it can be done and allows you to see the same or similar results, it is much easier if one uses one ring for C-14 analysis instead of homogenizing more than one ring. It will save you from having to grind the samples; one can send the entire cut-up ring for analysis. If you want to do multiple rings, then first measure length of ring to discern which year has more influence over another.

a. Cut up the sample into small intact 1 mm (or less) slivers if sample size is quite large: Using tweezers to hold the sample and an exacto knife to cut it should do the trick – always clean the tweezers and exacto knife with methanol in between every sample. For the cutting surface, place a NEW CLEAN piece of aluminum foil over the surface that is usually used for leaf punching (it is somewhere around the lab). This is so that you won't ding up the countertop. (It is recommended to cut instead of grinding up the samples first because if you grind it up too finely, samples may go through the Ankom bags and you will lose sample that way, and what is worse, it may cause cross contamination between samples.)
b. Weigh out the initial weight of the scintillation vial that will be used to contain the sample before and after sample is put in. Record it in your notebook. This way of measurement is much simpler (especially if there is static in the air – I guarantee that would drive you crazy since the sample are in tiny flakes now) and there is no unneeded transferring which would only increase chances of contamination.
c. Using the heat sealer (keep it at ~5.5 heat setting) and Ankom tissue digestion paper, seal the bags with samples inside. Ankom tissue digestion paper comes in large sheets; cut and seal accordingly. There is a slightly shiny/slick slide; this side should be on the inside. Cut the top of the Ankom paper in a unique pattern (See *Figure 1*) for each sample and record patterns on the sheet provided below. This will allow you to identify your samples later. During extraction, the solvent dissolves any markings made with a permanent marker.

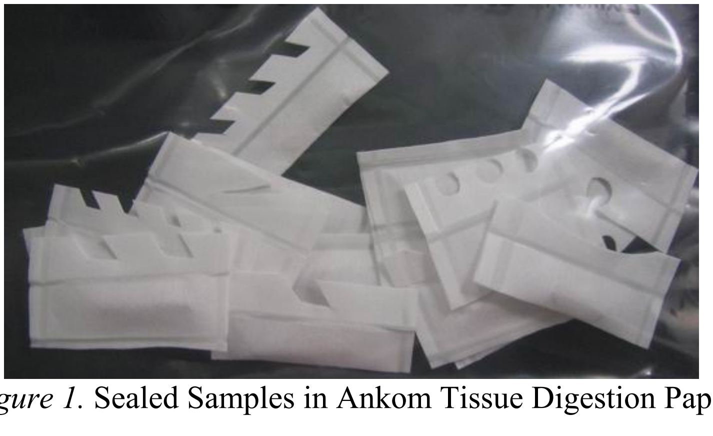

Figure 1. Sealed Samples in Ankom Tissue Digestion Paper

2. Put your samples into the soxhlet apparatus using the long tweezers (see *Figure 2*. below to note where samples should be placed). You also do not want to fill the middle section of the apparatus past the part of where the solvent will drain back into the round-bottom flask (see *Figure 3*).
3. Add boiling chips (boileezers) to the round bottom flask and fill with 390 ml 2:1 toluene:ethanol mixture. You can reuse this solution 2-3 times depending on how big and how many samples there are. Check the color – if the liquid that pool in the middle section of the soxhlet starts to get too brown, replace the solution. [**Note: You DO NOT want to fill up the round bottom flask over 400 ml because the solvent will expand when heated and may overflow/shoot up the soxhlet once it does start boiling] You will also want to put in fresh boiling chips every time you use the solvent, especially if the boiling chips have been sitting in solvent for a while. This is to prevent the boiling chips from becoming ineffective (which will cause "wild boiling"– which is a scary thing – trust me).
4. Place tubing on both ends of the top section of the soxhlet apparatus for water to go in and out if none are already in place (see *Figure 2.*) (the top part of the soxhlet is to condense solvent vapors). For the "Water In" tube, use a thick-walled tube (a yellow one) so that the tube does not bulge and burst when the water is turned on. For extra security, place a round-metal clamp around where the water source and tubing connect as well as where the tubing connects to the soxhlet.
5. Assemble the soxhlet apparatus, flask and condenser (see *Figure 2.*) in the hood. Put a thin layer of either vacuum grease or Vaseline where the glass pieces connect. Using a three pronged clamp, clamp the top section of the soxhlet to the metal rod to secure it in place.
6. Using a heavy duty metal clamp (see *Figure 2.*), compress the "Water In" tube – this is to prevent wasting more water than necessary. Adjust the clamp so that not too little or too much water is going down the drain (in the corner of hood). A prop may be necessary to hold the clamp steady. Place a weight (such a large flask in *Figure 2* below) on the "Water Out" tube so that the tubing will stay put and not move around when water is being forced out of the tube.
7. Turn the hot plate up to 5. Wait for it to boil and then turn it to a heat setting of 6.5. This should ensure that the condensed solvent drips down at around the rate of one drop per second (see *Figure 3.*). There is also a chance that there just isn't enough solvent to evaporate and reach up the soxhlet apparatus. If this is the case, then turn off the rounded-hot plate; let the solvent cool slightly, carefully open the soxhlet up and then add more solvent and turn it back on. Samples may have a tendency to float up as the middle section fills up with solvent. If this happens, turn off the rounded-hot plate, wait until the solvent stops boiling, and then disassemble the soxhlet apparatus, and re-arrange the configuration of the samples to prevent it from floating up. You may have to fold samples in half and stick it in between other samples, so that the samples altogether will be thick enough to "stick" to the bottom of the middle section and not float up.
8. Once the middle section fills up with solvent up to the (see *Figure 3.*) part where the thin glass tube on the side bends down, it will drain back down to the round bottom flask and it will start the process all over again.
9. Run this for 24 hours. Leave the blower on the whole time.
10. Turn off heat and then remove samples with long tweezers and put it in a large beaker. Let samples dry in the hood for 2 hours with the blower on.
11. Repeat extraction with 360 ml of pure ethanol (200 proof) for 24 hours. Again, leave the blower on the whole time. Then turn off the heat and remove samples from the solvent and place in a large beaker and let dry for 2 hours in the hood with the blower on. The ethanol can also be re-used 2-3 times as well.
12. The samples are now ready for bleaching.

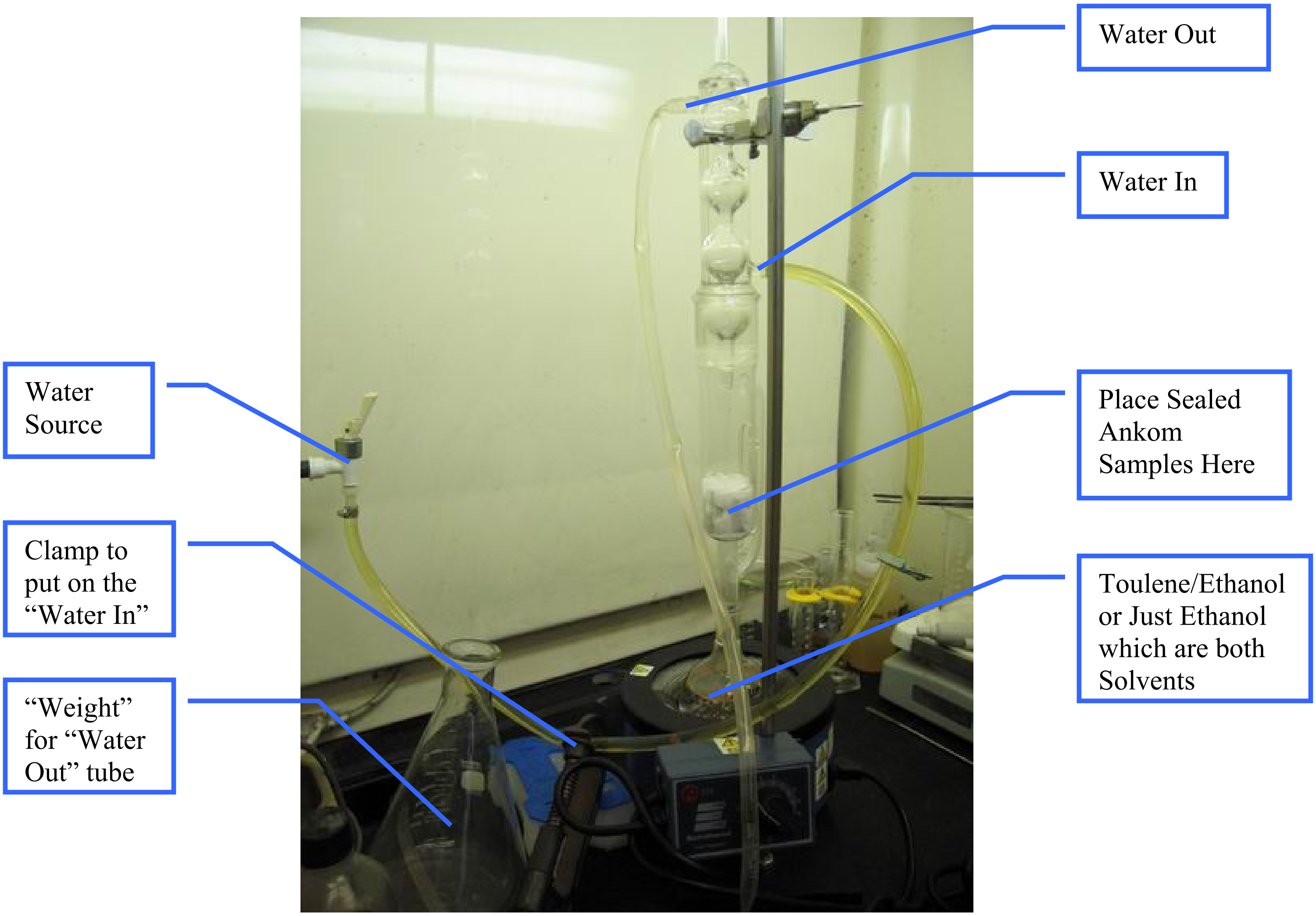

Water Out

Water In

Water Source

Place Sealed Ankom Samples Here

Clamp to put on the "Water In"

Toulene/Ethanol or Just Ethanol which are both Solvents

"Weight" for "Water Out" tube

Figure 2. Soxhlet Apparatus Assembly

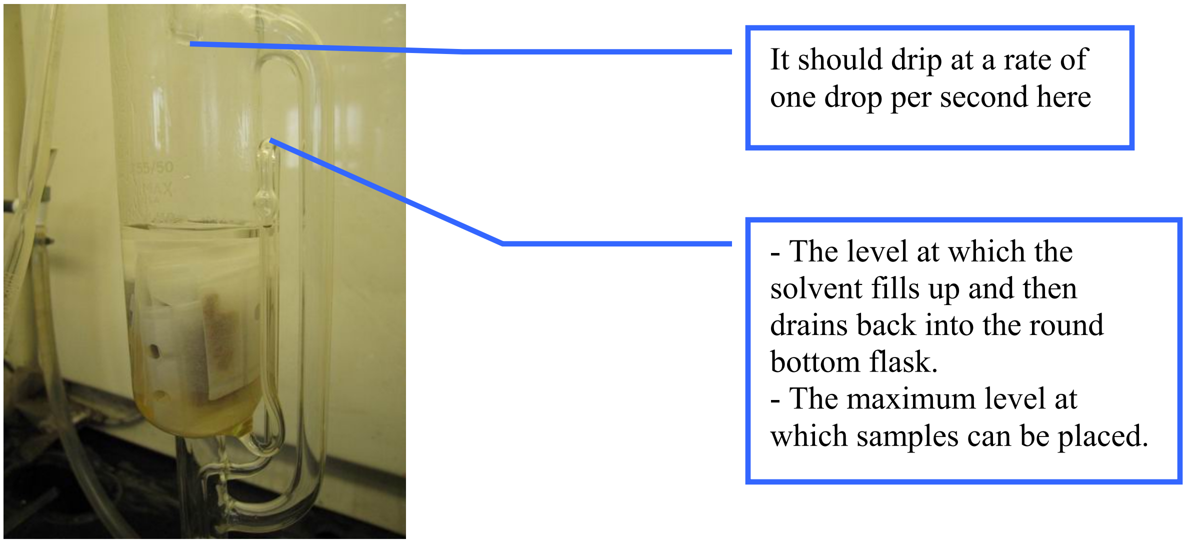

It should drip at a rate of one drop per second here

- The level at which the solvent fills up and then drains back into the round bottom flask.
- The maximum level at which samples can be placed.

Figure 3. Close-up of the middle section of the Soxhlet Apparatus

Modified from Susan Trumbore's Lab Extraction Method
Modified Last on 10/13/09 by Diana Hsueh
Questions? Contact Diana: hsueh.diana@gmail.com

Bleaching

1. Place digestion bags into a 1000 mL beaker.
2. Add 600 ml of DI water to the beaker and boil the samples for ~2 hours. Place a watch glass over the beaker to prevent too much evaporation.
3. Replace the solution with fresh 600 ml DI water, place stirbar in beaker and begin stirring solution. Adjust the heat setting to ~3-4 on the hotplate.
4. Wait until the water reaches 70°C. In the meantime weigh out 4 g of sodium chlorite with a scoopula and have 2 mL glacial acetic acid ready. (Note: It is much easier to use a pipette to put in 2 ml of glacial acetic acid instead of pouring it out; 1000 µL= 1mL)
5. Once the water has reached 70°C (use a thermometer), add the sodium chlorite and glacial acetic acid into the water at the same time. The water will eventually be a bright yellow color. Place a watch glass over the beaker to prevent too much evaporation.
6. Change this solution every 3-4 hours. You don't have to change the water, just add more sodium chlorite and glacial acetic acid. This may take up to 1-2 days depending on when you start during the day. At the end, the tissue should be really white (i.e. you can't see the wood through the Ankom Paper) If this procedure is not done by the end of the day, shut the heat and stirbar off. Resume the next day. This is so that the liquid does not evaporate overnight and burn (thus making your samples useless) in the beaker.
7. When you see that the tissue is white, rinse the samples several times with 600 ml DI water over a 3-4 hour period. At the end, no sodium chlorite (bleachy) smell should remain.
8. Remove the samples from the water and place on a piece of NEW aluminum foil. Place in the drying oven at 60-70°C and leave overnight.
9. When samples are dried, lay a sheet of NEW CLEAN aluminum foil on the countertop. Clean the aluminum foil you just placed down with methanol before use. Carefully cut an edge with scissors and put the samples into a NEW glass vial with tweezers. Clean scissors and tweezers and aluminum foil surface with methanol after each sample handling. You will also need to weigh out the sample again. Weigh out the initial weight of the glass vial that will be used to contain the sample before and after sample is put in and record it in your notebook. This again minimizes the chance of contamination through weighing and transferring. Use glass vials and not plastic containers (i.e. 1.5 mL centrifuge tubes) because this will reduce static (static is quite annoying for the person weighing out the sample for combustion)
10. Determine the % yield by dividing the final weight by the initial weight of the sample. The % yield should be in the 0.5-something area. However, a % yield of 0.7 not unheard of.
11. If needed, grind samples to homogenize the samples to be sent (Instructions Below)

At this point, you have produced holo-cellulose. This is fine for C-14 analysis.
To produce α-cellulose (for ^{18}O and D/H analysis), please refer to the original protocol below.

Modified from Susan Trumbore's Lab Extraction Method
Modified Last on 10/13/09 by Diana Hsueh
Questions? Contact Diana: hsueh.diana@gmail.com

Grinding (if necessary)

Use a 6750 Freezer/Mill. This machine can be found in a box below the hood. Obtain at least 10 L of liquid nitrogen. You will need to use a lot more if you will be grinding a lot of samples. Read the manual provided in the box to learn how to operate. Use the one that has 3 smaller metal containers in it to prevent potential contamination from the plastic if you are doing C-14 analysis. Play around with the prep-cool-down time, grinding time and number of cycles with a fake sample and adjust accordingly however you want the consistency to be. With wood, a 10.0 prep-cool-down time, 2.0 max grinding time and 1 cycle is enough to pulverize it into a fine powder to homogenize the sample. Don't stuff the metal containers with samples (split apart if necessary); samples may compact to one side instead of grinding. Once you are done with each sample, rinse/clean metal components with water and ultimately methanol to prevent cross contamination.

***

Name:_______________________________

Date Weighed and Put in Ankom Bags: _____________________________

draw cut designs above

ID	
wght of scint. vial (mg):	
wght of scint. vial+unprocessed sample (mg):	
start weight (mg):	
wght of glass vial (mg):	
wght of glass vial+processed sample (mg):	
final weight (mg):	
% yield	

draw cut designs above

ID	
wght of scint. vial (mg):	
wght of scint. vial+unprocessed sample (mg):	
start weight (mg):	
wght of glass vial (mg):	
wght of glass vial+processed sample (mg):	
final weight (mg):	
% yield	

draw cut designs above

ID	
wght of scint. vial (mg):	
wght of scint. vial+unprocessed sample (mg):	
start weight (mg):	
wght of glass vial (mg):	
wght of glass vial+processed sample (mg):	
final weight (mg):	
% yield	

draw cut designs above

ID	
wght of scint. vial (mg):	
wght of scint. vial+unprocessed sample (mg):	
start weight (mg):	
wght of glass vial (mg):	
wght of glass vial+processed sample (mg):	
final weight (mg):	
% yield	

draw cut designs above

ID	
wght of scint. vial (mg):	
wght of scint. vial+unprocessed sample (mg):	
start weight (mg):	
wght of glass vial (mg):	
wght of glass vial+processed sample (mg):	
final weight (mg):	
% yield	

draw cut designs above

ID	
wght of scint. vial (mg):	
wght of scint. vial+unprocessed sample (mg):	
start weight (mg):	
wght of glass vial (mg):	
wght of glass vial+processed sample (mg):	
final weight (mg):	
% yield	

Name:__________________________________

Date Weighed and Put in Pouches: _______________________________

Lipid Extraction

	Duration	Start	Finish
Toluene:ethanol	24 hrs.		
Air Dry	2 hrs		
Ethanol	24 hrs.		
Air Dry	2 hrs.		

Bleaching

	Duration	Start	Finish
DI H2O	2 hrs		
Sodium chlorite & glacial acetic acid	3-4 hours		
Add. Chem. added at:		__/__/__ @ __:__ am/pm ; __/__/__ @ __:__ am/pm ; __/__/__ @ __:__ am/pm	

	Duration	Start	Finish
DI H2O	3-4 hrs.		

Cellulose Lipid Extraction and Bleaching

Materials

heated stir plate
toluene
DI water
NaOH

soxhlet apparatus
ethanol
1000 ml beaker
drying oven

1000 ml round bottom flask
F57/41 Ankom tissue digestion bags
sodium chlorite (tech grade)
glacial acetic acid

Lipid Extraction

* it is best to start this extraction early Monday morning

1. Dry and grind samples. Weigh ~100 mg of sample into digestion bag. You can have up to four samples per bag and up to 10 digestion bags per batch.
2. Seal bags in unique patterns. This will allow you to identify your samples later. Record patterns and sample weight in notebook.
3. Place digestion bags in the soxhlet aparatus.
4. Add boiling chips (glass beads) to the round bottom flask and fill with 600 ml 2:1 toluene:ethanol mixture. You can reuse this solution about 3 times (check color before use).
5. Assemble soxhlet apparatus, flask, and condenser. Turn the hot plate on, use setting 6.5 or 7. Run for 24 hours.
6. Turn off heat and remove samples from the solvent. Let dry for 2 hrs.
7. Repeat extraction with 600 ml of ethanol for 24 hrs. The ethanol can also be reused.
8. Dry samples for 2 hrs.

Bleaching

1. Place digestion bags in 1000 ml beaker.
2. Add 600 ml DI water to the beaker and boil the samples for ~2 hrs.
3. Replace the solution with 600 ml DI H2O, place stirbar in beaker and begin stirring solution. Adjust the heat setting 2.75 or 3 on the hotplate.
4. Wait until the water reaches 70°C.
5. Measure out 4 g sodium chlorite and 2 ml glacial acetic acid ready.
6. Add the sodium chlorite and glacial acetic acid to the water at about the same time.
7. Change this solution every 3-4 hours. This can take 3-4 days. You don't have to change the water, just add more sodium chlorite and glacial acetic acid. Monitor the temperature – make sure it stays around 70°C.
8. When the tissue is white, rinse samples several times with 600 ml DI H2O over a 3-4 hour period. At the end no sodium chlorite smell should remain.

At this point you have produced holocellulose.

α-cellulose extraction (necessary for 18O and D/H analysis)

1. Fill beaker with 600 ml DI H2O, add 102 g NaOH and stir for 1 hour at room temperature (17% w/v NaOH)
2. Rinse tissue several times: 600 ml DI H2O over 3-4 hour period.

3. Fill beaker with 540 ml DI H2O, add 60 ml glacial acetic acid and stir for 1 hour at room temperature.
4. Rinse tissue several times with 600 ml DI H2O over a 3-4 hour period.
5. Check the pH of the water. It should be neutral.
6. Remove samples from the water and place on a piece of aluminum foil. Dry in the oven at 70°C.

References

Epstein, S., P. Thompson, and C.J. Yapp. 1988. Oxygen and hydrogen isotopic ratios in plant cellulose. Science 198:1209-1225.

Leaveitt, S. W. and S. R. Danzer. 1992. Methods for batch processing small wood samples to holocellulose for stable-carbon isotope analysis. Analytical Chemistry 65:87-89.

Sternberg, L. da S.L. 1988. Oxygen and hydrogen isotope ratios in plant cellulose: mechanisms and application, p. 124-141. In P. W. Rundel, J.R. Ehleringer, and K. Nagy, eds.) Stable Isotopes in Ecological Research. Springer Verlag.

Sternberg, L. da S.L.. Oxygen and hydrogen isotope measurements in plant cellulose. [notes from a visit to Miami]

Wise, L.E., (1944). Wood Chemistry, Reinhold.

Ordering information for chemicals

Chemical name	*Size*	*Fisher Scientific catalog #*
Toluene	4 L	T324-4
95% denatured ethyl alcohol	4 L	S73985
Glacial acetic acid	500 ml	A38-500
Sodium chlorite, tech grade	500 g	AA1426536
Sodium hydroxide pellets	500 g	S318-500

updated Jan. 2005